MICROBIOLOGY AND MOLECULAR BIOLOGY REVIEWS, Mar. 2001, p. 1–43 Vol. 65, No. 1
1092-2172/01/$04.00+0 DOI: 10.1128/MMBR.65.1.1–43.2001

Hyperthermophilic Enzymes: Sources, Uses, and Molecular Mechanisms for Thermostability

CLAIRE VIEILLE AND GREGORY J. ZEIKUS[1,2]*

Biochemistry Department, Michigan State University, East Lansing, Michigan 48824,[1] and MBI International, Lansing Michigan 48909[2]

* Corresponding author. Mailing address: Michigan Biotechnology Institute, 3900 Collins Rd., Lansing, MI 48909. Phone: (517) 337-3181. Fax: (517) 337-2122. E-mail: zeikus@mbi.org.

INTRODUCTION

Hyperthermophiles grow optimally at temperatures between 80 and 110°C. Only represented by bacterial and archaeal species, these organisms have been isolated from all types of terrestrial and marine hot environments, including natural and man-made environments. Enzymes from these organisms (or hyperthermophilic enzymes) developed unique structure-function properties of high thermostability and optimal activity at temperatures above 70°C. Some of these enzymes are active at temperatures as high as 110°C and above (349). Thermophilic organisms grow optimally between 50 and 80°C. Their enzymes (thermophilic enzymes) show thermostability properties which fall between those of hyperthermophilic and mesophilic enzymes. These thermophilic enzymes are usually optimally active between 60 and 80°C. Active at high temperatures, thermophilic and hyperthermophilic enzymes typically do not function well below 40°C.

Current theory and circumstancial evidence suggest that hyperthermophiles were the first life-forms to have arisen on Earth (318). Hyperthermophilic enzymes can therefore serve as model systems for use by biologists, chemists, and physicists interested in understanding enzyme evolution, molecular mechanisms for protein thermostability, and the upper temperature limit for enzyme function. This knowledge can lead to the development of new and/or more efficient protein engineering strategies and a wide range of biotechnological applications.

This review will encompass the sources and uses of thermophilic and hyperthermophilic enzymes, as well as the molecular determinants for protein stability. Emphasis will be placed on hyperthermophilic enzymes, because most current research is focused on these enzymes and on hyperthermophiles. What is the upper temperature for life? Back in 1969, when T. D. Brock and colleagues discovered *Thermus aquaticus*—now known for its *Taq* polymerase in PCR techniques—*T. aquaticus* was considered an extreme thermophile since it grew optimally at 75°C (41). Today, of course, hyperthermophiles such as *Pyrolobus fumarii*, which grows at up to 113°C (28), are considered extreme.

Thermophilic and hyperthermophilic enzymes (also called thermozymes [see reference 349]) are part of another enzyme category called extremozymes, which evolved in extremophiles. Extremozymes can function at high salt levels (halozymes), under highly alkaline conditions (alkalozymes), and under other extreme conditions (pressure, acidity, etc.) (see references 4, 144, 223, and 371). Intrinsically stable and active at high temperatures, thermophilic and hyperthermophilic enzymes offer major biotechnological advantages over mesophilic enzymes. (i.e., enzymes optimally active at 25 to 50°C) or psychrophilic enzymes (i.e., enzymes optimally active at 5 to 25°C): (i) once expressed in mesophilic hosts, thermophilic and hyperthermophilic enzymes are easier to purify by heat treatment, (ii) their thermostability is associated with a higher resistance to chemical denaturants (such as a solvent or guanidinium hydrochloride), and (iii) performing enzymatic reactions at high temperatures allows higher substrate concentrations, lower viscosity, fewer risks of microbial contaminations, and often higher reaction rates.

Already the object of extensive reviews (140, 317, 319, 320), hyperthermophiles are only briefly described here. No exhaustive description of all the enzymes isolated and characterized from thermophiles and hyperthermophiles is presented, since that information is available elsewhere (2, 3, 139, 263, 349). Instead, we will focus on the latest findings that explain the molecular determinants of extreme protein thermostability and on the thermophilic and hyperthermophilic enzymes with the highest commercial relevance.

HYPERTHERMOPHILE DIVERSITY

The interest shown by the scientific community in hyperthermophiles has constantly increased over the last 30 years. This growing interest is demonstrated by the increasing number of hyperthermophilic species that have been described (from 2 in 1972 [40, 372] to more than 70 at the end of 1999 [140, 320]), by the exponentially growing number of publications on the subject, and by the major central place occupied by hyperthermophiles in worldwide genome-sequencing projects (six completed genome sequences, and at least four genome-sequencing projects in progress) (see Table 1 and http//www.tigr.org) Studies of environmental 16S rRNA sequences (18, 19) in samples originating from a single continental hot spring (Obsidian Pool at Yellowstone National Park) and environmental lipid analysis (128) suggest that known hyperthermophiles represent only a fraction of hyperthermophilic species diversity.

Now that we are able to collect samples almost routinely from deep-sea floors, access to hyperthermophilic biotopes is not the limiting factor in studying hyperthermophile diversity. Isolating and growing pure cultures of new hyperthermophiles has been—and remains—a challenge. A striking example of this difficulty is the bacterium *Thermocrinis ruber* (147). This pink-filament-forming bacterium was described as early as 1967 by Brock (39), but it took more than 25 years to successfully cultivate this organism (147). A major task for scientists in

the near future will be to develop new isolation techniques for microorganisms with different, unforeseen metabolic requirements. Huber et al. (145) took the lead by cloning a new archaeal hyperthermophile by using optical tweezers.

Hyperthermophiles have been isolated almost exclusively from environments with temperatures in the range of 80 to 115°C. Hot natural environments include continental solfataras, deep geothermally heated oil-containing stratifications, shallow marine and deep-sea hot sediments, and hydrothermal vents located as far as 4,000 m below sea level (Table 1). Hyperthermophiles have also been isolated from hot industrial environments (e.g., the outflow of geothermal power plants and sewage sludge systems). Deep-sea hyperthermophiles thrive in environments with hydrostatic pressures ranging from 200 to 360 atm. Some of these species are barotolerant (281) or even barophilic (95, 233, 257). The most thermophilic organism known, *P. fumarii*, grows in the temperature range of 90 to 113°C. The upper temperature at which life is possible is still unknown, but it is probably not much above 113°C. Above 110°C, molecules such as amino acids and metabolites become highly unstable (ATP is spontaneously hydrolyzed in aqueous solution at temperatures below 140°C) and hydrophobic interactions weaken significantly (163).

Of the more than 70 species, 29 genera, and 10 orders of hyperthermophiles that have been described (320), most are archaea. *Thermotogales* and *Aquificales* are the only bacteria (Table 1). *Thermotogales* and *Aquificales* are the deepest branches in the bacterial genealogy, and for this reason they represent an obvious interest in evolutionary studies (1). One of the most striking findings extracted from the complete *Thermotoga maritima* genome sequence (258) is the abundance of evidence supporting lateral gene transfer between archaea and bacteria: (i) 24% of the *T. maritima* open reading frames (versus 16% in *Aquifex aeolicus*) encode proteins that are more similar to archaeal than to bacterial proteins; (ii) these archaea-like genes are not uniformly distributed among the biological categories; (iii) 81 of these genes are clustered in 15 4- to 20-kb regions, in which the gene order can be the same as in archaea; and (iv) The *T. maritima* genome sequence does not have a homogeneous G+C content—among the 51 regions having significantly different G+C contents, 42 contain "archaea-like" genes.

The archaeal domain is composed so far of two branches: the *Crenarchaeota* and the *Euryarchaeota*. A 16S rRNA isolated from a hyperthermophilic environment was recently sequenced that is not related to any other archaeal rRNA. This new rRNA species suggests the existence of a third branch in the archaeal domain, the *Korarcheota*, that branches deeper in the archaeal tree than the *Crenarchaeota* and the *Euryarchaeota* (18). Hyperthermophiles are represented in the *Crenarchaeota* and *Euryarchaeota*, and they systematically represent the deepest and shortest lineages in these two branches (see references 140 and 320 for phylogenetic trees). In addition to thermoacidophiles, *Crenarchaeota* include halophiles. Among the *Euryarchaeota*, methanogens have mesophilic relatives.

Hyperthermophile communities are complex systems of primary producers and decomposers of organic matter. All hyperthermophilic primary producers are chemolithoautotrophs (i.e., sulfur oxidizers, sulfur reducers, and methanogens) (104, 223). In relation to the high sulfur content of most hot natural biotopes, most hyperthermophiles are facultative or obligate chemolithotrophs: they either reduce S^0 with H_2 to produce H_2S (the anaerobes) or oxidize S^0 with O_2 to produce sulfuric acid (the aerobes). Extremely acidophilic hyperthermophiles belong to the order *Sulfolobales*. They are all strict aerobes (e.g., *Sulfolobus*) or facultative aerobes (e.g., *Acidianus*), and they have been isolated almost exclusively from continental solfataras (Table 1). While most heterotrophs are obligate sulfur reducers, all members of the *Thermotogales* and most members of the *Pyrococcales* and *Thermococcales* can grow independently of S^0, obtaining their energy from fermentations (Table 1). Because of the extremely low organic matter content of their submarine environments, hyperthermophilic heterotrophs typically obtain their energy and carbon from complex mixtures of peptides derived from the decomposition of primary producers. A few species are able to use polysaccharides (e.g., starch, pectin, glycogen, and chitin); to date, *Archeoglobus profundus* is the only known species that uses organic acids.

BIOCHEMICAL AND MOLECULAR PROPERTIES OF HYPERTHERMOPHILIC ENZYMES

Thermal and Catalytic Properties

Thermostability and optimal activity at high temperatures are inherent properties of hyperthermophilic enzymes. Enzyme thermostability encompasses thermodynamic and kinetic stabilities. Thermodynamic stability is defined by the enzyme's free energy of stabilization (ΔG_{stab}) and by its melting temperature (T_m, the temperature at which 50% of the protein is unfolded). For the enzymes that unfold irreversibly, only T_m can be determined. Kinetic stability depends on the energy barrier to unfolding (i.e., the activation energy [E_a] of unfolding). An enzyme's kinetic stability is often expressed as its half-life ($t_{1/2}$) at defined temperatures. In this review, an enzyme will be called mesophilic if it originates from a mesophilic organism, thermophilic if it originates from a thermophile, and hyperthermophilic if it originates from a hyperthermophile. Further, we will say that enzyme X is more thermophilic than enzyme Y if enzyme X is optimally active at higher temperatures than enzyme Y.

Most enzymes characterized from hyperthermophiles are optimally active at temperatures close to the host organism's optimal growth temperature, usually 70 to 125°C (see references 139 and 349 for lists of purified hyperthermophilic enzymes and their properties). Extracellular and cell-bound hyperthermophilic enzymes (i.e., saccharidases and proteases) are optimally active at temperatures above—sometimes far above—the host organism's optimum growth temperature and are, as a rule, highly stable. For example, *Thermococcus litoralis* amylopullulanase is optimally active at 117°C, which is 29°C above the organism's optimum growth temperature of 88°C (43). While they are usually less thermophilic than extracellular enzymes purified from the same host, intracellular enzymes (such as xylose isomerases) are usually optimally active at the organism's optimal growth temperature. Only a few enzymes have been described that are optimally active at 10 to 20°C below the organism's optimum growth temperature (108, 197, 278). While most hyperthermophilic enzymes are intrinsically very stable, some intracellular enzymes get their high

TABLE 1. Hyperthermophile diversity

Organism (references)	Growth conditions	Isolation/habitat	Metabolic properties
Bacteria			
Aquificales			
Aquifex pyrophilus (152)	85°C, pH 6.8, 3% NaCl	Shallow MHTV[c], Kolbeinsey Ridge, north off Iceland	Microaerophilic, strict chemolithoautotroph. H_2, S^0, and $S_2O_3^{2-}$ serve as electron donors; O_2 and NO_3^- serve as electron acceptors
Thermocrinis ruber (147)	80°C, pH 7.0–8.5, <0.4% NaCl	Octopus spring, Yellowstone	Chemolithoautotrophic microaerophile; grows chemoorganoheterotrophically on formate or formamide
Thermotogales			
Thermotoga maritima[a] (150)	80°C, pH 6.5, 2.7% NaCl	Heated sea floors, Vulcano, Italy, and Azores	Heterotroph anaerobe. Grows on cabohydrates and proteins; H_2 inhibits growth.
T. neapolitana (24)	77°C, pH 7.5	Shallow marine hot spring, Naples, Italy	Heterotroph anaerobe; grows on glucose, sucrose, lactose, starch, and YE[c]; reduces S^0 to H_2S
Thermotoga strain FjSS3-B.1 (153)	80–85°C, pH 7.0	Intertidal hot spring, Savusavu, Fiji	Anaerobe, chemoorganotroph; grows on carbohydrates, including glycogen, starch, and cellulose; produces acetate, H_2, and CO_2, does not reduce S^0 or SO_4^{2-}
Archaea: Crenarchaeota			
Sulfolobales			
Sulfolobus shibatae (122)	81°C, pH 3.0	Acidic geothermal spring, Beppu, Kiushu Island, Japan	Aerobe; facultative chemolithoautotrophic growth by S^0 oxidation; can grow on carbohydrates, YE[c], and tryptone
S. solfataricus[b] (383)	87°C	Solfataric fields	Heterotroph; grows on carbohydrates
S. islandicus (380)	Unknown	Solfataric fields, Iceland	Obligate heterotroph; grows on peptides and carbohydrates
Stygiolobus azoricus (302)	80°C, pH 2.5–3.0	Solfataric fields, Sao Miguel Island, Azores	Strict anaerobe; grows chemolithoautotrophically on H_2 by reducing S^0 to H_2S; no growth by anaerobic S^0 oxidation
Acidianus infernus (301)	90°C, pH 2.0, 0.2% NaCl	Hot water, mud, and marine sediments at hot springs in Italy, the Azores, and the United States	Facultative aerobe, obligate chemolithotrophic growth by S^0 oxidation (aerobic) or by S^0 reduction with H_2 (anaerobic)
A. ambivalens (106, 384)	80°C, pH 2.5	Solfataric source, Leirhnukur fissure, Iceland	Facultative anaerobe, chemolithoautotroph; uses either $S^0 + O_2$ (yielding H_2SO_4) or $S^0 + H_2$ (yielding H_2S) as energy source.
Thermoproteales			
Thermoproteus tenax (33, 382)	88°C, pH 5.0	Solfataric fields, Iceland	Anaerobe, facultative chemolithoautotroph; heterotrophic growth on glucose, starch, glycogen, a few alcohols, a few organic acids, peptides, and formamide by S^0 respiration; H_2S required; produces acetate, isovalerate, and isobutyrate from peptone + S^0
T. neutrophilus (104, 295)	85°C, pH 6.8	Hot spring, Iceland	Anaerobe, facultative autotroph; acetate >> succinate > propionate can be used as carbon sources
T. uzoniensis (33)	90°C, pH 5.6	Uzon caldera, Kamchatka peninsula	Anaerobe; ferments peptides, producing acetate, isovalerate, and isobutyrate; S^0 stimulates growth.
Pyrobaculum islandicum (148)	100°C, pH 6.0	Geothermal power plant, Iceland	Anaerobe, facultative heterotroph (growth on peptide substrates with S^0, $S_2O_3^{2-}$ sulfite, L-cystine, or oxidized glutathione as electron acceptors; grows chemolithoautotrophically on CO_2, $S^0 + H_2$, (produces H_2S)
P. organotrophum (148)	102°C, pH 6.0	Solfataric fields, Iceland, Italy, and Azores	Anaerobe, obligate heterotroph; growth on peptide substrates with S^0, L-cystine, or oxidized glutathione as electron acceptor
P. aerophilum[b] (355)	100°C, pH 7.0, 1.5% NaCl	Shallow marine boiling-water holes, Iischia, Italy	Grows by aerobic respiration or by dissimilatory nitrate reduction; heterotrophic growth on peptide substrates, propionate, and acetate; autotrophic growth by H_2 or $S_2O_3^{2-}$ oxidation; S^0 inhibits growth

Continued on following page

TABLE 1—*Continued*

Organism (references)	Growth conditions	Isolation/habitat	Metabolic properties
Thermofilum pendens (376)	85–90°C, pH 5.0–6.0	Solfataric fields, Iceland	Heterotrophic anaerobe, mildly acidophile; grows by S^0 respiration on complex peptide substrates; requires S^0, H_2S, and a polar lipid fraction from *T. tenax*
Desulfurococcales			
Desulfurococcus mobilis (381)	85°C, pH 6.0	Solfataric fields, Iceland	Strict heterotrophic anaerobe; grows on peptide substrates; S^0 respiration or fermentation
D. amylolyticus (34)	90–92°C, pH 6.4	Thermal springs, Kamchatka peninsula	Strict heterotrophic anaerobe; grows on peptide substrates and polysaccharides; S^0 stimulates growth
Staphylothermus marinus (103)	92°C, pH 4.5–8.5, 1–3.5% NaCl	Heated sea floor, Vulcano, Italy	Strict anaerobe; S^0dependent; heterotrophic growth on complex organic substrates; produces CO_2, acetate, isovalerate, and H_2S
Thermosphaera aggregans (146)	85°C, pH 6.5, 0% NaCl	Yellowstone, Obsidian pool	Heterotrophic anaerobe (YE, AA mix, glucose); S^0 inhibits growth
Pyrodictiales			
Pyrodictium occultum (276, 321, 322)	105°C, pH 5.5, 1.5% NaCl	Marine solfataric fields, Vulcano, Italy	Strict anaerobe; autotrophic growth on H_2 + CO_2 + S^0 (produces H_2S); in the presence of YE, can grow by reduction of $S_2O_3^{2-}$
P. abyssi (276)	97°C, pH 5.5, 0.7–4.2% NaCl	Deep-sea MHTV, Guaymas, Mexico; shallow MHTV, Kolbeinsey Ridge, north off Iceland	Anaerobe, strict heterotroph; grows by fermenting carbohydrates, cell extracts, proteins, and acetate; produces CO_2, isovalerate, isobutyrate, and butanol, reduces S^0 and $S_2O_3^{2-}$ in the presence of H_2
P. brockii (276, 322)	105°C, pH 5.5, 1.5% NaCl	Marine solfataric fields, Vulcano, Italy	Strict anaerobe; autotrophic growth on H_2 + CO_2 + S^0 (produces H_2S); YE stimulates growth yield; Reduces SO_3^{2-}, not $S_2O_3^{2-}$
Hyperthermus butylicus (377)	95–106°C, pH 7.0, 1.7% NaCl	Marine solfataric field, Azores	Heterotrophic anaerobe; uses peptide mixtures as carbon and energy sources; forms H_2S from S^0 + H_2 as accessory energy source; produces CO_2, L-butanol, acetate, phenylacetate, and hydroxyphenyl acetate
Thermodiscus maritimus (104)	85°C, pH 6.5	Hot sea water, Vulcano, Italy	Obligate autotroph
Pyrolobus fumarii (28)	106°C, pH 5.5, 1.7% NaCl	Deep-sea MHTV (3,650 m), Mid-Atlantic Ridge	Obligate H_2-dependent chemolithoautotroph, grows by NO_3^-, $S_2O_3^{2-}$, or O_2 (0.3%) reduction; S^0 and several organic nutrients inhibit growth; no growth at 85°C and below
Unclassified			
Aeropyrum pernix[a] (291)	90–95°C, pH 7.0, 3.5% salt	Coastal solfataric MHTV, Japan	Strict aerobe, heterotroph; grows on complex peptide substrates; no H_2S production
Caldococcus litoralis (385)	88°C, pH 6.4, 2.5% NaCl	Shallow MHTV, Kurile Islands	Strict anaerobic chemoorganotroph; grows on complex peptide substrates and amino acids; S^0 stimulates growth (reduced to H_2S)
Archaea: Euryarchaeota			
Thermococcales			
Palaeococcus ferrophilus (329)	83°C, pH 6.0, 4.7% sea salt	Deep-sea MHTV, Ogasawa-Bonin Arc, Japan	Strict anaerobic chemoorganotroph; grows on proteinaceous substrates in the presence of S^0 or Fe^{2+}
Thermococcus aggregans (57)	88°C, pH 7.0	Guaymas basin, Mexico	Chemoorganotrophic strict anaerobe
T. barophilus (233)	85°C, pH 7.0, 2–3% NaCl	MHTV (3,550 m), Mid-Atlantic Ridge	Obligate heterotroph; S^0 stimulates growth; obligate barophile at 95–100°C
T. guaymasensis (57)	88°C, pH 7.2	Guaymas basin, Mexico	Chemoorganotrophic anaerobe
T. celer (378)	88°C, pH 5.8, 4% NaCl	Shallow marine solfataric field, Vulcano, Italy	Obligate heterotrophic anaerobe; grows on peptide substrates by S^0 respiration or by fermentation; NaCl required
T. acidaminovorans (84)	85°C, pH 9.0, 1–4% NaCl	Shallow MHTV, Italy	Obligate heterotroph; grows on amino acids as sole carbon and energy source; S^0 stimulates growth
T. chitonophagus (151)	85°C, pH 6.7, 2% NaCl	Deep-sea MHTV, Guaymas, Mexico	Obligate heterotrophic anaerobe; grows on chitin, YE, and meat extract; produces H_2 (H_2S in the presence of S^0), CO_2, NH_3, acetate, and formate
T. barossii (89)	82.5°C, pH 6.5–7.5, 1–4% NaCl	Juan de Fuca Ridge	Obligate heterotrophic anaerobe, grows on peptides; S^0 required for growth

Continued on following page

TABLE 1—*Continued*

Organism (references)	Growth conditions	Isolation/habitat	Metabolic properties
T. litoralis (260)	85°C, pH 6.0, 1.8–6.5% NaCl	Marine solfataras, Vulcano and Naples, Italy	Obligate heterotrophic anaerobe; grows in complex peptide substrates; S^0 stimulates growth
T. profundus (186)	80°C, pH 7.5, 2–4% NaCl	MHTV (1,400 m), Mid-Okinawa Trough, Japan	Obligate heterotrophic anaerobe; S^0 dependent; uses complex peptide substrates, starch, pyruvate and maltose
T. stetteri (249)	75°C, pH 6.5, 2.5% NaCl	Marine solfararic fields, Northern Kurils	Strict anaerobe, S^0 dependent; uses complex peptide substrates, starch, and pectin; production of CO_2, acetate, isobutyrate, isovalerate, and H_2S
T. hydrothermalis[b] (117)	85°C, pH 6.0 2–4% NaCl	Deep-sea MHTV, East Pacific Rise	Obligate heterotrophic anaerobe; grows on proteolysis products, AA mix, and maltose in the presence of S^0
Pyrococcus furiosus[b] (102)	100°C, pH 7.0, 2% NaCl	Marine solfataric fields, Vulcano, Italy	Obligate heterotrophic anaerobe; grows on peptide substrates and carbohydrates; S^0 stimulates growth, probably by detoxifying H_2 (forming H_2S)
P. woesei (379)	100–103°C, pH 6.0–6.5, 3% NaCl	Marine solfataras, Vulcano, Italy	Obligate heterotrophic anaerobe (YE, peptides, PS); S^0 respiration, no fermentation
P. abyssi (95)	96°C, pH 6.8, 3% NaCl	Deep-sea MHTV, North Fiji Basin	Obligate chemoorganotroph, fermenting peptide substrates; Produces CO_2, H_2, acetate, propionate, isovalerate, and isobutyrate; produces H_2S in the presence of S^0; facultative barophilic; NaCl required
P. horikoshii[a] (119)	98°C, pH 7.0, 2.4% NaCl	Okinawa Trough, western Pacific	Obligate heterotrophic anaerobe; Trp auxotroph
Archaeoglobales			
Archaeoglobus fulgidus[a] (316)	83°C, pH 5.5–7.5	Heated sea floor, Vulcano, Italy	Strict anaerobe; chemolithoautotroph in the presence of H_2, CO_2, and $S_2O_3^{2-}$; heterotrophic growth on formate, formamide, lactate, glucose, starch, and peptide substrates; produces traces of methane
A. profundus (49)	82°C, pH 4.5–7.5, 0.9–3.6% NaCl	Deep-sea MHTV, Guaymas, Mexico	Strict anaerobe, mixotroph, requires H_2 for growth; uses organic acids, YE, peptide substrates as carbon sources; electron acceptors include sulfate, $S_2O_3^{2-}$, and sulfite
Methanococales			
Methanococcus jannaschii[a] (167)	85°C, pH 6.0, 2–3% NaCl	Deep-sea MHTV (2,600 m), East Pacific Rise	Autotrophic anaerobe, methanogen; NaCl and sulfide required for growth
M. vulcanius (165)	80°C, pH 6.5, 2.5% NaCl	East Pacific Rise	Anaerobe, methanogen; growth stimulated by YE, selenate, and tungstate; reduces S^0 in the presence of CO_2 and H_2
M. fervens (165)	85°C, pH 6.5, 3% NaCl	Guaymas Basin, Mexico	Anaerobe, methanogen; growth stimulated by YE, selenate, and tungstate, Casamino Acids, and trypticase
M. igneus (48)	88°C, pH 5.7, 1.8% NaCl	Shallow MHTV, Mid-Atlantic Ridge, north off Iceland	Anaerobe, methanogen, obligate chemolitho-autotroph; S^0 inhibits growth
M. infernus (166)	85°C, pH 6.5, 2.5% salt	Deep-sea MHTV, Mid-Atlantic Ridge	Chemolithotroph, obligate anaerobe, methanogen, reduces S^0; YE stimulates growth
Methanobacteriales			
Methanothermus fervidus (323)	83°C, pH 6.5	Icelandic hot spring	Anaerobe, methanogen; requires YE to grow in artificial medium
M. sociabilis (292)	88°C, pH 6.5	Continental solfatara fields, Iceland	Anaerobic S-independent autotroph; methanogen
Methanopyrales			
Methanopyrus kandleri (149)	98°C, pH 6.5, 1.5% NaCl	Deep-sea MHTV, Guaymas, Mexico	Strict anaerobe chemolithoautotroph; methanogen

[a] Fully sequenced genomes.
[b] Genome sequencing in progress
[c] Abbreviations: MHTV, marine hydrothermal vent; YE, yeast extract; AA, amino acid.

thermostability from intracellular factors such as salts, high protein concentrations, coenzymes, substrates, activators, or general stabilizers such as thermamine.

Arrhenius plots for hyperthermophilic and mesophilic enzymes are typically linear (20, 29, 62), suggesting that mesophilic and hyperthermophilic enzyme functional conformations remain unchanged throughout their respective temperature ranges. If enzyme structures changed in a catalytically signifi-

TABLE 2. Examples of hyperthermophile genes cloned by complementation or by activity screening at high temperature

Source	Gene	Cloning method[a]	Promoter	Reference
Thermotoga maritima	Endoxylanase	AS	Vector plac promoter	60
	β-Fructosidase	AS	Not known	217
	α-Galactosidase	AS	Not known	219
	β-Galactosidase	AS	Lambda p_L promoter	111
	β-Glucosidase	AS	Not known	111
	GDH	C	Not known (own promoter present)	193
	Maltosyltransferase	AS	Own promoter	243
Thermotoga neapolitana	Adenylate kinase	C	Own promoter	UD[b]
Pyrococcus furiosus	Methionine aminopeptidase	AS	Not known	341
	Ornithine carbamoyltransferase	C	Vector Tac promoter	282
	Amylopullulanase	AS	*E. coli*-like promoter	86
	α-Amylase	AS	*E. coli*-like promoter	85
	Pyrrolidone carboxyl peptidase	AS	Not known	342
	Esterase	AS	Not known	157
	Endoglucanase	AS	Not known	20
Pyrococcus woesei	Pullulanase	AS	Not known	283
Sulfolobus acidocaldarius	Aspartate carbamoyltransferase	C	Not known	90

[a] AS, activity screening; C, complementation.
[b] UD, A. Savchenko, H. H. Hyun, C. Vieille, and J. G. Zeikus, unpublished data.

cant manner with increasing temperature, one would expect to find (i) nonlinear Arrhenius plots for most enzymes and (ii) different types of plots for different enzyme classes. Biphasic Arrhenius plots reported for a number of hyperthermophilic enzymes (58, 98, 101, 133, 366) represent an important exception to the typical Arrhenius-like behavior. Biphasic Arrhenius plots can often be correlated with functionally significant conformational changes, detected by spectroscopic methods (101, 133, 222). Although not much information is typically available on the effect of temperature on the activity of mesophilic enzymes, a few examples exist of mesophilic enzymes showing bent Arrhenius plots (110), suggesting that such discontinuities are not a specific trait of hyperthermophilic enzymes.

Hyperthermophilic Proteins Are Highly Similar to Their Mesophilic Homologues

With the exception of phylogenetic variations, what differentiates hyperthermophilic and mesophilic enzymes is only the temperature ranges in which they are stable and active. Otherwise, hyperthermophilic and mesophilic enzymes are highly similar: (i) the sequences of homologous hyperthermophilic and mesophilic proteins are typically 40 to 85% similar (79, 350); (ii) their three-dimensional structures are superposable (16, 63, 143, 160, 227, 284, 327); and (iii) they have the same catalytic mechanisms (22, 350, 386).

Cloning and Expression of Genes from Hyperthermophiles in Mesophiles

More than 100 genes from hyperthermophiles have been cloned and expressed in mesophiles. Most of this work has been done in the last 5 years. Only a small fraction of them have been isolated by direct expression and activity screening (i.e., by complementation of growth or activity assay) of a genomic library in *Escherichia coli* (Table 2). Most other genes from hyperthermophiles have been isolated by hybridization or have been directly cloned after PCR amplification. Since archaeal transcription systems (including promoter sequences) are more closely related to eucaryal than to bacterial systems, it is not surprising that most archaeal genes are expressed in *E. coli* only when they are cloned under the control of strong promoters (plac, ptac, or T7 RNA polymerase promoter). Pyrococcal intergenic regions are particularly AT- rich, and *E. coli* consensus promoter-like sequences can be found that explain why some *P. furiosus* genes are directly expressed in *E. coli* (85, 86, 343). Another difficulty encountered in expressing archaeal genes in *E. coli* can be low expression due to a significantly different codon usage in the expressed gene. This difficulty is often alleviated by the expression in *E. coli* of rare tRNA genes together with the target gene (344). A few genes from hyperthermophilic archaea have been successfully expressed in yeast systems (77). They are able to complement yeast mutations (90, 275, 282).

When the properties of the native and recombinant hyperthermophilic enzymes are compared, the majority of hyperthermophilic enzymes expressed in *E. coli* retain all of the native enzyme's biochemical properties, including proper folding (121), thermostability, and optimal activity at high temperatures (8, 14, 115, 338, 350). Thus, while a few proteins from hyperthermophiles might require extrinsic factors (e.g., salts or polyamines), or posttranslational modifications (e.g., glycosylation) to be fully thermostable, most proteins from hyperthermophiles are intrinsically thermostable, and they can fold properly even at temperatures 60°C below their physiological conditions. The fact that most hyperthermophilic enzymes are properly expressed and folded in *E. coli* has greatly facilitated their study, since they can be purified from *E. coli* rather than from an often hard-to-grow hyperthermophilic organism. Additional indirect evidence for the correct folding of recombinant hyperthermophilic proteins is the fact that crystal structures of recombinant hyperthermophilic proteins are typically similar to that of their mesophilic homologues (160, 183, 227, 284, 327, 368). The idea that recombinant and native hyperthermophilic protein structures are identical has become so widely accepted that in some studies both the native and re-

combinant enzymes are used indifferently in crystallization studies (5).

It is unclear whether all hyperthermophilic proteins can be expressed in a mesophilic environment, since unsuccessful experiments are typically not reported. So far, fewer than 10% of all the hyperthermophilic enzymes expressed in *E. coli* have been reported to have stability, catalytic, or structural properties different from those of the enzyme purified from the native organism (51, 239). The recombinant *P. furiosus* ornithine carbamoyltransferase was as stable as the native enzyme when it was expressed in *Saccharomyces cerevisiae* but was less stable when expressed in *E. coli*. When expressed in *E. coli*, the *Sulfolobus solfataricus* 5′-methylthioadenosine phosphorylase (a hexameric enzyme containing six intersubunit disulfide bridges) forms incorrect disulfide bridges and is less stable and less thermophilic than the native enzyme (51). The recombinant *P. furiosus* glutamate dehydrogenase (GDH) is a partially active hexamer that can be fully activated upon incubation at 90°C but remains less stable than the native *P. furiosus* GDH (202). Such hyperthermophilic enzymes might require post-translational modifications (e.g., glycosylation) or specific chaperones to reach their fully functional and stable folded state.

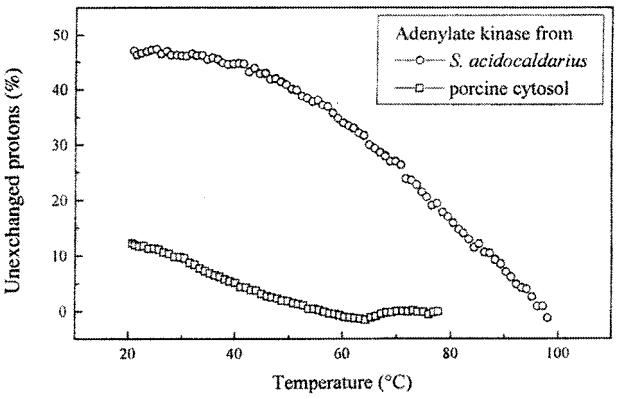

FIG. 1. Hydrogen-deuterium exchange recorded in *S. acidocaldarius* and porcine muscle cytosol adenylate kinases during a temperature gradient experiment. Fractions of unexchanged protons as a function of temperature were calculated from the normalized amide II intensities at 1,546 cm^{-1} (*S. acidocaldarius* enzyme) and 1,542 cm^{-1} (porcine enzyme). The exchange was completed at 56 and 97°C for the porcine and *S. acidocaldarius* enzymes, respectively. Reprinted from reference 35 with permission of the publisher. (Note that the two enzymes are not directly comparable because the pig enzyme is a monomer whereas the *Sulfolobus* enzyme is a trimer.)

Rigidity and Thermostability

A current working hypothesis is that hyperthermophilic enzymes are more rigid than their mesophilic homologues at mesophilic temperatures and that rigidity is a prerequisite for high protein thermostability. This hypothesis is supported by a growing body of experimental data that includes frequency domain fluorometry and anisotropy decay (229), hydrogen-deuterium exchange (35, 164, 370), and tryptophan phosphorescence (114) experiments. Figure 1 illustrates one of the hydrogen-deuterium exchange experiments. At 20°C a much smaller fraction of the amide protons in *Sulfolobus acidocaldarius* adenylate kinase (53%) are exchanged than in the porcine cytosolic enzyme (83%), indicating that considerable more amide protons are involved in stable hydrogen bonds in the thermophilic enzyme. Temperatures of 80 to 90°C are needed before *S. acidocaldarius* adenylate kinase can show an exchange level comparable to that of the catalytically active mesophilic enzyme (35). In protein structure determination, atomic temperature factors provide an adequate representation of local flexibility. In a 1987 study, Vihinen (351) calculated protein flexibility indexes for mesophilic and thermophilic proteins, starting from normalized atomic temperature factors. His results showed that flexibility decreased as thermostability increased. This study needs to be updated since Vihinen's sample was small and did not include data on hyperthermophilic proteins. A computer simulation showed that a mesophilic rubredoxin was more flexible, on the picosecond timescale, than its *P. furiosus* homologue at room temperature (201).

While most flexibility comparisons in mesophilic and hyperthermophilic proteins have reached the same conclusion that hyperthermophiliic proteins are more rigid enzymes, one recent study (134) does not support this conclusion. Using amide hydrogen exchange data, Hernández et al. show that (i) all the hydrogen bonding involving the amide hydrogens of *P. furiosus* rubredoxin are disrupted in less than 1 s at temperatures close to *P. furiosus* rubredoxin's temperature of maximal thermodynamic stability; (ii) conformational opening for solvent access takes place in the millisecond range for the entire protein; and (iii) at alkaline pHs, the maximum enthalpy contributed by hydrogen-bonded amides accounts for less than 5% of the total activation enthalpy normally associated with protein unfolding. These results suggest that the most stable protein characterized so far shows a degree of conformational flexibility comparable to that of mesophilic proteins.

Lazaridis et al. (201) argue that there is no single measure of flexibility (a protein can be rigid on a nanosecond scale but flexible on a millisecond scale) and that there is no fundamental reason for stability and rigidity to be correlated. Flexibility implies increased conformational entropy of the folded state, and it should therefore be favorable to thermodynamic stability. More studies on hyperthermophilic enzyme flexibility at various temperatures are needed before we can get a better understanding of the role of conformational rigidity in protein stability.

It has also been proposed that excessive rigidity explains why hyperthermophilic enzymes are often inactive at low temperatures (i.e., around 20 to 37°C). One set of evidence that tends to support this hypothesis is that denaturants (e.g., guanidinium hydrochloride and urea) (23, 195, 364), detergents (e.g., Triton X-100 and sodium dodecyl sulfate) (82, 283, 290), and solvents (78, 195) often activate hyperthermophilic enzymes at suboptimal temperatures. This activation tends to disappear as the temperature gets closer to the enzyme's temperature of maximal activity (T_{opt}) (23). At that temperature, the enzyme is flexible enough in the absence of a denaturant to show full activity. Recent findings that show increasing levels of hydrogen tunneling with in-

TABLE 3. Comparison of the ΔG_{stab}-versus-T curves for some mesophile, thermophile, and hyperthermophile proteins

Thermophilic/mesophilic source (reference)	Protein	Characteristics of $_{\Delta}G$-vs-T curve for thermophilic enzyme, ΔG^a (kcal/mol)
Thermus thermophilus/*E. coli* (142)	RNase H	ΔG-vs-T curve shifted toward higher ΔGs and flattened
Bacillus stearothermophilus/yeast (79)	PGK	ΔG-vs-T curve probably shifted toward higher ΔGs $\Delta\Delta G^b$ = 5 kcal/mol at 20°C
T. thermophilus/yeast (265)	PGK	ΔG-vs-T curve shifted toward higher ΔGs and flattened (smaller ΔCp) *T. thermophilus*: ΔG = 6.32 kcal/mol at 25°C; yeast: ΔG = 3.63 kcal/mol at 25°C
T. thermophilus/horse (264)	Cytochrome *c*-552	ΔG-vs-T curve shifted toward higher ΔGs and higher temperatures *T. thermophilus*: ΔG = 28.5 kcal/mol at 25°C; horse: ΔG = 12.7 kcal/mol at 25°C
Sulfolobus acidocaldarius/assortment of mesophilic proteins (241)	Sac7d DNA binding protein	ΔG-vs-T curve flattened
T. maritima/*E. coli* (76)	Dihydrofolate reductase	ΔG-vs-T curve shifted toward higher ΔGs and higher temperatures
T. maritima/yeast (121)	PGK	ΔG-vs-T curve shifted toward higher ΔGs *T. maritima*: $\Delta G_{max}{}^c$ = 28.7 kcal/mol at 30°C; yeast: ΔG_{max} = 6.0 kcal/mol at 30°C
T. maritima/bovine adrenal cortex (274)	Ferredoxin	ΔG-vs-T curve shifted toward higher ΔGs and higher temperatures *T. maritima*: ΔG_{max} = 9.3 kcal/mol at 45°C; bovine: ΔG_{max} = 4.8 kcal/mol at 25°C
P. furiosus and *M. fervidus* (a and b)/*M. formicicum* (216)	Histone	ΔG-vs-T curve shifted toward higher ΔGs and higher temperatures *P. furiosus*: ΔG_{max} = 17.2 kcal/mol at 44°C (T_m = 114°C); *M. fervidus* a: ΔG_{max} = 15.5 kcal/mol at 35°C (T_m = 104°C), *M. fervidus* b: ΔG_{max} = 14.6 kcal/mol at 40°C (T_m = 113°C), *M. formicicum*: ΔG_{max} = 7.2 kcal/mol at 32°C (T_m = 75°C)
P. furiosus/mesophilic proteins in general (141)	Rubredoxin	ΔG-vs-T curve shifted toward higher ΔGs and higher temperatures ΔG_{max} = 18 kcal/mol at 65°C (T_m = 176–195°C)
S. solfataricus/pig (14)	Aspartate aminotransferase	ΔG-vs-T curve flattened (smaller ΔC_p) and probably shifted toward higher ΔGs *S. solfataricus*: ΔG = 16.8 kcal/mol at 25°C; pig: ΔG = 13.8 kcal/mol at 25°C

[a] ΔG, ΔG_{stab}.
[b] $\Delta\Delta G$, difference in ΔG_{stab} between the thermophilic and mesophilic enzymes.
[c] ΔG_{max}, maximal ΔG_{stab}.

creasing temperature in a thermophilic alcohol dehydrogenase provide additional evidence for the role of thermally induced protein motions in modulating enzyme activity (190). A few hyperthermophilic enzymes have been characterized that are more active than their mesophilic counterparts, even at 37°C (156, 246, 315). Since they are thermostable, these enzymes are expected to be quite rigid at mesophilic temperatures. Their high catalytic activity at mesophilic temperatures suggests that these enzymes combine local flexibility in their active site (which is responsible for their activity at low temperatures) with high overall rigidity (which is responsible for their thermostability). The existence of such enzymes (and of highly stable, engineered mesophilic enzymes [116, 374]) also suggests that thermostability is not incompatible with high activity at moderate temperatures. Hyperthermophiles probably only need enzymes with activities at their optimal temperatures comparable to that of their mesophilic homologues. While there is probably no evolutionary pressure for an organism to have more efficient enzymes, this does not mean that more efficient thermostable enzymes cannot be engineered in the laboratory.

Thermophilic and Hyperthermophilic Proteins and Free Energy of Stabilization

The free energy of stabilization (ΔG_{stab}, where $\Delta G_{stab} = \Delta H_{stab} - T\Delta S_{stab}$) of a protein is the difference between the free energies of the folded and the unfolded states of that protein. It directly measures the thermodynamic stability of the folded protein. ΔH_{stab} (the stabilization enthalpy) and ΔS_{stab} (the stabilization entropy) are large numbers that vary almost linearly with temperature in the temperature range of the activities of most enzymes. Also a function of temperature, ΔG_{stab} is usually small (83, 162) (Table 3). The ΔG_{stab} of globular mesophilic proteins is typically between 5 and 15 kcal/mol at 25°C (Table 3). Not many proteins have been studied to determine the free energies of stabilization. Such studies are hindered by the fact that the thermal denaturation of most proteins is irreversible: complete denaturation is often almost immediately followed by aggregation and precipitation (see below). Thus, most ΔG_{stab} data are for small monomeric proteins (277) (Table 3). ΔG_{stab} calculations are made even more difficult for hyperthermophilic proteins, since their de-

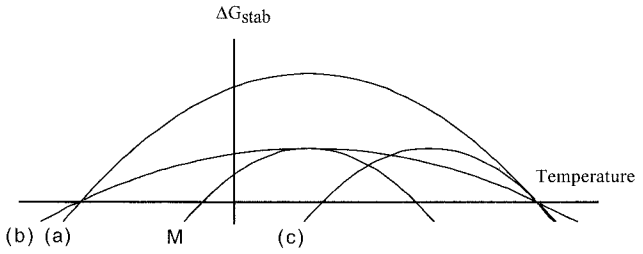

FIG. 2. Comparison of theoretical ΔG_{stab}-versus-T curves for mesophilic and hyperthermophilic proteins. M, theoretical ΔG_{stab}-versus-T curve for a mesophilic protein. (a), (b), and (c), theoretical ΔG_{stab}-versus-T curves for a hyperthermophilic protein. In curve (a), the hyperthermophilic protein has the same temperature of maximal stability (T_s) as the mesophilic protein, and the ΔG_{stab}-versus-T curve of the hyperthermophilic protein is shifted upward to higher ΔG_{stab} values. In curve (b), hyperthermophilic and mesophilic protein have same T_s values and the same ΔG_{stab} values at T_s. The ΔG_{stab}-versus-T curve of the hyperthermophilic protein is flatter. In curve (c), hyperthermophilic and mesophilic proteins have different T_s values but have the same ΔG_{stab} at their respective T_s. The ΔG_{stab}-versus-T curve of the hyperthermophilic protein is shifted toward higher temperatures.

naturation transitions take place outside the temperature range of most calorimeters (141, 274). To overcome this difficulty, most thermodynamic studies of hyperthermophilic protein stability are performed in the presence of guanidinium hydrochloride (168) or at pHs outside the physiological conditions (241). These various conditions allow the temperature of the denaturation transition to become accessible to physical measurement, and in some cases they allow the enzyme to unfold reversibly. In one case, the stability parameters of a hyperthermophilic protein were determined under native conditions using hydrogen exchange to measure the reversible cycling between the native and unfolded proteins (141). Table 3 shows that in most cases the difference in ΔG_{stab} values of hyperthermophilic and mesophilic proteins is small, usually in the range of 5 to 20 kcal/mol. Stability studies of enzyme mutants (173, 261), showing that differences in ΔG_{stab} as small as 3 to 6.5 kcal/mol can account for thermostability increases of up to 12°C, are in complete agreement with the stability data listed in Table 3.

As a consequence of the enthalpic and/or entropic stabilizations occurring in a hyperthermophilic protein, the ΔG_{stab}-versus-T curve of this protein will be different from that of its mesophilic counterpart. Figure 2 illustrates the three theoretical ways by which increased protein thermodynamic stability can be achieved (265): (a) the ΔG_{stab}-versus-T curve of a hyperthermophilic protein can be shifted toward higher ΔG_{stab} values, (b) it can be shifted toward higher temperatures, or (c) it can be flattened (due to a smaller difference in partial molar heat capacity between the protein's folded and unfolded states [ΔC_p]). As seen in Table 3, a majority of thermophilic and hyperthermophilic proteins use various combinations of these three mechanisms to reach their superior thermodynamic stabilities. For example, the ΔG_{stab}-versus-T curve of the *P. furiosus* histone is shifted by approximately 12°C toward higher temperatures and by 10 kcal/mol toward higher ΔG_{stab} values, compared to the ΔG_{stab}-versus-T curve of the *Methanobacterium formicicum* histone. The most common stabilization mechanism among both thermophilic and hyperthermophilic proteins is the shift of their ΔG_{stab}-versus-T curves toward higher ΔG_{stab} values.

MECHANISMS OF PROTEIN INACTIVATION

Unfolding, Formation of Scrambled Structures, and Aggregation

Native, active proteins are held together by a delicate balance of noncovalent forces (e.g., H bonds, ion pairs, and hydrophobic and Van der Waals interactions). When high temperatures disrupt these noncovalent interactions, proteins unfold. Protein unfolding can be observed by different techniques, including differential scanning calorimetry, fluorescence, circular dichroism spectroscopy, viscosity, and migration patterns. The T_m, as determined by calorimetry and spectroscopic techniques, is typically the same (216). Numerous studies have shown that inactivation becomes significant only a few degrees below the T_m. In most cases, the loss of secondary and tertiary structures is concomitant with enzyme inactivation at high temperature. Small monomeric proteins commonly unfold via a two-state transition (i.e., unfolding intermediates are barely detectable or not detectable). Some proteins might regain their native, active conformation upon cooling. This unfolding is called thermodynamically reversible unfolding, and the thermodynamic parameters describing the folded and unfolded states can be determined (it is most easily done using calorimetry data) (17, 277).

Most mesophilic proteins, however, unfold irreversibly. They unfold into inactive but kinetically stable structures (scrambled structures), and they often form aggregates (intermolecular mechanism). During aggregation, the hydrophobic residues that are normally buried in the native protein become exposed to the solvent and interact with hydrophobic residues from other unfolding protein molecules to minimize their exposure to the solvent (354). Such irreversible unfolding usually follows the general model proposed by Tomazic and Klibanov (334):

$$\underset{\text{(active)}}{\text{native enzyme}} \rightleftharpoons \underset{\text{(inactive)}}{\text{nonnative enzyme}} \rightarrow \underset{\text{(often precipitate)}}{\text{scrambled structures}}$$

This model is consistent with an intramolecular rate-determining step in thermal inactivation. The natural logarithm of the residual activity is a linear function of the inactivation time:

$$\ln(\text{residual activity}) = -kt$$

where k is the inactivation rate and t is the inactivation time. In this model, the inactivation rate constant is independent of the initial protein concentrations.

Hyperthermophilic proteins that denature reversibly are probably as rare as reversibly denaturing mesophilic proteins. High E_a values for inactivation of hyperthermophilic enzymes (above 100 kcal/mol) suggest that the limiting step in their inactivation is still unfolding (55, 268, 352). These different observations suggest that chemical modifications (e.g., deamidation, cysteine oxidation, and peptide bond hydrolysis) take place only once the protein is unfolded. Accelerated at elevated temperatures, chemical modifications are another process that make denaturation irreversible.

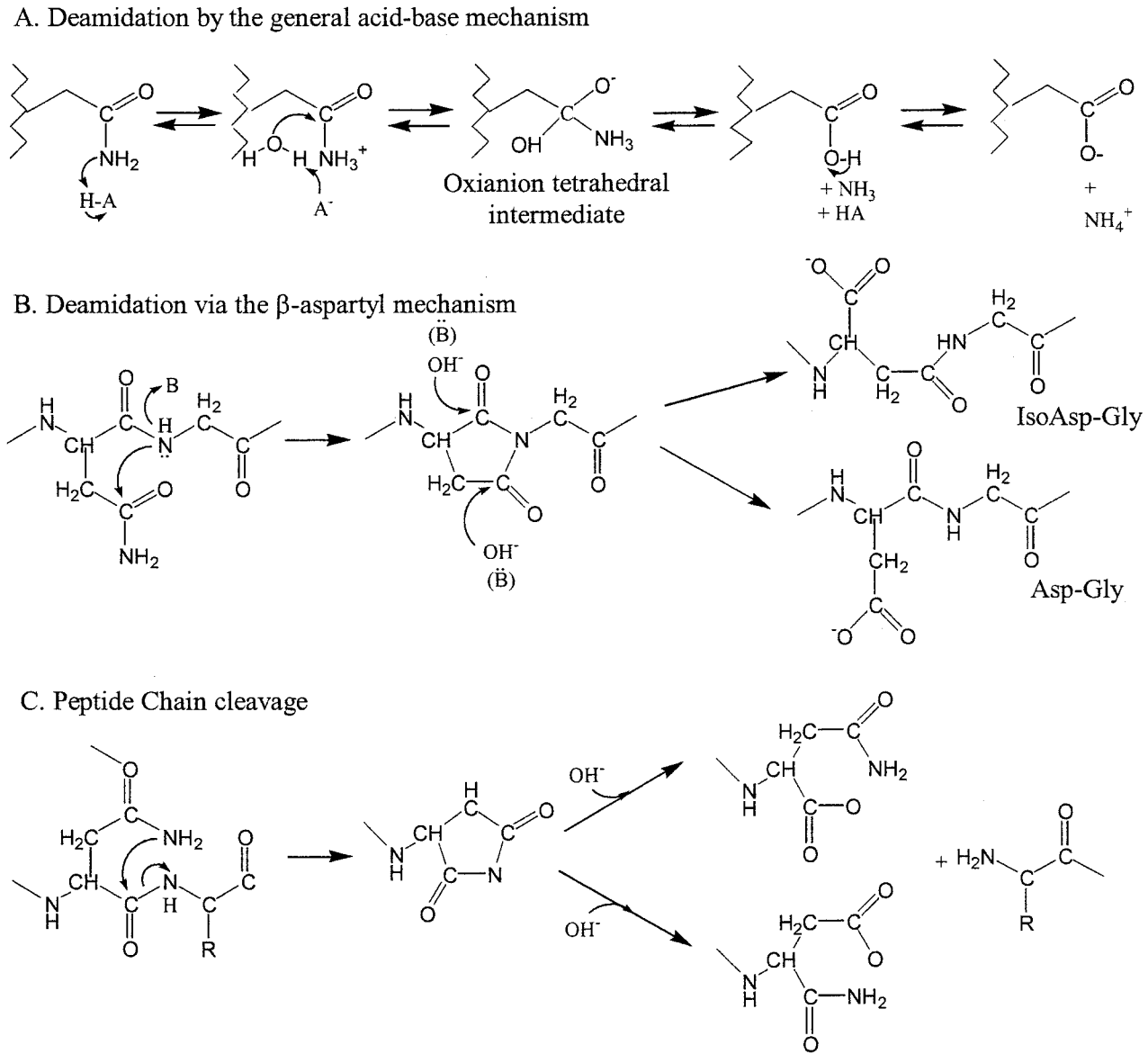

FIG. 3. Mechanisms of protein degradation involving Asn residues.

Covalent Mechanisms

While there have been numerous studies of mesophilic enzymes affected by deamidation in vivo (reference 367 and references therein), it is still unclear whether some hyperthermophilic proteins are inactivated via covalent mechanisms. Studies performed with a few enzymes (e.g., hen egg white lysozyme, RNase A, and *Bacillus* α-amylases) at temperatures neighboring or even above their melting temperatures clearly showed that elevated temperatures trigger chemical modifications that irreversibly inactivate reversibly denatured proteins (6, 334, 335, 369).

Deamidation. Two deamidation mechanisms are known for Asn and Gln residues (367), but it not often known which mechanism is responsible for an enzyme deamidation. In the general acid-base mechanism, a general acid (HA) protonates the Asn (or Gln) amido (—NH) group. A general base (A^- or OH^-) attacks the carbonyl carbon of the amido group or activates another nucleophile (Fig. 3). The transition state is supposed to be an oxyanion tetrahedral intermediate. The order of the acid and base attacks varies with pH. In the β-aspartyl shift mechanism, the Asn side chain amide group is attacked by the $n + 1$ peptide nitrogen (acting as a nucleophile). The succinimide intermediate then breaks down to yield an α-linked (Asp) or β-linked (isoAsp) residue, typically in the ratio 1:3 (Fig. 3). In this mechanism, Gly, Ser, and Ala are favored in $n + 1$ because their small side chains do not obstruct the cyclization into the succinimide intermediate. In both deamidation mechanisms, conformation and rigidity seem to be instrumental in limiting the extent of deamidation. Conformation probably also explains the approximately 10-fold-higher propensity of Asn to deamidate than Gln.

An RNase Asn residue located in a β-turn, with its side

chain mobile in the solvent, was shown to be much more susceptible to deamidation once the enzyme was unfolded (362). In one of the only studies of hyperthermophilic protein chemical degradations, *Methanothermus fervidus* and *Pyrococcus woesei* glyceraldehyde 3-phosphate dehydrogenases (GAPDHs) were shown to inactivate significantly faster than they deamidated (132), indicating that deamidation was not a major inactivation mechanism. Once unfolded, the *P. woesei* GAPDH deamidated at a much higher rate than the native enzyme did. Zale and Klibanov (369) showed that deamidation rates were similar in a few selected enzymes and suggested that deamidation was not affected by local structure. Their studies, however, were always performed under conditions in which the enzyme would be mostly unfolded; thus, their results cannot be interpreted in terms of the role of local conformation in a residue's susceptibility to deamidation. Indirect evidence for the role of conformation and rigidity in controlling the rate of deamidation is found in the existence of hyperthermophilic proteins that are functional and stable up to 120°C. In these proteins, noncovalent structural interactions are strong enough to protect the Asn residues from deamidation. Deamidation can take place in native enzymes (reference 367 and references therein), however, but all examples are of mesophilic proteins. It is not clear if deamidation is a major inactivation process for hyperthermophilic proteins.

Hydrolysis of peptide bonds. Hydrolysis of peptide bonds happens most often at the C-terminal side of Asp residues, with the Asp-Pro bond being the most labile of all (354). Two factors seem to be responsible for this lability. The proline nitrogen is more basic than that of other residues, and Asp has an increased propensity for α-β isomerization when linked on the N side of a proline. Peptide chain cleavage can also occur at Asn-Xaa linkages in a β-aspartyl shift-like mechanism (367). In this reaction the Asn amido (—NH_2) group acts as the nucleophile, attacking its own main-chain carboxyl carbon (Fig. 3) (132). Such cleavage occurs in five positions in the *M. fervidus* GAPDH when conditions favor unfolding (i.e., temperatures above 85°C and low salt concentrations). Less susceptible to hydrolysis, the more thermostable *P. woesei* GAPDH contains substitutions in three of these cleavage positions. Cleavage at the two remaining Asn-Xaa locations is probably inhibited by the higher conformational rigidity of the *P. woesei* enzyme.

β-Elimination of disulfide bridges. Destruction of disulfide bridges under alkaline conditions is known to occur via a β-elimination reaction, yielding dehydroalanine and thiocysteine. Dehydroalanine then reacts with nucleophilic groups—especially the ε-amino group of lysine—to form lysinoalanine. The fate of thiocysteine is not completely understood (354). The β-elimination reaction produces free thiols that can catalyze disulfide interchange and further inactivate the enzyme (369).

Cysteine oxidation. Cysteines are the most reactive amino acids in proteins. Their autooxidation, usually catalyzed by metal cations (especially copper), leads to the formation of intramolecular and intermolecular disulfide bridges or to the formation of sulfenic acid (354). Cysteines can also catalyze disulfide interchange, causing disulfide bond reshuffling as well as important structural variations. The recombinant *S. solfataricus* 5′-methylthioadenosine phosphorylase forms incorrect intersubunit disulfide bridges that make it less stable and less thermophilic than the native enzyme (51).

Other reactions. Aside from the above commonly observed degradative reactions, other, less frequent chemical inactivation mechanisms have been identified (354). Methionine can be oxidized to its sulfoxide counterpart, and some residues (Asp and Ser, in particular) can be racemized to their D-form. Lysine can react with reducing sugars via the Maillard reaction (279). Last, thermolysin-like neutral proteases are susceptible to autolysis. Local unfolding of one of their surface loops determines their inactivation by autolysis (93).

MECHANISMS OF PROTEIN THERMOSTABILIZATION

The hydrophobic effect is considered to be the major driving force of protein folding (83). Hydrophobicity drives the protein to a collapsed structure from which the native structure is defined by the contribution of all types of forces (e.g., H bonds, ion pairs, and Van der Waals interactions). Dill (83) reviewed the evidences supporting this theory: (i) nonpolar solvents denature proteins; (ii) hydrophobic residues are typically sequestered into a core, where they largely avoid contact with water; (iii) residues and hydrophobicity in the protein core are more strongly conserved and related to structure than any other type of residue (replacements of core hydrophobic residues are generally more disruptive than other types of substitutions); and (iv) protein unfolding involves a large increase in heat capacity. Given the central role of the hydrophobic effect in protein folding, it was easy to assume that the hydrophobic effect is also the major force responsible for protein stability. The sequencing, structure, and mutagenesis information accumulated in the last 20 years confirm that hydrophobicity is, indeed, a main force in protein stability. Two observations suggest that mesophilic and hyperthermophilic homologues have a common basic stability afforded by the conserved protein core: (i) hydrophobic interactions and core residues involved in secondary structures are better conserved than surface area features, and (ii) numerous stabilizing substitutions are found in solvent-exposed areas (as observed in mesophilic and hyperthermophilic protein structures comparisons and in protein directed-evolution experiments, see below). The high level of similarity encountered in the core of mesophilic and hyperthermophilic protein homologues suggests that even mesophilic proteins are packed almost as efficiently as possible and that there is not much room left for stabilization inside the protein core. Stabilizing interactions in hyperthermophilic proteins are often found in the less conserved areas of the protein. As illustrated below, factors such as surface ion pairs, decrease in solvent-exposed hydrophobic surface, and anchoring of "loose ends" (i.e., the N and C termini and loops) to the protein surface seem to be instrumental in hyperthermophilic protein thermostability.

Enough experimental evidence (e.g., sequence, mutagenesis, structure, and thermodynamics) has been accumulated on hyperthermophilic proteins in recent years to conclude that no single mechanism is responsible for the remarkable stability of hyperthermophilic proteins. Increased thermostability must be found, instead, in a small number of highly specific mutations that often do not obey any obvious traffic rules.

TABLE 4. Relative amino acid compositions of mesophilic and hyperthermophilic proteins[a]

Residue(s)	Amino acid composition (%) of:		Variation of composition in hyperthermophilic relative to mesophilic proteins
	Mesophilic proteins[b]	Hyperthermophilic proteins[c]	
A	8.09 ± 1.54	6.82 ± 1.42	−1.27
C	1.10 ± 0.18	0.86 ± 0.27	−0.24
D	5.06 ± 0.18	4.63 ± 0.54	−0.43
E	6.45 ± 0.54	8.55 ± 0.95	+2.10
F	4.61 ± 0.78	4.40 ± 0.82	−0.21
G	6.70 ± 0.96	7.16 ± 0.68	+0.46
H	2.04 ± 0.21	1.57 ± 0.16	−0.47
I	7.40 ± 1.69	7.82 ± 1.64	+0.42
K	6.81 ± 2.00	7.61 ± 2.16	+0.80
L	10.43 ± 0.55	10.21 ± 0.68	−0.22
M	2.42 ± 0.28	2.29 ± 0.25	−0.13
N	4.90 ± 1.20	3.52 ± 0.94	−1.38
P	3.77 ± 0.77	4.36 ± 0.99	+0.59
Q	3.99 ± 0.75	1.78 ± 0.22	−2.21
R	4.33 ± 0.98	5.57 ± 1.16	+1.24
S	6.08 ± 0.57	5.54 ± 1.01	−0.54
T	5.09 ± 0.57	4.34 ± 0.23	−0.75
V	6.35 ± 0.75	8.05 ± 0.68	+1.70
W	1.02 ± 0.31	1.06 ± 0.20	+0.04
Y	3.30 ± 0.43	3.82 ± 0.33	+0.52
A, G	14.79	13.98	−0.81
D, E	11.51	13.18	+1.67
K, R, H	13.18	14.75	+1.57
S, T	11.17	9.88	−1.29
N, Q	8.99	5.3	−3.69
I, L, M, V	26.60	28.37	+1.77
F, W, Y	8.93	9.28	+0.35

[a] Data from references 81, 175, and GenBank.
[b] From the genome sequences of *B. subtilis, Campylobacter jejuni, E. coli, Haemophilus influenzae, Helicobacter pylori, Neisseria meningitidis, Rickettsia prowazekii*, and *Synechocystis*.
[c] From the genome sequences of *A. fulgidus, A. aeolicus, A. pernix, M. jannaschii, P. abyssi, P. horikoshii*, and *T. maritima*.

Amino Acid Composition and Intrinsic Propensity

Protein amino acid composition has long been thought to be correlated to its thermostability. The first statistical analyses comparing amino acid compositions in mesophilic and thermophilic proteins indicated trends toward substitutions such as Gly→Ala and Lys→Arg. A higher alanine content in thermophilic proteins was supposed to reflect the fact that Ala was the best helix-forming residue (10). As more experimental data accumulate (in particular, complete genome sequences), it is becoming obvious that "traffic rules of thermophilic adaptation cannot be defined in terms of significant differences in the amino acid composition" (31). The comparison of residue contents in hyperthermophilic and mesophilic proteins based on the genome sequences of eight mesophilic and seven hyperthermophilic organisms shows only minor trends (Table 4). More charged residues are found in hyperthermophilic proteins (+3.24%) than in mesophilic proteins, mostly at the expense of uncharged polar residues (−4.98%; in particular Gln, −2.21%). Hyperthermophilic proteins also contain slightly more hydrophobic and aromatic residues than mesophilic proteins do. These data obtained from genome sequencing cannot be generalized, since large variations exist among hyperthermophile genomes themselves: the *Aeropyrum pernix* protein pool actually contains fewer charged residues (23.64%), fewer large hydrophobic residues (27.29%), and fewer aromatic residues (7.42%) than do the mesophiles listed in Table 4. Instead, *A. pernix* proteins contain more Ala, Gly, Pro, Ser, and Thr residues. Thus, a bias in a hyperthermophilic protein amino acid composition might often be evolutionarily relevant, rather than an indication of its adaptation to high temperatures. Probably more relevant to thermostability than amino acid composition are the distribution of the residues and their interactions in the protein. The two homologous proteases *Bacillus amyloliquefaciens* subtilisin BPN′ and *Thermoactinomyces vulgaris* thermitase contain the same number of charged residues, but the thermophilic enzyme thermitase contains eight more ion pairs (331).

In relation to the idea that protein stability was determined by the stability and tight packing of its core, the propensity of the individual residues to participate in helical or strand structures was studied as a potential stability mechanism. In their comparison of mesophilic and thermophilic protein structures, Facchiano et al. (99) observed that helices of thermophilic proteins are generally more stable than those of mesophilic proteins. The only trend they detected was a decreasing content in β-branched residues (Val, Ile, and Thr) in the helices of thermophilic proteins (β-branched residues are not as well tolerated in helices as linear residues are) (99). A number of examples exist in which this trend is not followed. The *P. furiosus* and *T. litoralis* GDHs contain a larger number of isoleucines. If Leu and Ile residues are compared, these two residues have the highest (and equivalent) partial specific volumes. In proteins, the Leu side chain is most often found in one of two rotamer conformations ($\chi 1$ of 180° and 300°) but not in the one with $\chi 1 = 60°$. The Ile side chain frequently adopts four different rotamer conformations, and the three $\chi 1$ values are found. With this conformational flexibility, Ile might be better able to fill various voids that can occur during protein core packing (38). Dill (83) also noted that context effects (e.g., salt bridge formation, aromatic interactions, burial of hydrophobic surface, and cavity filling) could be as important as the intrinsic helical propensity. In many cases, secondary structures found in protein structures do not correspond to the secondary structures predicted by intrinsic propensity, suggesting that intrinsic propensity is not enough to account for the stability of α-helices in proteins (83).

Several properties of Arg residues suggest that they would be better adapted to high temperatures than Lys residues: the Arg δ-guanido moiety has a reduced chemical reactivity due to its high pK_a and its resonance stabilization. The δ-guanido moiety provides more surface area for charged interactions than the Lys amino group does. Figure 4 illustrates the ability of Arg to participate in multiple noncovalent interactions. Because the Arg side chain contains one fewer methylene group than Lys, it has the potential to develop less unfavorable contacts with the solvent. Last, because its pK_a (approximately 12) is 1 unit above that of Lys (11.1), Arg more easily maintains ion pairs and a net positive charge at elevated temperatures (pK_a values drop as the temperature increases) (252, 354). The average Arg/Lys ratios in the protein pools of the mesophiles and hyperthermophiles listed in Table 4 (0.73 ± 0.37 and 0.87 ± 0.60, respectively) are associated with large standard deviations. (Among hyperthermophiles, Arg/Lys ratios vary from 0.52 in *Aquifex aeolicus* proteins to 2.19 in *Aeropyrum pernix* proteins.) These results suggest that if an increased Arg

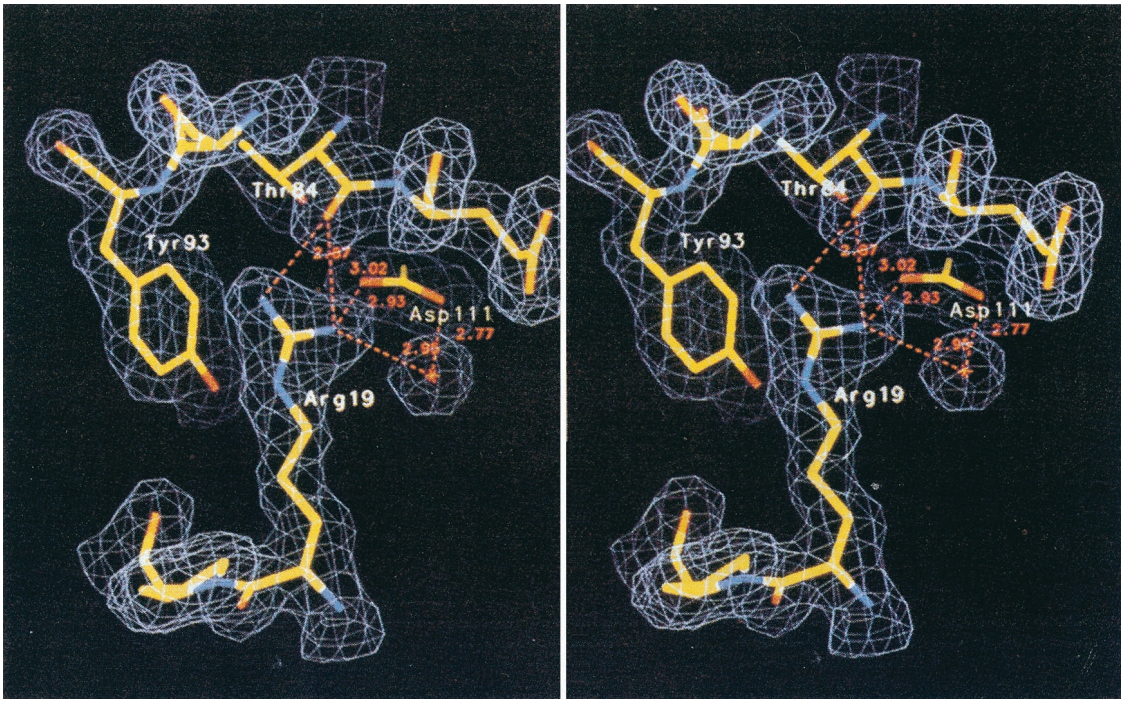

FIG. 4. Stereo view of the ion pair between Arg19 and Asp111 in *S. solfataricus* indole-3-glycerol phosphate synthase. The Arg19 guanidinium group also forms a cation-π interaction with the Tyr93 π system and two H bonds with Thr84. Reprinted from reference 185 with permission of the publisher.

content is indeed stabilizing, this mechanism is not universally used among hyperthermophiles.

An indirect indication that deamidation affects hyperthermophilic proteins (156) is the high activity of *T. maritima* L-isoaspartyl methyltransferase. This enzyme methylates L-isoAsp residues that result from Asn deamidation or from Asp isomerization. Its high activity suggests that it has been adapted for the high load of protein damage that could occur at high temperatures. Resistance to deamidation seems to result from at least three adaptation mechanisms. (i) Some hyperthermophilic enzymes contain less Asn than their mesophilic homologues do. *P. woesei* 3-phosphoglycerate kinase (PGK) contains less Asn than the *Methanobacterium bryantii* enzyme does. In both Asn-Ala and two of the three Asn-Gly sequences present in *M. bryantii* PGK, the Asn residue is substituted in the *P. woesei* enzyme (136). The only conserved Asn-Gly sequence is conserved in all PGKs. It is possible that the four nonconserved sequences would have been susceptible to deamidation at high temperatures and that they have been selected against in the hyperthermophilic PGK. A direct correlation was also shown between the Asn+Gln content in type II D-xylose isomerases and their respective temperatures of maximal activity (ranging from 55 to 95°C) (350). (ii) Other hyperthermophilic enzymes contain as many Asn residues, but these residues are in locations and in conformations in which they are not susceptible to deamidation. The resistance of *P. woesei* GAPDH to deamidation and peptide bond hydrolysis was shown to be related to the enzyme's higher conformational stability (132). *S. solfataricus* 5′-methylthioadenosine phosphorylase is optimally active at 120°C, and its T_m is 132°C. It is not inactivated after 2 h at 100°C (52). It is interesting that it contains twice as many Asn as a related enzyme from *E. coli*, including one Asn in the sequence Asn-Gly, a sequence normally highly susceptible to deamidation.

The Asn and Gln contents listed in Table 4 suggest that hyperthermophilic proteins do not acquire their resistance to deamidation only through a decreased Asn content. Instead, it is curious that the seven hyperthermophiles show the same significant decrease in Gln residues in their proteins.

Cysteine's high sensitivity to oxidation at high temperature suggests that hyperthermophilic enzymes contain fewer cysteines than their mesophilic counterparts do. While Table 4 indicates that hyperthermophilic proteins in average contain fewer cysteines than mesophilic proteins do, large variations exist among species. *Archaeoglobus fulgidus* and *Methanococcus jannaschii* proteins contain more cysteines (1.17 and 1.27%, respectively), in fact, than an average mesophile protein pool does (1.10%). From the seven hyperthermophilic organisms included in Table 4, *A. aeolicus* and *A. pernix* are microaerophilic and aerophilic organisms, respectively, whereas the others are strict anaerobes. Interestingly, *A. aeolicus* and *A. pernix* proteins contain more cysteines (0.79 and 0.93%, respectively) than *Pyrococcus abyssi, P. horikoshii*, and *T. maritima* proteins do (0.55, 0.63, and 0.71%, respectively). One would expect a high selection pressure against the presence of cysteines in proteins from aerobic hyperthermophiles (and the absence of such selection pressure in anaerobic hyperthermophiles). Cysteines that are present in proteins from aerobic hyperthermophiles are often involved in specific stabilizing interactions (e.g., disulfide bridges and metal liganding) and/or are inaccessible to the solvent. Drastic denaturing conditions are required (2 h at 70°C in the presence of 6 M

guanidinium HCl) for 10 mM dithiothreitol to reduce most of the six intersubunit disulfide bridges in native *S. solfataricus* 5′-methylthioadenosine phosphorylase (51). In contrast, the GAPDH from the anaerobe *T. maritima* contains three Cys residues, one of them essential in the active site and two others described by Schultes et al. as "unnecessary" (299).

Disulfide Bridges

Disulfide bridges are believed to stabilize proteins mostly through an entropic effect, by decreasing the entropy of the protein's unfolded state (237). The entropic effect of the disulfide bridge increases in proportion to the logarithm of the number of residues separating the two cysteines bridged.

Because of the susceptibility of cysteines and disulfide bridges to destruction at high temperatures, 100°C was believed to be the upper limit for the stability of proteins containing disulfide bridges (353). This notion was based on the fact that early studies characterizing protein inactivation mechanisms were performed with the only enzymes available at that time: mesophilic enzymes. These studies determined that all proteins studied that contained disulfide bridges had the same rate of β-elimination at 100°C. This rate was independent of the protein structure and was higher at pH 8.0 ($t_{1/2}$ of 1 h) than at pH 6.0 ($t_{1/2}$ of 12.4 h). The limitation of these studies was that at 100°C all the proteins studied were in the unfolded state. The recent characterization of disulfide bridge-containing proteins that are optimally active and stable at temperatures above 100°C suggests that disulfide bridges can be a stabilization strategy above 100°C and that conformational environment and solvent accessibility are determining factors in the protection of disulfide bridges against destruction. When expressed in *E. coli, S. solfataricus* 5′-methylthioadenosine phosphorylase forms incorrect, destabilizing disulfide bridges. This observation indirectly suggests that the disulfide bridges present in the native enzyme are stabilizing (52). An *Aquifex pyrophilus* serine protease was recently described that contains eight cysteines (none are present in subtilisin BPN') (64). A dithiothreitol treatment reduced its $t_{1/2}$ at 85°C from 90 h to less than 2 h. This destabilization by dithiothreitol at high temperature suggests that this enzyme indeed contains disulfide bridges and that they are highly inaccessible. The enzyme's 6-h $t_{1/2}$ at 105°C and pH 9.0, which is much longer than the $t_{1/2}$ calculated for disulfide bridges in unfolded proteins at pH 8.0 (1 h), suggests that this enzyme's disulfide bridges are protected from destruction by their inaccessibility in the protein. Thus, not all disulfide bridges have equal susceptibility to thermal destruction.

Hydrophobic Interactions

As suggested in Table 4 and illustrated in Table 5, hydrophobic interactions are a stabilization mechanism in hyperthermophilic proteins. An average increase in stability of 1.3 (± 0.5) kcal/mol was calculated for each additional methyl group buried in protein folding (269) (based on cavity-creating mutations in which a large aliphatic residue was replaced with a smaller aliphatic residue). Mutations attempting to fill cavities are often less stabilizing when they create unfavorable Van der Waals interactions that need local rearrangements (158). While Table 5 gives crystallographic evidence for the potential role of hydrophobic interactions in thermostability, not much direct, experimental evidence is available to confirm the stabilizing role of hydrophobic interactions in hyperthermophilic proteins. The stability properties of an enzyme chimera constructed between the *Methanococcus voltae* and *M. jannaschii* adenylate kinases indicated that a larger and more hydrophobic enzyme core (which is due to an increase in aliphatic residue content and in aliphatic side chain volume) may be responsible for *M. jannaschii* adenylate kinase's thermostability (124). The 3-isopropylmalate dehydrogenase from the thermophile *Thermus thermophilus* contains intersubunit hydrophobic interactions that do not exist in the *E. coli* enzyme. *Thermus* 3-isopropylmalate dehydrogenase Leu246Glu/Val249Met and *E. coli* Glu256Leu/Met259Val mutant derivatives were constructed that destabilized and stabilized the *Thermus* and *E. coli* enzymes, respectively. Polyacrylamide gel electrophoresis of the mutant and wild-type enzymes in the presence of urea showed that the hydrophobic interactions made the dimer more resistant to dissociation (180).

Aromatic Interactions

Aromatic-aromatic interactions (aromatic pairs) are defined by a distance of less than 7.0 Å between the phenyl ring centroids. The following characteristics of aromatic pairs were extracted from the analysis of 272 aromatic pairs in 34 high-resolution structures of mesophilic proteins: in two-thirds of the pairs, the interacting rings are not far from perpendicular; most are involved in a network; most link distinct secondary structural elements (i.e., nonlocal interactions); most are energetically favorable (80% have potential energies between 0 and −2 kcal/mol); and most take place between buried or partially buried residues (50). Among the hyperthermophilic proteins whose structures have been solved (Table 5), at least one might be stabilized by extra aromatic interactions. *P. furiosus* α-amylase also contains 5% more aromatic residues than the homologue from *Bacillus licheniformis*, but is it unknown whether these additional residues are involved in stabilizing interactions (85). A few examples also exist among thermophilic proteins. Thermitase, the serine proteinase produced by *Thermoactinomyces vulgaris*, contains 16 aromatic residues involved in aromatic pairs; the mesophilic homologue *Bacillus amyloliquefaciens* subtilisin BPN' contains only 6 aromatic pairs (331). Two clusters of aromatic interactions also exist in the *Thermus* RNase H that are not present in the *E. coli* enzyme (159). The solvent-exposed aromatic pair, Tyr13-Tyr17, in *B. amyloliquefaciens* RNase was replaced with Ala or Phe residues (single and double mutations). Both Tyr-Tyr and Phe-Phe pairs contributed approximately -1.3 kcal/mol toward thermodynamic stabilization (303).

Another type of interaction involving aromatic residues exists in proteins, but it has not been studied in relation to thermostability. In cation-π interactions, positive charges (most often metal cations but possibly cationic side chains of Arg and Lys) typically interact with the center of the aromatic ring (an example is shown in Fig. 4). The stabilization energy of the cation-π interaction does not decrease as a function of $1/r^3$ but, rather, exhibits a $1/r^n$ dependence with $n < 2$, which resembles more a Coulombic ($1/r$) than a hydrophobic interaction. The low dependence of the cation-π interaction on distance—and the fact that Phe, Tyr, and Trp do not have high

TABLE 5. Crystal structures of hyperthermophilic proteins and potential stabilizing features

Enzyme (resolution)	Stabilizing features	Reference
T. maritima holo-GAPDH (2.5 Å)	Additional intramolecular, surface IPs[a]	192
T. maritima ferredoxin (1.75 Å)	More charged-neutral H bonds that stabilize the structure of turns or fix turns together; conformational strain release: left-handed helical residues substituted with Gly; strong docking of the protein N terminus	226
T. maritima PGK (2.0 Å)	Dipole stabilization of the C and N caps of helices; extension of helix α6 by 4 more residues; more IPs, including 2 IPs that link the enzyme C and N termini together	15
T. maritima phosphorybosyl anthranilate isomerase (2.0 Å)	More prolines in loops or at the N terminus of helices; loop $\alpha_2\beta_3$ is highly hydrophobic, completely buried into the interior of another subunit; each subunit's N and C termini form a hydrophobic cluster included in the intersubunit surface	131
T. maritima GDH (3.0 Å)	More intrasubunit IPs; smaller intrasubunit cavities; hydrophobic intersubunit interfaces (different from the *P. furiosus* enzyme)	183
T. maritima lactate dehydrogenase (2.1 Å)	More intrasubunit IPs; fewer exposed hydrophobic residues/more Glu and Arg on the surface; higher secondary structure (α and β) content; one more helix on the surface shortens a flexible loop; tighter, hydrophobic, intersubunit contacts	16
T. maritima triosephosphate isomerase (2.85 Å)	Increased buried hydrophobic surface; more IPs; protein fusion with PGK	227
T. maritima dihydrofolate reductase (2.1 Å)	Dimerization involves intersubunit H bonds participating in forming two intermolecular antiparallel β-sheets and tight dimer interface packing	75
A. pyrophilus Fe-superoxide dismutase (1.9 Å)	Docking of loop 2 and C terminus in intersubunit contacts; large number of IPs (0.1/residue, not involved in networks)	220
P. furiosus aldehyde ferredoxin oxidoreductase (2.3 Å)	Reduced surface area/volume ratio (increased packing); more IPs	59
P. furiosus citrate synthase (1.9 Å)	Increased packing (loop shortening, more buried atoms, no cavities, more intimate intersubunit interactions); more intersubunit IPs; fewer thermolabile residues (Met); loop docking by more IPs	284
P. furiosus GDH (2.2 Å)	More IPs and IP networks (on the surface and at the intersubunit interfaces)	368
P. furiosus methionine aminopeptidase (1.75 Å)	More IPs and IP networks; more charged-neutral H bonds in α and β structures; same number of buried waters, but the buried waters cross-link areas that are distant in the sequence; stabilization of 2 antiparallel β-strands by prolines; shortening of N and C termini and loop stabilization	327
P. kodakaraensis O^6 methylguanine-DNA methyltransferase (1.8 Å)	Less hydrophobic, less polar, and more charged enzyme surface; more aromatic residues and aromatic clusters; more intra- and interhelix IPs	127
T. litoralis pyrrolidone carboxyl peptidase (1.73 Å)	Intersubunit disulfide bridge; hydrophobic intersubunit interface	310
T. gorgonarius DNA polymerase type B (2.5 Å)	Two disulfide bridges; enhanced electrostatic complementarity at the protein-DNA interface; better packing of surface loops	143
M. fervidus histone B (NMR)	Less unfavorable surface ionic interactions; filling of a hydrophobic cavity	375
M. kandleri methenyl:tetrahydromethanopterin cyclohydrolase (2.0 Å)	Trimer instead of dimer; Increase in hydrophobic intersubunit interactions; docking of loops and N and C termini by intersubunit contacts; decreased hydrophobic surface area and more surface acidic residues prevent enzyme aggregation at high salt concentration	120
M. kandleri formylmethanofuran: tetrahydromethanopterin formyltransferase (1.73 Å)	Uses the high intracellular salt concentration as stabilizing mechanism; enhanced surface ion pairing probably involving inorganic solvated cations; salting-out effect strengthens the intersubunit hydrophobic interactions; docking of loops and of C and N termini	96
S. solfataricus adenylate kinase (2.6 Å)	Strong and rigid central trimer interface, strengthened by a laterally extended β-sheet; trimer rather than monomer	356

Continued on following page

TABLE 5—*Continued*

Enzyme (resolution)	Stabilizing features	Reference
S. solfataricus GAPDH (2.05 Å)	One large IP network (15 residues) at a subunit interface (conserved in other thermophilic archaeal GAPDHs, but not entirely conserved in mesophilic archaeal GAPDHs); one interdomain disulfide bridge	160
S. solfataricus β-glycosidase (2.6 Å)	More IP networks; docking of the C terminus on the protein surface; buried water molecules involved in H-bond networks (Hypothesis: the internal solvent clusters and surface IP networks absorb the energy of molecular collisions and damp molecular vibrations, thus increasing the kinetic barrier to unfolding)	5
S. solfataricus indole-3-glycerol phosphate synthase (2.0 Å)	Docking of the N terminus by H bonds and IPs; more IPs (24 against 11) that clamp secondary structures together, helix dipole stabilization with Asp or Glu; conformational strain release: helix C capping with Gly; ionic strength has little effect on the number and specificity of intramolecular IPs	130, 185
S. solfataricus Fe superoxide dismutase (2.3 Å)	No clear reason for stability (far fewer IPs than in the *A. pyrophilus* enzyme)	345
Sulfolobus strain 7 ferredoxin (2.0 Å)	Zinc atom holds the core fold and the N-terminal extension together	107
T. aggregans β-glycosidase (2.4 Å)	More intersubunit IPs (including buried IPs); more buried waters, involved in H-bond networks; enzyme is a tetramer	63

[a] IP, ion pair.

desolvation energies and can easily be accommodated in hydrophobic environments—makes these interactions a potential stabilization mechanism (88).

Hydrogen Bonds

H bonds are typically defined by a distance of less than 3 Å between the H donor and the H acceptor and by donor-hydrogen-acceptor angle below 90°. The effect of hydrogen bonds on RNase T1 stability has been carefully studied (307). RNase T1 contains 86 H bonds with an average length of 2.95 Å. Their contribution to RNase T1 stability (approximately 110 kcal/mol, as determined by mutagenesis and unfolding experiments) was found to be comparable to the contribution of hydrophobic interactions; individual H bonds contributed an average of 1.3 kcal/mol to the stabilization (307). Because the identification of H bonds is highly dependent on the distance cutoff and because a number of hyperthermophilic protein structures have not been refined to sufficiently high resolutions, studying the role of H bonds in thermostability by structure analysis has not provided clear-cut answers.

One study done by Tanner et al. showed a strong correlation between GAPDH thermostability and the number of charged-neutral H bonds (i.e., between a side chain atom of a charged residue and either a main chain atom of any residue or a side chain atom of a neutral residue) (330). Tanner et al. list two reasons why this type of H bond might be particularly thermodynamically stabilizing: (i) the desolvation penalty associated with burying such H bonds is less than the desolvation penalty for burying an ion pair (that involves two charged residues), and (ii) the enthalpic reward of a charged-neutral H bond is greater than that of a neutral-neutral H bond because of the charge-dipole interaction. This correlation between charged-neutral H bonds and GAPDH stability suggests that the role of charged residues in protein stabilization may not be limited to forming ion pairs. An increased number of charged-neutral H bonds was also found in the *T. maritima* ferredoxin (Table 5). These H bonds either stabilize the structure of turns or anchor turns to one another.

Ion Pairs

Because ion pairs are usually present in small numbers in proteins and because they are not highly conserved, they are not a driving force in protein folding (83). Earlier work by Perutz (272) had suggested, however, that electrostatic interactions represent a significant stabilizing force in folded proteins. He stated that ion pairs are stronger in proteins than in solvents because they are formed between fixed charges. (In bulk water, solvation makes the stability of opposite charges almost independent of distance.) A single ion pair was calculated to be responsible for a 3 to 5-kcal/mol stabilization of T4 lysozyme (7). The desolvation contribution [$\Delta\Delta G$(desolvation)] to the free energy of folding associated with bringing oppositely charged side chains together is large and unfavorable. It has been suggested that ion pairs are destabilizing in proteins, because this $\Delta\Delta G$(desolvation) is not sufficiently compensated by the electrostatic energy provided by the ion pair. This unfavorable $\Delta\Delta G$(desolvation), however, decreases at high temperatures, partially because of a decrease in the water dielectric constant. This reduction is almost entirely electrostatic, primarily affecting the surface charged residues (the water molecules are less ordered and, on average, farther away from charged residues at high temperatures). Thus, charged residues tend to rearrange their conformations to improve their direct electrostatic interactions among each other, and the loss in solvation free energy is almost exactly compensated by a gain in interaction energy with other charged residues in the protein (80, 94). While ion pairing might not be the optimum stabilizing mechanism—or might even be destabilizing for mesophilic proteins—it can represent a strong stabilizing mechanism for hyperthermophilic proteins, as illustrated in Table 5. *P. furiosus* GDH is 34% identical to the *Clostridium symbiosum* enzyme. The main difference between these two

TABLE 6. Comparison of the ion pair contents of *P. furiosus* and *Clostridium symbiosum* GDHs[a]

Characteristic	Value for:	
	C. symbiosum	*P. furiosus*
No. of IPs[b] per subunit	26	45
No. of IPs per residue	0.06	0.11
% of charged residues forming IPs	40	54
% of IPs formed by Arg/Lys/His	46/31/23	64/27/9
% of IPs formed by Asp/Glu	46/54	47/53
% of all Arg forming IPs	55	90
No. of residues forming 2 IPs	6	17
No. of residues forming 3 IPs	1	5
No. of 2/3/4-residue networks[c]	72/24/12	54/24/12
No. of 5/6/18-residue network[c]	0/0/0	12/6/3
% of IPs in networks of >3 residues[c]	23	62
No. of intersubunit IPs[c]	30	54
No. of interdomain IPs	1	7

[a] Adapted from reference 368 with permission of the publisher.
[b] IP, ion pair.
[c] Numbers refer to the hexamers.

enzyme structures is found in their ion pair contents (Table 6). A higher percentage of charged residues participate in ion pairs, in particular Arg (90% of all the Arg residues in the *P. furiosus* GDH form ion pairs). The *P. furiosus* enzyme contains 0.11 ion pairs per residue against 0.06 in the *C. symbiosum* GDH (the average for mesophilic enzymes is approximately 0.04). Arg residues form ion pairs plus H bonds with the carboxylic acids. The ion pairs form large networks that criss-cross the protein surface and the subunit interfaces. P. *furiosus* GDH's largest ion pair network (Fig. 5) is composed of 24 residues (belonging to four different subunits) connected by 18 ion pairs. Ion pair networks are energetically more favorable than an equivalent number of isolated ion pairs, because for each new pair the burial cost is cut in half: only one additional residue must be desolvated and immobilized (368).

The stabilizing potential of buried ion pairs has been investigated, but it remains controversial because of the large $\Delta\Delta G$(desolvation) associated with burying two charged residues. In a recent study using continuum electrostatic calculations, an average $\Delta\Delta G$(desolvation) of $+12.9 \pm 5.6$ kcal/mol was calculated for buried ion pairs. The large $\Delta\Delta G$(desolvation) was compensated for by the large Coulombic energy created by the ion pair. (Buried ion pairs are in a low dielectric-constant environment and thus are not exposed to a large screening.) The study's conclusion was that salt bridges with favorable geometry were likely to be stabilizing anywhere in the protein (196). Four additional buried ion pairs between α-helices have been suggested as a stabilization mechanism in *P. kodakaraensis* O^6-methylguanine-DNA methyltransferase. For these four pairs, distances are short: between 2.74 and 3.02 Å. Residues Arg50 and Glu93 form a double ion pair NH1-Oε1 (2.74 Å) and NH2-Oε2 (2.83 Å) that connects the N- and C-terminal domains (Table 5). A stabilizing function has also been proposed for buried ion pairs in *Thermosphaera aggregans* β-glycosidase (Table 5).

The *P. furiosus* methyl aminopeptidase was shown to contain more ion pairs and ion pair networks than the *E. coli* enzyme (Table 5). The *P. furiosus* enzyme stability decreased at low pH values (where acidic residues are protonated and disrupt favorable ionic interactions) and at high salt concentrations (salts are known to destabilize protein ion pairs). These results suggest that ion pairs are essential in maintaining this enzyme stability at high temperatures (266). In similar experiments, NaCl was shown to destabilize *S. solfataricus* carboxypeptidase at pH 7.5, but not at pH 9.0 (where the stabilizing ion pairs probably do not exist any more), suggesting that ion pairs are involved in the stabilization of this *S. solfataricus* enzyme (352). Since other *S. solfataricus* enzymes are destabilized by NaCl, ion pairing might represent a general stabilization strategy in this organism (as *Sulfolobale* strains do not thrive in the presence of high salt concentrations).

Ion pairing's involvement in hyperthermophilic protein stabilization has already been extensively studied by site-directed mutagenesis (SDM). Because all studied hyperthermophilic enzymes unfold irreversibly, the only stability data available refer to kinetic stability. A 4-residue surface ion pair network that connects the N- and C-terminal helices was shown by SDM to participate in the stabilization of *T. maritima* GAPDH. In this network, Arg20 is connected to three other residues by ion pairs or H bonds. The mutations Arg20Ala and Arg20Asn increased the enzyme denaturation rate at 100°C by a factor of 3.5 (270). In *T. maritima* indoleglycerol phosphate synthase, the stabilization provided by ion pair Arg241-Glu73 (between $[\alpha/\beta]_8$ barrel helices α_8 and α_1) was also tested by SDM. At 85.5°C, mutation Arg241Ala increased the enzyme denaturation rate by a factor of almost 3. The enzyme E_a of unfolding at 85°C decreased by 3.2 kJ/mol, suggesting that the Arg241-Glu73 pair participates in the kinetic stabilization of this enzyme (246).

The ion pair networks identified in the *P. furiosus, P. kodakaraensis*, and *T. litoralis* GDH structures (Table 5) were studied by SDM. The three enzymes are 83 to 87% identical, but their thermostabilities decrease in the direction P. *furiosus* GDH > *P. kodakaraensis* GDH > *T. litoralis* GDH. They all contain the same 18-ion-pair network at their hexamer interface (Fig. 5). The mutation Glu158Gln, which removed two ion pairs at the center of this network, significantly destabilized *P. kodakaraensis* GDH (280). One ion pair network involving six charged residues is present only in *P. furiosus* GDH. The same ion pair network was created in *P. kodakaraensis* GDH and *T. litoralis* GDH by SDM. Both enzymes were stabilized by the newly introduced ion pair network (280, 348). These studies confirmed the role of ion pair networks in the *P. furiosus, P. kodakaraensis*, and *T. litoralis* GDH thermostabilities. Lebbink et al. (203) introduced a 16-residue ion pair network at the subunit interface in *T. maritima* GDH to create an interface similar to the 18-ion-pair network in *P. furiosus* GDH. The combination of three destabilizing mutations yielded a triple mutant enzyme (Ser128Arg-Thr158Glu-Asn117Arg) that was slightly more stable and thermophilic than the wild-type enzyme. This result illustrates the high level of cooperation that exists among the different members of this ion pair network. This result also supports the role of the 18-residue ion pair network in *P. furiosus* GDH stabilization.

In an earlier study, Tomschy et al. (337) had removed two ion pairs located on the surface of two α-helices in *T. maritima* GAPDH. Because these mutations did not affect the enzyme stability, the authors concluded that surface ion pairs could not be considered a general strategy of thermal adaptation. Both

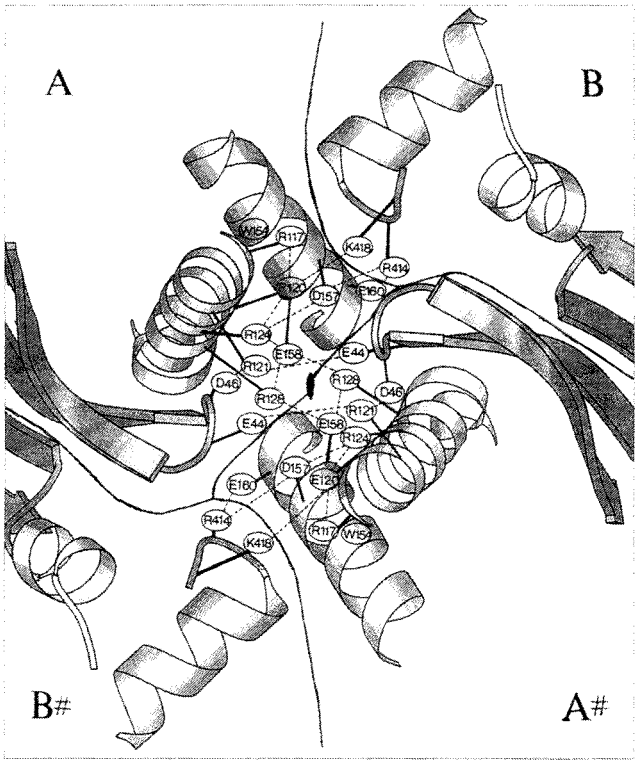

FIG. 5. Schematic representation of the ion-pair network that stabilizes the intersubunit interactions in the hexameric *P. furiosus* GDH. The twofold axis of symmetry between the dimers is indicated by the dyad symbol. Dotted lines represent ion pair interactions. Reprinted from reference 368b with permission of the publisher.

ion pairs chosen in this study were intrahelical ion pairs. These two pairs might have been located in protein areas that were overconstrained and that were not among the protein areas most susceptible to unfolding. In contrast, the other examples described above illustrate the thermostabilization effect of non-local ion pairs and ion-pair networks, which link nonadjacent residues (and secondary structures) in the sequence.

Additional, indirect evidence for the role of ion pairing in thermostability comes from genome sequencing. The major trend observed in Table 4 is toward an increased number of charged residues in hyperthermophilic proteins compared to mesophilic proteins, mostly at the expense of uncharged polar residues.

Prolines and Decreasing the Entropy of Unfolding

Matthews et al. (238) proposed that proteins of known three-dimensional structure could be stabilized by decreasing their entropy of unfolding. In the unfolded state, glycine, without a β-carbon, is the residue with the highest conformational entropy. Proline, which can adopt only a few configurations and restricts the configurations allowed for the preceding residue (313), has the lowest conformational entropy. Thus, the mutations Gly→Xaa or Xaa→Pro should decrease the entropy of a protein's unfolded state and stabilize the protein, as long as the engineered residue does not introduce unfavorable strains in the protein structure. This technique has been used to engineer enzymes that are more thermodynamically stable. For example, *B. stearothermophilus* neutral protease inactivates by autolysis, which targets a specific flexible surface loop (residues 63 to 69) (93). Prolines were introduced in that loop to make it less susceptible to unfolding. Only positions 65 and 69 were suitable for proline substitutions. In other positions, a proline would eliminate noncovalent interactions, create conformational strains, or have inappropriate torsion angles. Only mutations Ser65Pro and Ala69Pro proved thermostabilizing, as had been predicted by modeling (125). A number of thermophilic and hyperthermophilic proteins also use this stabilization mechanism (255) (Table 5). The *Thermoanaerobium brockii* secondary alcohol dehydrogenase contains eight more prolines than its *Clostridium beijerinckii* mesophilic homologue. Residues Pro177 and Pro316 at the N termini of two helices and Pro24 in position 2 of a β-turn were shown to be stabilizing (215). (Prolines were introduced in the corresponding locations in the *C. beijerinckii* enzyme.) There are at least 22 locations in which prolines occur only in thermophilic *Bacillus* oligo-1,6-glucosidases. The majority of these prolines are in position 2 of solvent-exposed β-turns (seven of these prolines), in coils within loops (nine of them), or at the N-cap of α-helices in the barrel structure (four of them). Prolines were introduced at the corresponding locations in the mesophilic *Bacillus cereus* oligo-1,6-glucosidase. Thermostability usually increased with the number of prolines introduced. The stability increase was most significant when prolines were added at position two of β-turns or at N caps of α-helices. The less stabilizing mutations probably introduced unfavorable Van der Waals interactions or removed stabilizing H bonds (361).

The *Thermotoga neapolitana* xylose isomerase contains two prolines in a loop that is involved in intersubunit interactions. These prolines are absent in the less stable *Thermoanaerobacterium thermosulfurigenes* enzyme (Fig. 6). The kinetic stability properties of the two *T. thermosulfurigenes* xylose isomerase mutants Gln58Pro and Ala62Pro illustrate how important the mutation location is for the outcome of SDM (313). Both Gln58 and Ala62 had backbone dihedral angles which allowed for prolines, neither was involved in noncovalent stabilizing interactions, and Asp57 and Lys61 had dihedral angles that allowed for residues preceding prolines. The conformation of the Gln58 side chain was very close to that of the proline pyrrolidone ring (Fig. 6), and so no conformational strain was introduced by Pro; the mutation Gln58Pro stabilized the protein mainly by decreasing the entropy of unfolding. In contrast, the mutation Ala62Pro created a volume interference between the proline pyrrolidone ring (Cδ atom) and the Ly61 side chain (Cβ atom) that probably led to destabilizing conformational changes. The mutation Ala62Pro reduced the enzyme's $t_{1/2}$ at 85°C by a factor of 10.

Intersubunit Interactions and Oligomerization

For almost half of the hyperthermophilic proteins listed in Table 5, intersubunit interactions are mentioned as a potential major stabilization mechanism. The only strong experimental evidence available that supports the role of intersubunit interactions in the stability of hyperthermophilic proteins was obtained with *P. kodakaraensis* and *T. litoralis* GDHs: ion pairs were created to match the structure of the more thermostable *P. furiosus* GDH (280, 348) (see "Ion Pairs" above). More

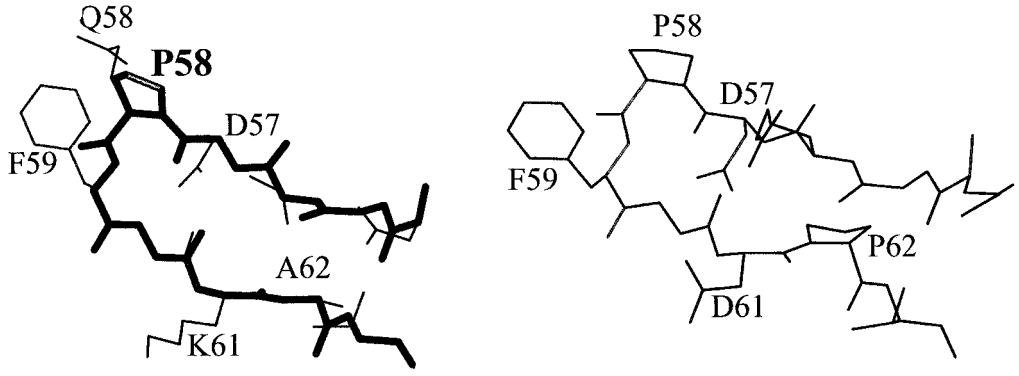

FIG. 6. Comparison of the Phe59 loop structures in *Thermoanaerobacterium thermosulfurigenes* (left) and *Thermotoga neapolitana* xylose isomerases (right). Thin lines represent the structures of the wild-type enzymes; thick lines represent the model of the *T. thermosulfurigenes* xylose isomerase Gln58Pro mutant derivative.

work has been done using thermophilic enzymes as models. The mutation Gly281Arg in *B. subtilis* GAPDH (matching the sequence of the more stable *B. stearothermophilus* GAPDH) created kinetically stabilizing intersubunit ion pairs. The enzyme $t_{1/2}$ increases from 19 min at 50°C to 198 min at 75°C (252). Compared to the *E. coli* 3-isopropylmalate dehydrogenase, the *Thermus thermophilus* enzyme shows a more hydrophobic subunit interface. SDM experiments showed than the hydrophobic interactions present in the *Thermus* enzyme made the dimer more resistant to dissociation (180, 250) (see "Hydrophobic Interactions" above). Mutagenesis of a hydrophobic core at the dimer interface in the *T. thermophilus* elongation factor EF-Ts showed that this hydrophobic core contributed to the enzyme dimerization and that dimer formation considerably contributed to the thermodynamic stability of *T. thermophilus* EF-Ts, (259). *Methanopyrus kandleri* formylmethanofuran:tetrahydromethanopterin (H_4MPT) formyltransferase (MkFT) is monomeric and inactive at low salt concentrations. It adopts active dimeric and tetrameric forms at higher salt concentrations. The activity of MkFT in dimeric or tetrameric forms in the presence of potassium phosphate is stimulated by the addition of NaCl, suggesting that oligomerization is a prerequisite for activity and that the mechanisms of salt-induced activation and salt-induced oligomerization are different. In the enzyme crystal structure, subunit interfaces are mostly hydrophobic. Lyotropic salts increase hydrophobic interactions and probably strengthen subunit interactions. Oligomer formation requires higher concentrations of NaCl than of potassium phosphate (a stronger lyotropic salt), suggesting a dominant role for salting-out effects in MkFT thermostability (306). Both MkFT thermodynamic and kinetic stabilities increased with oligomerization (306). From the examples listed in Table 5 and above, it appears that intersubunit interactions play indeed a major role in the stabilization of hyperthermophilic proteins. Interestingly, there is no single type of intersubunit interaction responsible for this stabilization.

An ever-increasing number of hyperthermophilic proteins are known that have a higher oligomerization state than their mesophilic homologues (Table 7). Only for *T. maritima* phosphoribosylanthranilate isomerase is experimental evidence available demonstrating that dimerization is a stabilization factor (332). Thoma et al. (332) engineered monomeric variants of this enzyme by SDM. These monomeric variants remained as active as the wild-type enzyme. Their X-ray structure differed from that of the wild-type enzyme only in the restructured interface, but their kinetic stability at 85°C decreased by factors of 60 to 100 (from a $t_{1/2}$ of 310 min for the wild-type enzyme to 3 to 5 min for the variants). For *M. kandleri* methenyl H_4MPT cyclohydrolase (MkCH), trimerization probably increases the enzyme stability, since it leads to an enlarged buried surface area and increased packing density. Not only are the hydrophobic interactions between subunits strength-

TABLE 7. Comparison of subunit numbers in hyperthermophilic versus mesophilic enzymes

Source	Enzyme	No. of subunits in:		Reference
		Hyperthermophilic enzyme	Mesophilic enzymes	
Pyrococcus woesei	PGK	2	1	136
Methanothermus fervidus	PGK	2		
Pyrococcus furiosus	β-Glucosidase	4	1	357
Sulfolobus solfataricus	β-Glucosidase	4		
Thermotoga maritima	β-Glucosidase	2		
T. maritima	Anthranilate synthase	2	1	315
T. maritima	Dihydrofolate reductase	1 or 2	1	364
T. maritima	Phosphoribosyl-anthranilate isomerase	2	1	332
S. solfataricus	β-Glycosidase	4	2	63
Thermosphaera aggregans	β-Glycosidase	4		
Methanopyrus kandleri	MkCH	3	2	120

ened but also several loops and the N and C termini are fixed by contacts to the neighboring subunits (120). Triosephosphate isomerase (TIM) is only expressed as a fusion enzyme with PGK in *T. maritima*. The *T. maritima* PGK-TIM fusion and the tetrameric structure were shown to enhance the stability and activity of TIM but not the stability of PGK (23). Based on stability studies of dimeric globular proteins, Neet and Timm (256) calculated that quaternary interactions could provide 25 to 100% of the conformational stability in protein dimers. This study, although performed with mesophilic proteins, suggests that oligomerization can be a significant stabilizing mechanism for hyperthermophilic enzymes. *T. maritima* xylanase XynA is organized in five domains. Domains N1 and N2 were shown to be necessary for optimal kinetic thermostability (365). These two domains were also present in *T. saccharolyticum* XynA (207) and are also needed for that enzyme kinetic stability. Modular organization may be another factor contributing to stability.

Conformational Strain Release

Residues in the left-handed helical conformation (ϕ = 40 to 60°, Ψ = 20 to 80°) have marginal conformational stability unless they are stabilized by intramolecular non-covalent interactions. (Non-Gly residues with a left-handed helical conformation are supposed to be less stable than the right-handed conformation by 0.5 to 2.0 kcal/mol.) The close contact between the β-carbon and the carbonyl oxygen within the residue in the left-handed helical conformation creates a local conformational strain on the protein structure. Two residues in the left-handed helical conformation, Glu15 in *B. subtilis* DNA binding protein HU and Lys95 in *E. coli* RNase H1, both in turn regions, are replaced by Gly residues in their thermophilic counterparts. Mutations Glu15Gly and Lys95Gly in *B. subtilis* DNA binding protein HU and *E. coli* RNase H1, respectively, eliminated the conformational strain created by the residues in the left-handed helical conformation, and significantly increased the thermodynamic stabilities of the two proteins (173, 179). In these two examples, the stability gained by the conformational strain release was enhanced by its stabilizing effect on secondary structure interactions. *E. coli* RNase H1 contains two additional non-Gly residues with left-handed helical conformation. Residues Trp90 and Asn100, in contrast to Lys95, point to the interior of the enzyme, and they make compensatory polar or hydrophobic interactions. Mesophilic ferredoxins contain three residues in the left-handed helical conformation in their [4Fe-4S] cluster binding region. In the *T. maritima* and *T. litoralis* homologs, the steric hindrance in the cluster binding region is released by the substitution of the residues in the left-handed helical conformation with three Gly residues. These three Gly residues are involved in H bonds with the cluster sulfur atoms (226).

Other types of conformational strain releases have been proposed as stabilizing mechanisms. In α-helices, for example, residues with a low helical propensity can be replaced by residues that have a high helical propensity. Such substitutions usually take place when a residue's side chain is not well accommodated in the α-helix. One particular substitution location in α-helices is the C terminus (or C cap). Gly is the most favorable residue at the C cap, because its lack of side chain allows it to adopt a left-handed helical conformation without strain and because the main chain carbonyl oxygen can form H bonds with solvent molecules. The *P. furiosus* citrate synthase contains at least seven helices that have a C-cap Gly. Their effect on stability is still unknown (254). In general, though, these types of conformational strain releases are not expected to provide significant stabilization, and they have not been characterized in detail in hyperthermophilic protein structures. They also compete with other stabilization mechanisms (e.g., propensity for hydrophobic interactions, for H bonds, or for ion pairs) (83).

Helix Dipole Stabilization

Helix dipoles can be stabilized by negatively charged residues near their N-terminal end, as well as by positively charged residues near their C-terminal end. In the *S. solfataricus* indole-3-glycerol phosphate synthase, every helix dipole in the $(\alpha/\beta)_8$ barrel is stabilized versus six in the *E. coli* enzyme (130). The helices' dipoles are also stabilized in the *B. stearothermophilus* and *T. maritima* PGKs: while mesophilic enzymes have only 9 N caps and 12 C caps (pig PGK) and 10 N caps and 9 C caps (yeast PGK) stabilized by opposite charges, the numbers of stabilized N and C caps increase to 16 N caps and 13 C caps in the *B. stearothermophilus* PGK and to 17 N caps and 14 C caps in the *T. maritima* PGK (15). Nicholson et al. showed that N-cap stabilization could increase an enzyme's ΔG_{stab} by approximately 0.8 kcal/mol (262). In general, though, N and C capping compete with other stabilization and destabilization mechanisms (e.g., propensity for H bonds or ion pairs, and conformational strain), and the stabilization provided is often marginal.

Packing and Reduction in Solvent-Accessible Hydrophobic Surface

In a recent study, Karshikoff and Ladenstein (169) compared the partial specific volumes, voids, and cavity volumes in a set of 80 nonhomologous mesophilic, 20 thermophilic, and 4 hyperthermophilic proteins. They concluded that none of these factors could be considered a common thermostabilization mechanism. A few examples exist, however, of hyperthermophilic proteins that gain part of their stability from better packing (Table 5). For one of these proteins, thermodynamic stabilization by better packing was demonstrated experimentally: a solvent-accessible cavity in the *Methanobacterium formicicum* histone is partially filled by bulkier hydrophobic side chains in the *M. fervidus* protein (375). The mutations Ala31Ile and Lys35Met increased the *M. formicicum* protein T_m by 11 and 14°C, respectively, while the mutations Ile31Ala and Met35Lys decreased the *M. fervidus* histone T_m by 4 and 17°C, respectively (216). Britton and colleagues (38) suggested that the strongly increased Ile content in *P. furiosus* GDH was consistent with a general increase in packing when compared to the mesophilic *C. symbiosum* GDH. With the ability of Ile to adopt more conformations than Leu in proteins (see "Amino Acid Composition and Intrinsic Propensity" above), it is better able to fill various voids in the protein core (38). While better core packing is often linked to increased hydrophobicity, in some cases it can affect stability in different ways. Based on the ability of high short peptide densities to form α-helices in crystals, it has been proposed that an increasing peptide con-

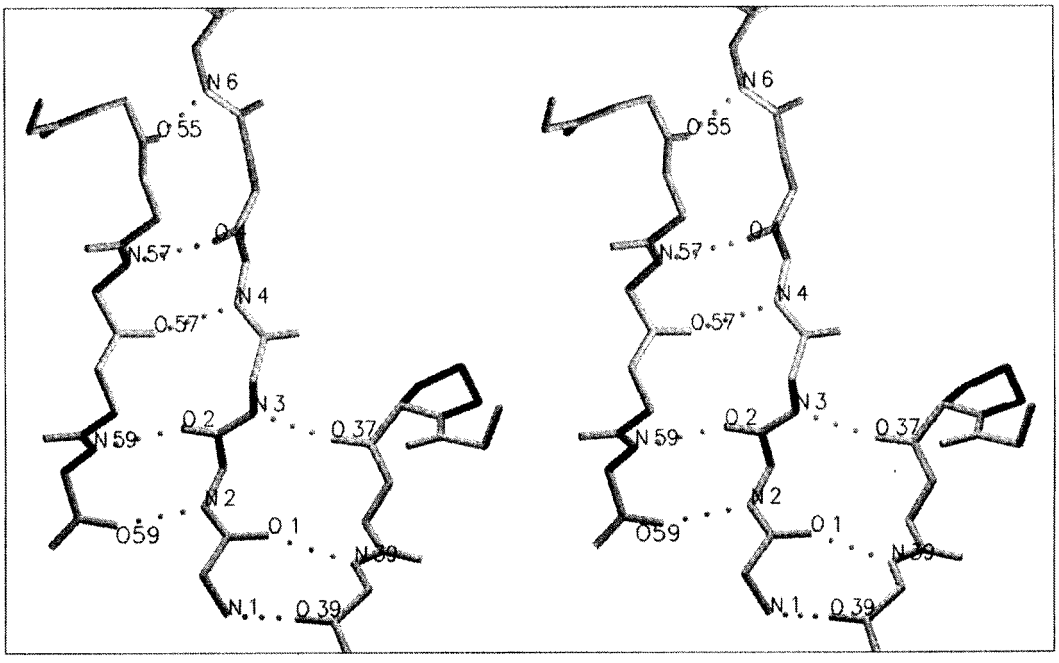

FIG. 7. Stabilization of the N-terminal β-strand by H bonding in *T. maritima* ferredoxin. β-Strand Lys2-Val5 forms a two-stranded β-sheet with β-strand Ile56-Glu59. The N-terminal β-strand is fixed to the protein core by three H bonds (gray dotted lines) to turn D: two bonds between Met1 and Thr39, and one bond between Val3 and Pro37. Reprinted from reference 226 with permission of the publisher.

centration increases the stability of helices (83). Internal packing, therefore, could be involved in protein thermostability either as a general stabilizing force or as a factor altering the stability of secondary structures.

Since surface hydrophobic residues cannot participate in stabilizing interactions with the solvent, they are detrimental to protein stability and solubility. A number of hyperthermophilic proteins show significantly reduced hydrophobic accessible surface areas (ASA): *T. maritima* lactate dehydrogenase, *P. kodakaraensis* O^6-methylguanine-DNA methyltransferase, *M. kandleri* MkCH, and *S. acidocaldarius* anthranilate synthase (Table 5). In *S. acidocaldarius* superoxide dismutase, the hydrophobic ASA represents only 18% of the total ASA, as opposed to 26.8% in mesophilic enzymes. This decrease in hydrophobic ASA is balanced by an increase in polar ASA (184).

Docking of the N and C Termini, and Anchoring of Loose Ends

Loops and N and C termini are usually the regions with the highest thermal factors in a protein crystal structure. They are likely to unfold first during thermal denaturation. Going against the earlier belief that loops had no bearing on protein stability, loops in hyperthermophilic proteins show structural features that could lead to protein stabilization. Two loop-stabilizing trends have been observed (Table 5): loops are either shortened or better anchored to the rest of the protein. Loop shortening can be the consequence of the extension or the creation of a secondary structure (*T. maritima* PGK and lactate dehydrogenase in Table 5). Loop anchoring is achieved through ion pairing, H bonding, or hydrophobic interactions. Stabilization of the N and C termini involves similar mechanisms to those in loop stabilization. In Fig. 7, the N terminus of *T. maritima* ferredoxin is fixed to the protein core by H bonds. N and C termini often interact with each other for mutual stabilization (*T. maritima* PGK and phosphoribosyl anthranilate isomerase in Table 5), N and C termini—as well as loops—can also be anchored by participating in subunit interfaces (*T. maritima* PGK and MkCH in Table 5).

One of the best examples of multiple dockings in found in *M. kandleri* MkFT. An insertion region that is loosely attached to its subunit interacts extensively with the β-meander region from another subunit, docking each area to the other. Loops are linked to adjacent regions in the same or different subunit by multiple interactions (mainly H bonds); the N- and C-terminal residues are connected to each other and to the protein (they even have average B factors) (96). In *A. pyrophilus* superoxide dismutase, loop 2 is extended and plays a key role in forming a compact tetramer. This loop is not flexible (it has low B factors), and it makes extensive contacts with other subunits in the tetramer. The C terminus is 10 or 11 residues longer than in other superoxide dismutases. These additional residues extend the C-terminal α-helix by two more turns, and this C-terminal helix makes extended contacts with the C-terminal helix of another subunit (220). Trimerization of MkCH is probably a stabilization mechanism in itself, but it also allows several loops and the N and C termini to be fixed by contacts to the neighboring subunits (120).

Metal Binding

Metals have long been known to stabilize and activate enzymes. Xylose isomerases bind two metal ions (chosen from Co^{2+}, Mg^{2+}, and Mn^{2+}). One cation is directly involved in catalysis; the second is mainly structural (232, 363). The two

TABLE 8. Effect of metals (chloride salts) on the kinetic and thermodynamic stabilities of *B. licheniformis* xylose isomerase[a]

Metal	Half-life (min)	E_a of inactivation (kcal/mol)	T_m (°C)
None	24 (40°C)	92	50.3
Mg^{2+}	35 (56°C)	144	53.3
Co^{2+}	18 (70.5°C)	279	73.4
Mn^{2+}	50 (71.5°C)	257	73.6

[a] C. Vieille, K. L. Epting, R. M. Kelly, and J. G. Zeikus, submitted for publication.

metal binding sites have different specificities, and replacing one cation with another often significantly alters enzyme activity, substrate specificity, and thermostability (171, 232). A study of *Bacillus licheniformis* xylose isomerase stability in the presence and absence of metals showed that the evolution of kinetic stability followed that of thermodynamic stability and that both types of stabilities were functions of the nature of the metal present (Table 8). These observations suggest that major stabilizing forces are associated with the presence of metal in the holoenzyme.

Indirect evidence for the role of metals in the stability of hyperthermophilic proteins is the difficulty encountered in removing the metals from the enzymes. α-Amylases specifically bind Ca^{2+}. The α-amylase catalytic site is located in a cleft between two domains (an $[\alpha/\beta]_8$ barrel and a large loop). Coordinated by ligands belonging to these two domains, Ca^{2+} is essential for the enzyme's catalytic activity and thermostability (30). The *P. furiosus* extracellular α-amylase was initially described as a Ca^{2+}-independent enzyme, because room temperature EDTA treatments had no effect on its activity (85). Further characterization revealed that this enzyme contains at least two Ca^{2+} cations that cannot be removed by EDTA at temperatures below 70°C. A 30-min EDTA treatment at 90°C removed approximately 60 to 70% of the bound Ca^{2+} (A. Savchenko, C. Vieille, and J. G. Zeikus, unpublished results). Similar observations were made with the *Thermococcus profundus* α-amylase (approximately 80% identical to the *P. furiosus* extracellular α-amylase). This enzyme was activated and stabilized by Ca^{2+}, but room temperature EDTA treatments had no effect on activity (65).

Some thermophilic and hyperthermophilic enzymes have been described that contain metal atoms that are not present in their mesophilic homologs. The ferredoxin from *Sulfolobus* sp. strain 7 contains an extra 40-residue N-terminal extension that is linked to the protein core by a Zn binding site. The zinc atom is liganded by three His residues from the N-terminal domain and one Asp residue from the core domain. This structure (N-terminal extension plus Zn binding site) is absent in eubacterial homologs but is conserved in all other thermoacidophiles (107). Progressive N-terminal deletions and SDM of two of the three His ligands showed that both the N-terminal extension and the zinc atom are important for thermodynamic stability. Their presence or absence has no effect, though, on ferredoxin function. The zinc atom is responsible for a 9°C increase in T_m. It is so tightly bound inside the protein that it cannot be removed without removing the two FeS clusters (191). *Thermoactinomyces vulgaris* subtilisin-type serine-protease thermitase contains three Ca^{2+}-binding sites; one of them is not present in its mesophilic homologues (331). A thermophilic homologue of thermitase, the *Bacillus* Ak1 protease, contains one more Ca^{2+} than thermitase does, and it is significantly more kinetically stable than thermitase in the presence of Ca^{2+} ($t_{1/2}$ of 15 h at 80°C versus 19 min for thermitase) (311). Since Ca^{2+} preferentially binds carboxylate and other oxygen ligands (which are the metal ligands most likely to be located on the protein surface), this metal is more likely than others to play a significant stabilizing role in proteins.

Nonlocal versus Local Interactions

Perutz and Raidt (273) suggested that ion pairs linking portions of the protein that are juxtaposed in the structure but nonadjacent in the sequence can significantly contribute to protein thermostability. Recent information accumulated on hyperthermophilic proteins strongly supports this hypothesis. Figure 4 shows three types of nonlocal interactions involving residues from one α-helix (Tyr93) and three different loops (Arg19, Thr84, and Asp111). While most information available concerns ion pairs (Table 5 and references therein), the hypothesis of Perutz and Raidt might also extend to other types of noncovalent interactions. Chimeras were constructed between *P. furiosus* and *Clostridium pasteurianum* rubredoxins. Their relative stabilities (compared to the *P. furiosus* and *C. pasteurianum* rubredoxins) indicate that essential stabilizing interactions exist between the protein core and the β-sheet (H bonds or hydrophobic interactions). Individually, neither the core nor the β-sheet provides extensive stabilization (92).

The stabilization provided by a few nonlocal ion pairs was tested by SDM. In *T. maritima* indoleglycerol phosphate synthase, the ion pair Arg241-Glu73 links helices α_8 and α_1 in the $(\alpha/\beta)_8$ barrel. At 85.5°C, the mutation Arg241Ala increased the enzyme denaturation rate by a factor of almost 3. The enzyme E_a of unfolding at 85°C decreased by 3.2 kJ/mol, suggesting that the Arg241-Glu73 ion pair participates in the kinetic stabilization of this enzyme (246). In *Bacillus polymyxa* β-glucosidase A, the mutation Glu96Lys created a stabilizing surface salt bridge (Lys96-Asp28) between two distant parts of the protein sequence: a loop (Asp28) and the N terminus of a helix (Lys96) (293). The docking of loops and N and C termini on the protein surface also involve numerous nonlocal interactions. Figure 7 illustrates the docking of a protein N terminus to a surface turn.

Posttranslational Modifications

Protein glycosylation is widespread among eucaryal enzymes, and a number of bacterial extracellular enzymes are glycosylated. Only a few examples are known of hyperthermophilic proteins that are glycosylated, and their carbohydrate moieties have not been extensively characterized (100, 138). Most glycosylated enzymes (bacterial, archaeal, and eucaryal), though, retain their catalytic and stability properties when expressed in bacteria. A few studies using naturally glycosylated eucaryal proteins showed that glycosylation could cause significant thermal stabilization without affecting the protein folding pathways or their conformations. The higher tendency of the deglycosylated enzymes to aggregate during thermal inactivation suggested that glycosylation could also prevent partially folded or unfolded proteins from aggregating (163, 359). Bo-

vine pancreatic RNase A and RNase B differ only by a carbohydrate moiety attached on Asn34 in RNase B. This carbohydrate moiety is responsible for the higher kinetic and thermodynamic stability of RNase B. Progressive hydrolysis of the carbohydrate moiety showed that the stability difference was due to the attachment of the first carbohydrate unit to Asn34 (13).

The effect of glycosylation on thermostability was also studied with two *Bacillus* β-glucanases expressed in *E. coli* and in *Saccharomyces cerevisiae*. One of the two enzymes was strongly kinetically stabilized by glycosylation at 70°C, and its optimum temperature for activity was higher. The thermostabilization level depended more on the location of the carbohydrate moiety on the protein than on the extent of glycosylation (267). While glycosylation is probably not a thermostabilization method commonly found in nature, the few examples cited above suggest that it could represent an alternative method for either enzyme thermostabilization or for solubilization.

Posttranslational lysine methylation (formation of *N*-ε-monomethyllysine) has been described for a number of *Sulfolobus* proteins (91, 231, 240). The native small DNA binding protein Sac7d from *S. acidocaldarius* (monomethylated on Lys 5 and Lys7) reversibly denatures at 100°C (pH 7.0) (91). The recombinant Sac7d denatures at 92.7°C. The 7°C difference in T_m between native and recombinant Sac7d has been attributed to Lys methylation, which is absent in the recombinant protein (240). It is unclear, though, if Lys methylation is a general thermostabilization mechanism in members of the *Sulfolobales*, since the stability of Sso7d (the Sac7d homologue in *S. Sulfolobus*) is methylation-independent.

Extrinsic Parameters

While most pure hyperthermophilic enzymes are intrinsically very stable, some intracellular hyperthermophilic proteins get their high thermostability from intracellular environmental factors such as salts, high protein concentrations, coenzymes, substrates, activators, polyamines, or an extracellular environmental factor such as pressure.

Stabilization by salts. Inorganic salts stabilize proteins in two ways: (i) through a specific effect, where a metal ion interacts with the protein in a conformational manner (see "Metal binding" above), and (ii) through a general salt effect, which mainly affects the water activity. Thauer and colleagues studied the effect of salts on the thermostability and the activity of five *M. kandleri* methanogenic enzymes (36, 37, 181, 224, 225). While the five enzymes are activated and kinetically stabilized by salts, the extent of the salt effect is enzyme dependent. K^+ and NH_4^+ typically stabilize enzymes more efficiently than other cations do. Of all the anions, SO_4^{2-} and HPO_4^{2-} have the strongest activating effect (36). Enzyme salt requirements are not always satisfied by the intracellular salt concentration. The *M. kandleri* intracellular salt concentration (>1 M potassium plus 1 M cyclic 2,3-diphosphoglycerate [cDPG]) seems to favor MkCH activity (maximal at 1.5 M salt) over its stability (optimal below 0.1 M salt) (37). The effects of salts on CHO-tetrahydromethanopterin (H_4MPT) formyltransferases from *M. kandleri, M. thermoautotrophicum, Archaeoglobus fulgidus*, and *Methanosarcina barkeri* were compared. The difference in formyltransferase activation by salts was directly correlated to the intracellular cDPG concentration in the different organisms (36). The structure of MkFT was analyzed in terms of its stabilization by salts. Two features were suggested to be related to this property: (i) MkFT presents a decrease in accessible surface hydrophobicity, as well as intersubunit interfaces that are largely hydrophobic; and (ii) the tetramer surface presents an excess of negatively charged residues (48 versus 24 basic residues). Acidic residues can form strong H bonds and multiple H bonds to water molecules, enabling these residues to compete with inorganic cations or water. Of all the residues, Glu has the highest capacity to bind water molecules. Of the 48 surface negative residues, 33 are Glu and 15 are Asp (96). High lyotropic salt concentrations are supposed to enhance the surface ionic interactions due to an increasing number of inorganic cations at the negatively charged surface and to enhance intersubunit hydrophobic interactions due to the salting-out effect. MkFT oligomer formation was shown to require higher concentrations of NaCl than of potassium phosphate (a stronger lyotropic salt), suggesting a dominant role for salting-out effects in MkFT thermostability (306). This protein might have evolved to be optimally stable in the presence of a high intracellular salt concentration. *M. kandleri* cells contain approximately 1 M cDPG when grown at 98°C. Potassium salts of cDPG, 2,3-DPG, and phosphate are equally effective at activating *M. kandleri* cyclohydrolase. However, at equal ion concentrations cDPG is more effective at stabilizing MkFT. In *M. kandleri*, the cDPG concentration is optimal for the activities and stabilities of MkCH and MkFT. Synthesizing cDPG requires 4 ATP molecules. The last reaction in this synthesis is the only one exergonic enough to drive the synthesis up to cDPG rather than to its precursor 2,3-DPG. Also, at pH 7.0, cDPG is a trianion whereas 2,3-DPG is a penta-anion; thus cDPG has a smaller effect on the ionic strength than would 2,3-DPG (305).

M. fervidus GAPDH is intrinsically kinetically stable only up to 75°C. A study of this enzyme's thermostabilization by salts indicated that the relative salt effects—$K_3PO_4 > Na_3PO_4 > K_2SO_4 > Na_2SO_4 > KCl > NaCl$—were consistent with their respective abilities to reduce the enzyme solubility in an aqueous solvent. Their action was attributed to their salting-out effects (98). *M. fervidus* GAPDH is probably stabilized in vivo by cDPG, which is present in this organism at approximately 0.2 to 0.3 M (305). It is interesting that other *M. fervidus* enzymes are only stable up to temperatures below the organism's optimal growth temperature, suggesting that stabilization by salts is a common mechanism in this organism (98).

The *Thermoanaerobacterium thermosulfurigenes* xylose isomerase was also stabilized by K^+. This enzyme's $t_{1/2}$ increased sevenfold in the presence of 100 mM KCl (244).

Stabilization by the substrate. Substrate molecules have long been known to stabilize enzymes specifically by stabilizing their active site. This observation is also valid for hyperthermophilic enzymes (9, 98, 182, 187, 309, 328). *T. maritima* dihydrofolate reductase was shown to be strongly kinetically stabilized by substrates, in particular by NADPH (sixfold increase in $t_{1/2}$ at 80°C) (364). NADPH is quite unstable at high temperatures. This strong stabilization of *T. maritima* dihydrofolate reductase by NADPH could also be associated to a strong stabilization of the cofactor.

Pressure effects. Because many high-temperature environments are also high-pressure environments and because microorganisms cannot evade pressure and temperature, all the macromolecular cell components have to be adapted to high pressures. Thus, it is not surprising to find hyperthermophilic organisms that are also barophilic (such as *Thermococcus barophilus* [Table 1]) and to find enzymes that are stabilized and activated by high pressures (e.g., *M. jannaschii* protease and hydrogenase) (129, 247, 248). The theory behind stabilization by pressure says that pressure favors the structure with the smallest volume. Proteins stabilized mainly by hydrophobic interactions are therefore expected to be stabilized at high pressure, whereas proteins stabilized by ionic interactions should be destabilized (247). *P. furiosus* rubredoxin, for example, is stabilized mostly by electrostatic interactions. This enzyme is destabilized by high pressures. Since numerous chemical reactions are performed at high temperatures and pressures, enzyme stability at high pressures has great potential benefits for biocatalysis.

PROTEIN THERMOSTABILITY ENGINEERING

Potential for Protein Thermostabilization

The Q_{10} rule indicates that many reaction rates double with each 10°C increase in temperature. According to this rule, one would expect hyperthermophilic enzymes to have specific activities between 50 and 100 times higher than mesophilic enzymes. What is observed instead is that hyperthermophilic and mesophilic enzymes have approximately the same activities and catalytic efficiencies in their respective physiological conditions. The fact that hyperthermophilic enzymes are not as catalytically optimized catalysts as their mesophilic homologues was attributed to the principle that there had to be a trade-off between thermostability and activity, i.e., that a protein could not be both a hyperstable and a catalytically optimized catalyst. This principle came from the observation of natural proteins. Numerous protein engineering studies performed in the last 10 years suggest instead that protein stability can be enhanced without deleterious effects on activity and that actually stability and activity can be increased simultaneously (116, 346, 374).

The facts that mesophilic enzymes are not optimized in terms of stability and that hyperthermophilic enzymes are not catalytically optimized is probably only a reflection of the absence of selection pressure for these characteristics. Organisms need to have proteins that they are able to degrade, in order to rapidly adapt to changes in environmental stimuli. Hence, mesophilic as well as hyperthermophilic enzymes are only marginally stable under their respective physiological conditions. Unless their substrate is highly unstable, there is no selection pressure in nature for hyperthermophilic enzymes to be highly active. A protein engineer should be able to increase an enzyme's thermostability without negatively affecting its catalytic properties. The limit to this thermostability increase is the upper temperature of protein stability (which is still unknown).

Mechanism of Inactivation, and Choice of Thermostabilization Strategy

Two types of protein stability (thermodynamic and long term) are of interest from an applied perspective. Increasing the thermodynamic thermostability is the main issue when an enzyme is used under denaturing conditions (i.e., high temperatures or organic solvents). Industrialists need active enzymes rather than enzymes that are in a reversibly inactivated state. For other enzymes, for example diagnostics enzymes, it is often long-term stability that needs to be improved (251).

Depending on an enzyme's first inactivation step, i.e., chemical inactivation or unfolding, stabilizing the native, active conformation should involve either substituting temperature-sensitive residues with chemically more stable residues or increasing the enzyme's resistance to unfolding, respectively. A number of attempts at stabilizing (or destabilizing) proteins by SDM have failed because they did not target protein areas that were critical for the unfolding process (173, 174, 337). On the other hand, mutations targeted at areas whose unfolding is limiting in the protein denaturation process can provide extensive stabilization. Good illustrations can be found in the stability studies of *Bacillus stearothermophilus* thermolysin-like protease. This enzyme is irreversibly inactivated by autolysis that is made possible by partial unfolding of local surface areas. Stabilizing mutations were all located on the surface, around one flexible loop located in the β-pleated N-terminal domain (125, 230, 347). The association of eight mutations in the same area resulted in a 340-fold kinetic stabilization of *B. stearothermophilus* thermolysin-like protease at 100°C and did not affect the catalytic activity at 37°C (346). In this enzyme, since the target for autolysis is a loop belonging to the N-terminal domain, any attempt to stabilize the enzyme introducing mutations into the C-terminal domain would have been doomed to fail.

While improving thermodynamic thermostability can have a beneficial effect on long-term stability, other strategies can also be used to increase long-term stability. In this case, the focus for stabilization is decelerating the irreversible inactivation process that usually follows reversible unfolding. The strategies that can be used include (i) eliminating protein diffusion to block aggregation and other bimolecular processes (the most effective approach so far is immobilization), (ii) replacing temperature-sensitive residues by chemically more stable residues (reference 251 and references therein), and (iii) stabilizing the reversibly unfolded state by introducing more hydrophilic residues on the enzyme surface or by adding low-molecular-weight compounds to the solute (i.e., inorganic and organic salts, organic cosolvents, or classical denaturants). Hen egg-white lysozyme slowly deamidates once reversibly unfolded (6). In their 1995 study, Tomizawa et al. (336) replaced Gly residues by Ala in the potentially deamidable Asn-Gly sequences of lysozyme. These mutations generally increased the rate of reversible unfolding, but they decreased the rate of irreversible inactivation and, as a result, stabilized the enzyme against irreversible inactivation. This study is a good illustration of the fact that resistance against irreversible inactivation is not synonymous to thermodynamic thermostability.

Strategies for Stabilization by Site-Directed Mutagenesis

The different stabilization strategies (e.g., better core packing, surface ion pairing, surface loop stabilization, and reduction of the entropy of unfolding) discussed in this review do not have comparable potential for protein stability engineering today. The high conservation of the protein core (mostly defined by α-helices and β-strands) between mesophilic and hyperthermophilic protein homologues suggests that the protein core is already quite optimized for stability, even in mesophilic enzymes. For this reason, mutations in the protein core are often destabilizing, with stabilizing effects often being masked by destabilizing conformational constraints or repulsive van der Waals interactions. The stability gain from α-helix stabilization by introducing residues with high helix propensity is also usually small (373). More promising strategies are directed at the protein surface loops and turns: surface residues are typically involved in less intramolecular interactions than internal residues, and newly introduced residues are less likely to create volume interferences. Substitutions in these areas are accommodated by rearrangements of the neighboring residues more easily than in rigid parts of the protein. Successes in substituting left-handed helical residues with Gly or Asn, in introducing prolines in surface turns or loops, in introducing nonlocal surface ion pairs, and in creating disulfide bridges docking loops to the protein surface are well documented (173, 179, 238, 293, 346). Natural examples along these lines are the docking of the N and C termini and the anchoring of "loose ends" observed in the structures of many hyperthermophilic enzymes (Table 5).

The most promising strategies for thermostabilization using SDM should focus on the surface areas, mostly on loops and turns, and on creating additional nonlocal ion pairs. Loops can be made more rigid by decreasing their intrinsic entropy of unfolding. Two types of mutations, Gly→Xaa and Xaa→Pro, can be introduced (238). In the first case, the newly introduced β-carbon should not interfere with neighboring atoms. In the second case, the substitution site should have specific dihedral angles (φ and ψ) in the regions −50 to −80 and 120 to 180 or −50 to −70 and −10 to −50 and the residue preceding the potential proline should also have a specific conformation. In addition, the proline ring should not interfere with neighboring atoms, and the substitution should not eliminate stabilizing noncovalent interactions. Another method is to anchor the loops to the protein surface, either by noncovalent interactions or with a disulfide bridge. Introducing a disulfide bridge in a semiflexible area of the protein should help compensate for any conformational strain created by the disulfide bridge (230). Ion pairs linking nonadjacent sequences in a protein have a great stabilizing potential, and since they can be designed on the protein surface, they do not tend to create as many destabilizing conformational constraints or repulsive van der Waals interactions as substitutions of buried residues. Metal-mediated protein cross-linking can also be a stabilizing strategy. Such cross-linking stabilizes the protein by reducing the entropy of the denatured state; therefore, it depends on the size of the loop formed by the cross-link. β-sheets offer both the geometry and rigidity required for metal ion chelating by dihistidine sites (253).

Computational Methods in the Design of Stabilizing Strategies

Although not reviewed here in detail, a number of computer algorithms based on physical and chemical principles are being developed to predict protein rigidity and stability and to design stabilizing mutations. Initial results are encouraging and suggest that computer algorithms will become a powerful tool for protein engineers in the near future. Using a computer algorithm based on the dead-end elimination theorem, Malakauskas and Mayo (228) designed a hyperthermostable variant of the streptococcal protein G β1 domain. The variant had a T_m that was increased by more than 20°C and a ΔG_{stab} that was increased by 4.3 kcal/mol at 50°C. Structural analysis of the variant indicated that the main stabilization mechanisms were the release of a strained rotamer conformation, the increased burial of hydrophobic area, and higher helical propensity.

The FIRST software was developed to predict flexible and stable regions in proteins of known structure (161). Based on the hypothesis that thermostable enzymes are more rigid than their less stable counterparts, we are now using mesophilic, thermophilic, and hyperthermophilic adenylate kinases as model enzymes to test the ability of FIRST to predict the interactions important for thermostability. The energy levels at which breakups occur in the hydrogen bond networks are related to the relative thermostability of the enzymes. We will attempt to identify H bonds that could be responsible for the higher stabilities of the thermophilic and hyperthermophilic adenylate kinases, The potential role of these H bonds in stabilization will be tested by SDM.

The last 10 years have seen the development of molecular dynamics (MD) simulations applied to protein unfolding (53, 54, 71, 74, 155, 200, 201, 212–214, 360). Due to limiting computing power, these simulations have been confined to the study of very small proteins (e.g., barnase and rubredoxin) or of protein fragments. Multiple MD trajectories of the same protein under identical conditions confirm the newest description of protein unfolding as a funnel-like pathway (155, 200, 214): the trajectories typically differ widely from one another, but a statistically preferred unfolding pathway emerges from these comparisons, at least up to an early unfolding intermediate (200, 214). The structural properties of this intermediate are often similar to those deduced from unfolding experimental data (200, 214). They are also often similar for simulations run with different algorithms, under different environmental conditions (e.g., different temperatures, different solvent conditions) (71, 214, 360), or with homologous proteins of different thermostabilities (201). These observations suggest that MD simulations can provide clues about how enzymes start to unfold and which regions to target for stabilization (71, 201). The comparison of MD simulations reproducing the thermal movements at room temperature and of MD simulations inducing unfolding allows the distinction between movements related to catalysis and movements related to unfolding, and it allows the identification of regions that could sustain stabilization without affecting activity (71).

Continual algorithmic improvements and improvements in computer power and speed should extend the use of MD simulations to bigger proteins (73). Investigation by SDM of

hypotheses drawn from MD simulations and comparisons between MD simulations and nuclear magnetic resonance (NMR) or hydrogen exchange data should soon provide us with a clearer understanding of how MD can be used to study protein thermostability and flexibility.

Directed Evolution

Directed evolution is a powerful engineering method, and it is now often used to design enzymes with increased thermostability (297). This method has also been used for a variety of other needs, such as developing enzymes active in solvents, enzymes with altered substrate specificity (12, 61), or thermostable enzymes with high activity at 20 to 37°C. Enzymes improved by directed evolution have already been commercialized (297). A major advantage of this engineering method over SDM is that no knowledge about enzyme structure is necessary. Since there is still much to be learned about thermostabilization mechanisms, SDM approaches often yield disappointing results. To date, directed evolution has proven to be a much more powerful engineering method than SDM.

Two directed-evolution method have been developed. The first one, DNA shuffling, involves random fractionation of a gene with DNase I followed by PCR-mediated reassembly of the full gene. This method introduces point mutations at a rate of approximately 0.7% (314). Each round of mutagenesis is followed by screening for the desirable trait. This mutagenesis procedure can be accelerated by shuffling a family of genes together (70). One limitation to any random-mutagenesis method is the generation of deleterious mutations. For this reason, mutagenesis rates must be kept low to avoid multiple mutations in a single gene copy. Shuffling several homologous genes provides sequence diversity as well as functional diversity, and hence it can increase the mutagenesis rate without increasing the risk of creating deleterious variants. Genes from mesophiles and hyperthermophiles can be shuffled to select for the combination of high catalytic activity at mesophilic temperatures and high stability.

The second evolution method involves error-prone PCR together with DNA shuffling. In short, sequence diversity is created by one or several cycles of error-prone PCR, with each cycle being followed by screening for the desirable trait. Variants with the best characteristics are then recombined by the DNA-shuffling technology. A couple of examples illustrate remarkably clearly the power of this technology. *Bacillus subtilis* substilisin E was converted into an equivalent of its thermophilic homologue thermitase through a succession of one error-prone PCR, one step of DNA shuffling (to combine the properties of the best variants), and four additional rounds of error-prone PCR. The evolved enzyme was 15 times more active than subtilisin E at 37°C, it showed a 16°C increase in T_{opt}, and its $t_{1/2}$ at 65°C was more than 200 times that of subtilisin E (Fig. 8) (374). Sequence information and structural analysis indicated that most of the stabilizing mutations were in loops connecting elements of secondary structure (i.e., the most variable regions). The fact that some of these substitutions could not be modeled illustrates the limitations of SDM engineering approaches. In another experiment, *B. subtilis p*-nitrobenzyl esterase thermostability was enhanced through five cycles of error-prone PCR followed by one step of DNA shuffling (116). The evolved esterase showed a 14°C increase in T_m and a 10°C increase in T_{opt}, and it was more active than the wild-type enzyme at any temperature. Although activity was screened at 30°C (instead of higher temperatures) after each mutagenesis cycle, increases in T_m always resulted in increased T_{opt}. In both sets of experiments, *B. subtilis* subtilisin E and esterase variants could be generated that were significantly more thermostable while still as active at low temperatures as the wild-type enzyme. These results suggest that activity and thermostability are at least partially independent properties and that they can be optimized in the same enzyme (116).

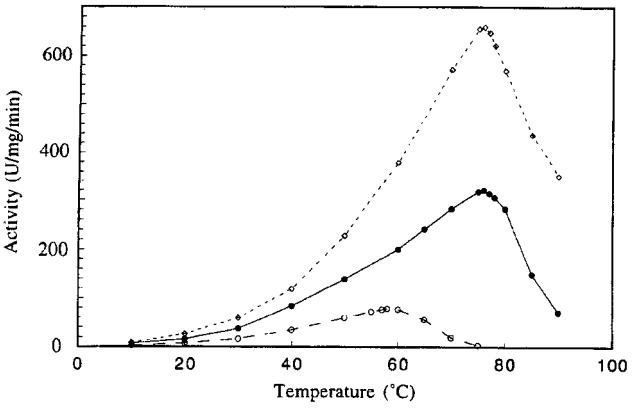

FIG. 8. Activity-temperature profiles of wild-type subtilisin E (○), subtilisin E variant 5-3H5 (●), and thermitase (◇). Variant 5-3H5 was obtained by directed evolution. It is the subtilisin E eightfold mutant derivative Pro14Leu-Asn76Asp-Asn118Ser-Ser161Cys-Gly166Arg-Asn181Asp-Ser194Pro-Asn218Ser. Reprinted from reference 374 with permission of the publisher.

HYPERTHERMOPHILIC ENZYMES WITH COMMERCIAL APPLICATIONS

The characterization of *T. aquaticus Taq* DNA polymerase followed by the quick popularization of PCR-related technologies was instrumental in the ever-growing interest of the scientific and industrial communities in thermophilic and hyperthermophilic enzymes. Only a few of today's industrial and specialty enzymatic processes utilize thermophilic and hyperthermophilic enzymes. The ever-growing number of enzymes characterized from hyperthermophilic organisms and the recent advent of powerful protein engineering tools suggest that thermophilic and hyperthermophilic enzymes will see more and more use in a variety of applications. This section assesses the interest thermophilic and hyperthermophilic enzymes hold for a few major industrial and specialty enzyme applications.

Applications in Molecular Biology

DNA polymerases. The cloning and expression of *T. aquaticus Taq* DNA polymerase in *E. coli* was instrumental in the development of the PCR technology. Thermophilic DNA polymerases have since been cloned and characterized from a number of thermophiles and hyperthermophiles. The multiple applications of the PCR technology make use of two major properties of these DNA polymerases: processivity and fidelity. Devoid of 3′-5′ proofreading exonuclease activity, the *Taq* polymerase synthesizes DNA faster (but with a higher error

TABLE 9. Examples of thermophilic and hyperthermophilic enzymes with applications as molecular biology reagents

Enzyme	Origin	Applications	Properties	Source or reference(s)
Taq polymerase	*T. aquaticus*	PCR technologies	Optimal activity at 75°C, pH 9.0	26, 199
Vent DNA polymerase	*T. litoralis*		Optimal activity at 75°C, proofreading activity	2, 271
Deep Vent DNA polymerase	*P. furiosus*		Optimal activity at 75°C, proofreading activity; $t_{1/2}$, 23 h (95°C)	2, 343
C. therm DNA polymerase	*Carboxydothermus hydrogenoformans*	Reverse transcription-PCR	Reverse transcriptase activity, 3′→5′ proofreading activity; optimal activity as 60–70°C	Roche Molecular Biochemicals
DNA polymerase	*Thermus thermophilus*		Reverse transcriptase activity	Roche Molecular Biochemicals
Pfu DNA ligase	*P. furiosus*	Ligase chain reaction and DNA ligations	Active at 45–80°C; $t_{1/2}$ >60 min (95°C)	Stratagene
Tcs DNA ligase	*Thermus scodoductus*	Ligase chain reaction	Optimal activity at 45°C	Roche Molecular Biochemicals
DNA binding protein Ssod7	*S. solfataricus*	Time-reducing and specificity-enhancing in DNA-DNA hybridizations; locking of antisense oligonucleotide to target sequence	Sequence-aspecific DNA binding; ATP-independent, homology-dependent DNA annealing at 60°C	123
Serine protease (PRETAQ)	*Thermus* strain Rt41A	DNA and RNA purifications; cellular structures degradation prior to PCR	Optimal activity at 90°C, pH 8.0; $t_{1/2}$, 20 min (90°C) (+$CaCl_2$)	Life Technologies
Protease S	*P. furiosus*	Protein fragmentation for sequencing	Optimal activity at 85–95°C, pH 6.0–8.0; 80% active after 3 h (95°C)	TaKaRa Biomedicals
Methionine aminopeptidase	*P. furiosus*	Cleavage of the N-terminal Met in proteins	Optimal activity at 85–95°C, pH 7.0–8.0; stable for 1 h (75°C)	TaKaRa Biomedicals
Pyroglutamate aminopeptidase	*P. furiosus*	Cleavage of the N-terminal L-pyroglutamate in proteins	Optimal activity at 95–100°C, pH 6.0–9.0; 95% active after 2.5 h (75°C)	TaKaRa Biomedicals
Carboxypeptidase	*S. solfataricus*	C-terminal sequencing	Broad specificity (can release basic, acidic, and aromatic residues); stable in solvents at 40°C	66
Alkaline phosphatase	*T. neapolitana*	Enzyme-labeling applications where high stability is required	Optimal activity at 85°C, pH 9.9; $t_{1/2}$, 4 h (90°C) (+ Co^{2+})	87

rate) than do enzymes with 3′-5′ proofreading activity. *Taq* DNA polymerase's high processivity make it the enzyme of choice for sequencing or detection procedures. Proofreading enzymes (such as Vent and Deep Vent polymerases [Table 9] are preferred when high fidelity is required. While thermophilic DNA polymerases have partially replaced mesophilic enzymes in a few applications, most applications were developed after the advent of PCR (e.g., PCR in situ hybridization and reverse transcription-PCR). These applications have been extensively reviewed (135, 198, 308).

DNA ligases. Thermophilic DNA ligases are commercially available (Table 9). Optimally active in the range 45 to 80°C, they represent an excellent addition to PCR technology. These enzymes are perfect for ligating adjacent oligonucleotides that are hybridized to the same target DNA. This property can be used for ligase chain reaction (a DNA amplification method), for mutational analysis (by oligonucleotide ligation assay), or for gene synthesis (from overlapping oligonucleotides).

Other research enzymes. A number of thermophilic and hyperthermophilic proteases are now used in molecular biology and biochemistry procedures. Some proteins, in particular thermophilic proteins, resist proteolytic digestion at moderate temperatures (20 to 60°C). They only start to unfold and to become sensitive to proteolytic attack above 70°C. Proteases like the *Thermus* Rt41A serine protease PRETAQ (Table 9), which is rapidly inactivated by EGTA, can be used in DNA and RNA purification procedures. Once inactivated, PRETAQ will not interfere with other enzymes during further treatment of the DNA or RNA. This enzyme can be used as an adjunct to PCR to break down cellular structures prior to PCR. The *P. furiosus* protease S has a broad specificity, so it is used to fragment proteins before peptide sequencing. Other hyperthermophilic proteases are used for protein N- or C-terminal sequencing (Table 9). Numerous thermophilic restriction endonucleases are now commercialized. Most of them, isolated from *Bacillus* and *Thermus* strains, are optimally active in the range of 50 to 65°C.

Applications in Starch Processing

Most industrial starch processes involve starch hydrolysis into glucose, maltose, or oligosaccharide syrups. These syrups are then used as fermentation syrups to produce a variety of chemicals (e.g., ethanol, lysine, and citric acid). High-fructose corn syrup (HFCS) is produced by the enzymatic isomerization of high-glucose syrup. Starch bioprocessing usually involves two steps, liquefaction and saccharification, both run at high temperatures. During liquefaction, starch granules are gelatinized in a jet cooker at 105 to 110°C for 5 min in aqueous solution (pH 5.8 to 6.5) and then partially hydrolyzed at α-1,4

linkages with a thermostable α-amylase at 95°C for 2 to 3 h. Temperature and pH controls are critical at this stage. If the gelatinization temperature drops below 105°C, incomplete starch gelatinization occurs, which causes filtration problems in the downstream process. If the gelatinization temperature increases much above 105°C, the α-amylases typically used (from *Bacillus licheniformis* and *B. stearothermophilus*) are inactivated. The enzymes are also inactivated at pHs below 5.5, and higher pH values cause by-product and color formation. After liquefaction, the pH is adjusted to 4.2 to 5.0 and the temperature is lowered to 55 to 60°C for the saccharification step. During saccharification (which runs for 24 to 72 h), the liquefied starch is converted into low-molecular-weight saccharides and ultimately into glucose or maltose. Glucose syrups (up to 95 to 96% glucose) are produced using pullulanase and glucoamylase in combination, while maltose syrups (up to 80 to 85% maltose) are produced using pullulanase and β-amylase (25, 69).

The natural pH of the starch slurry is approximately 4.5. Present starch-processing methods require adjusting the pH of the starch slurry to 5.8 or above for starch liquefaction and then reducing it to 4.2 to 4.5 for the saccharification step. These two pH adjustments increase chemical costs. They also create the need for ion-exchange refining of the final product to remove the added salts. An α-amylase able to work at lower pH would reduce these costs, simplify the process, and reduce the formation of high-pH by-product (e.g., maltulose) (69). The pullulanase, isoamylase, β-amylase, and glucoamylase used in industrial starch processing originate from mesophilic organisms and are only marginally stable at 60°C. There is a need today for thermostable pullulanases, β-amylases, and glucoamylases. α-Amylases which do not require added Ca^{2+} and which operate above 100°C at acid pH values are also targeted for improved processing. Increasing the saccharification process temperature would result in many benefits: (i) higher substrate concentrations, (ii) decreased viscosity and lower pumping costs, (iii) limited risks of bacterial contaminations, (iv) increased reaction rates and decrease of operation time, (v) lower costs of enzyme purification, and (vi) longer catalyst half-life, due to increased enzyme thermostability.

α-Amylases. Able to grow at temperatures in the range 80 to 110°C, hyperthermophiles are great potential sources for α-amylases functioning in the same temperature range. Representatives of the most thermophilic α-amylases known are listed in Table 10 (see also reference 263). Their optimal activities range from 80 to 100°C at pH 4.0 to 7.5. An optimal catalyst for starch liquefaction should be optimally active at 100°C and pH 4.0 to 5.0 and should not require added Ca^{2+} for stability. None of the enzymes listed in Table 10 present these combined characteristics. Greater characterization of some of these enzymes is needed to determine if they are stable and retain significant activity at pH 4.0. With the recent development of powerful engineering tools (see above), we can expect that an α-amylase with these features will soon be available. Some of the α-amylases listed in Table 10 were initially believed to be independent of calcium. EDTA has no effect on *P. furiosus* α-amylase activity and stability at temperatures below 90°C. A 30-min EDTA treatment at 90°C followed by extensive dialysis removes part of the enzyme-linked Ca^{2+} and partially inactivates the enzyme. Full activity is restored by adding $CaCl_2$ to the enzyme and heating the enzyme solution for 30 min at 90°C (A. Savchenko, C. Vieille, and J. G. Zeikus, unpublished). At least 80% identical in sequences to the *P. furiosus* α-amylase, the *P. kodakaraensis* and *T. profundus* enzymes are likely to be calcium dependent. Despite its Ca^{2+} dependency, *P. furiosus* α-amylase is highly stable and active at 100°C in the absence of added Ca^{2+} (Table 10), suggesting that starch liquefaction could soon be performed in the absence of Ca^{2+}.

β-Amylases. Due to the risk of unwanted side-reactions at alkaline pHs and to the length of the saccharification processes (48 to 72 h), thermophilic β-amylases will improve starch saccharification only if they are active at acidic pHs and only if they can reduce the saccharification time by increasing the reaction rate. Two sources of thermophilic β-amylases exist (Table 10). If intermediate temperatures (70 to 80°C) are required to limit the browning side reactions, *T. thermosulfurigenes* β-amylase is an option, since it is stable and 70% active at pH 4.0 (154). Optimally active at 95°C and pH 4.3 to 5.5 and in the absence of Ca^{2+}, *T. maritima* β-amylase could be a good enzyme for testing the impact of high temperatures on the saccharification process. This enzyme, however, has not been cloned or characterized in detail. Production of maltose syrups using these β-amylases would still require a compatible debranching enzyme.

Glucoamylases and α-glucosidases. Hyperthermophiles typically hydrolyze starch via an α-amylase and/or an amylopullulanase (Table 10). Oligosaccharides are then degraded intracellularly by an α-glucosidase. Like β-amylases, glucoamylases are rare in thermophiles and hyperthermophiles. Glucoamylases have been purified from only a few anaerobes, and a putative glucoamylase gene has been identified in the *M. jannaschii* genome (21). Extensive work remains to determine if the putative *M. jannaschii* glucoamylase gene is functional and if its product has catalytic properties close to the properties required for starch saccharification. Stable in the presence of starch, the *T. thermosaccharolyticum* glucoamylase (Table 10) represents an alternative catalyst for the development of a starch saccharification process at 70 to 75°C.

Pullulanases and amylopullulanases. Type I pullulanases (hydrolyzing only α-1,6-glucosidic linkages) are used as debranching enzymes in starch saccharification. Until recently, type I pullulanases were known only in mesophilic organisms and in thermophilic aerobic bacteria. A selection of thermophilic type I pullulanases and some of their properties are listed in Table 10. The *Thermotoga maritima* enzyme is the only one characterized in a hyperthermophile. These pullulanases are all optimally active at acidic pHs. Their potential for starch saccharification remains to be tested. These pullulanases seems to have temperature and pH requirements compatible with those of recently characterized thermophilic glucoamylase and β-amylases (Table 10).

Amylopullulanases (or type II pullulanases) show dual specificity for starch α-1,4- and α-1,6-glucosidic linkages (234). For this reason, they cannot be used as debranching enzymes in maltose and glucose syrup productions. Amylopullulanases have been suggested, however, as alternative enzymes to replace α-amylases during starch liquefaction for producing fermentation syrups. Since certain amylopullulanases specifically produce maltose, maltotriose, and maltotetraose (DP2 to

TABLE 10. Examples of thermophilic and hyperthermophilic enzymes with potential applications in starch processing

Enzyme	Origin	Properties	Reference
α-Amylase	*Desulfurococcus mucosus*	Optimal activity at 100°C, pH 5.5[a]	56
	Pyrococcus furiosus	Optimal activity at 100°C, pH 5.5–6.0; sp act, 3,900 U/mg (98°C); $t_{1/2}$, 13 h (98°C)	85
	Pyrococcus woesei	Optimal activity at 100°C, pH 5.5	188
	Pyrodictium abyssi	Optimal activity at 100°C, pH 5.0	263
	Staphylothermus marinus	Optimal activity at 100°C, pH 5.0[a]	56
	Thermococcus profundus	Optimal activity at 80°C, pH 4.0–5.0	65, 205
	Dictyoglomus thermophilum	Optimal activity at 90°C, pH 5.5	109
	Thermotoga maritima	Optimal activity at 85–90°C, pH 7.0	263
Pullulanase	*Bacillus flavocaldarius*	Optimal activity at 75–85°C, pH 6.3; $t_{1/2}$, 10 min (107°C)	170, 325
	Thermotoga maritima	Optimal activity at 90°C, pH 6.0	263
	Thermus caldophilus	Optimal activity at 75°C, pH 5.5; $t_{1/2}$, 72 h (78°C, pH 6.0)	177
	Fervidobacterium pennavorans	Optimal activity at 80–85°C, pH 6.0; $t_{1/2}$, 2 h (80°C) and > 50 h (80°C + starch)	27, 187
Amylopullulanase	*Desulfurococcus mucosus*	Optimal activity at 100°C, pH 5.0[a]	56
	ES4	Optimal activity on starch at 120°C, pH 5.5–6.5; $t_{1/2}$, 6.5 h (98°C) and 20 h (98°C) (+$CaCl_2$)	298
	Pyrococcus furiosus	Optimal activity at 105°C, pH 6.0; V_{max}(starch), 88 U/mg (98°C), $t_{1/2}$, 44 h (90°C) (5 mM $CaCl_2$)	86
	Thermococcus celer	Optimal activity at 90°C, pH 5.5[a]	56
	Thermococcus litoralis	Optimal activity at 117°C, pH 5.5 (5 mM $CaCl_2$)	43
	Thermococcus hydrothermalis	$t_{1/2}$, >8 h (95°C) and 1 h (105°C)	97, 113
	Thermoanaerobacter ethanolicus	Optimal activity at 90°C, pH 5.5; sp act (starch), 175 U/mg (60°C); $t_{1/2}$, 40 min (90°C)	235, 236
Glucoamylase	*Clostridium thermosaccharolyticum*	Optimal activity at 70°C, pH 5.0; >90% active after 6 h (70°C)	312
	Methanococcus jannaschii	Putative gene identified in the genome sequence	21
	Thermoanaerobacterium thermosaccharolyticum	Optimal activity at 50–60°C, pH 4.0–5.5; stable for 8 h (65°C)	112
α-Glucosidase	*Thermoanaerobacter ethanolicus*	Optimal activity at 75°C, pH 5.0–5.5; $t_{1/2}$, 46 h (60°C) and 35 min (75°C)	288
β-Amylase	*Thermotoga maritima*	Optimal activity at 95°C, pH 4.3–5.5; $t_{1/2}$, ca. 30 min (90°C)	300
	Thermoanaerobacterium thermosulfurigenes	Optimal activity at 75°C, pH 5.5–6.0; stable at pH 3.5–6.5; >80% active after 1 h (75°C)	154, 304
CGTase	*Thermococcus* sp.	Optimal activity at 90–100°C, pH 5.0–5.5 (can work at pH 4.5); sp act in CD synthesis, 1,400 U/mg (90°C) (between 69 and 90% α-CD formed); $t_{1/2}$, 40 min (110°C)	326
Xylose isomerase	*Thermoanaerobacterium thermosulfurigenes*	Optimal activity at 80°C, pH 7.5; $t_{1/2}$, 35 min (85°C)	204, 244
	Thermoanaerobacterium strain JW/SL-YS 489	Optimal activity at 80°C, pH 6.8; $t_{1/2}$, 1 h (80°C)	221
	Thermus aquaticus	Optimal activity at 85°C, pH 7.0; $t_{1/2}$, 4 days (70°C)	210
	Thermotoga maritima	Optimal activity at 100–110°C; $t_{1/2}$, 10 min (120°C)	44
	Thermotoga neapolitana	Optimal activity at 97°C, pH 7.1; $t_{1/2}$, 2.5 h (80°C)	137, 313, 350

[a] Data obtained with crude enzyme (either culture supernatant or cell extract).

DP4) as the major end products of starch degradation, they have been suggested as catalysts in a one-step liquefaction-saccharification process for the production of high-DP2-to-DP4 syrups (289). Because amylopullulanases purified from the hyperthermophiles *P. furiosus*, ES4, *Thermococcus litoralis*, and *T. hydrothermalis* are active at high temperatures (105 to 120°C) and at low pHs and because they are exceptionally thermostable, they are strong candidates for this process (Table 10). Their low activity levels on starch, however, represent a major limitation to their use in starch liquefaction. As an example, at 98°C the *P. furiosus* α-amylase is approximately 44 times more active on starch than the *P. furiosus* amylopullulanase (Table 10).

Cyclomaltodextrin glucanotransferases. Cyclomaltodextrin glycosyltransferases (CGTases) convert oligodextrins into cyclodextrins (CDs). α-, β-, and γ-CDs are cyclic compounds composed of 6, 7, or 8 α-1,4-linked glucose molecules, respectively. The internal cavities of CDs are hydrophobic, and they can encapsulate hydrophobic molecules. This property makes CDs suitable for numerous applications in the food, cosmetic,

TABLE 11. Catalytic parameters of *T. thermosulfurigenes* xylose isomerase at 65°C and *T. neapolitana* xylose isomerase at 80°C and of their mutant derivatives[a]

Xylose isomerase	Glucose				Xylose			
	K_m (mM)	V_{max} (U/mg)	K_{cat} (min^{-1})	K_{cat}/K_m	K_m (mM)	V_{max} (U/mg)	K_{cat} (min^{-1})	K_{cat}/K_m
T. thermosulfurigenes								
Wild type	110	12.8	640	5.8	12	21.6	1,100	97.2
W138F	65	19.4	970	15.0	46	12.2	620	13.6
V185T	91	17.6	880	9.7	13	14.5	740	55.4
W138F/V185T	29	19.0	950	32.9	36	15.3	780	32.9
T. neapolitana								
Wild type	139	14.5	737	5.3	11	14.1	717	64.4
W138F	133	15.9	808	6.1	13	8.1	410	31.1
V185T	62	20.0	1,018	16.4	15	15.6	795	54
W138F/V185T	52	12.7	644	12.5	14	10.4	530	38.9

[a] Data from references 245 and 313.

and pharmaceutical industries, where they are used to capture undesirable tastes or odors, stabilize volatile compounds, increase a hydrophobic substance's water solubility, and protect a substance against unwanted modifications. CD production involves α-amylase-catalyzed starch liquefaction followed by CD formation using a mesophilic CGTase. A CGTase was recently characterized in a *Thermococcus* species (Table 10). This enzyme is highly stable at 100 to 105°C. Optimally active at 90 to 100°C under acidic conditions, it also shows high α-amylase activity. This *Thermococcus* CGTase could probably be used to develop a one-step CD production in which it would replace α-amylase for starch liquefaction.

Xylose isomerases. Used in HFCS production, xylose isomerases (also called glucose isomerases) catalyze the equilibrium isomerization of glucose into fructose. Xylose isomerases represent the first large-scale industrial use of immobilized enzymes (72). The isomerization process is typically run in packed-bed reactors at 58 to 60°C for 1 to 4 h, and the converted syrup reaches 42% fructose. An additional strong acid cation-exchange chromatographic step further increases the fructose concentration to 55%—the concentration required by most of today's HFCS applications. The glucose-to-fructose conversion rate at equilibrium is shifted toward fructose at high temperatures: at 60 and 90°C, the fructose contents at equilibrium are 50.7% and 55.6%, respectively. Two major parameters are responsible for the moderate temperatures used in this process. (i) the xylose isomerases currently used are only moderately stable at 60°C. (Due to enzyme inactivation, the reactors need to be repacked every 2 months.) (ii) Unwanted side reactions (Maillard reactions) occur at high temperatures and alkaline pHs. For this last reason, HFCS producers are interested in a process that would take place at temperatures close to those of today's processes but at a lower pH. HFCS producers are also interested in using a more stable enzyme.

Highly thermophilic and thermostable xylose isomerases have been characterized from *Thermus thermophilus, Thermus aquaticus, Thermotoga maritima*, and *Thermotoga neapolitana* (Table 10). Despite their optimal activity at elevated temperatures (95 to 100°C) and their attractive, high catalytic efficiency at 90°C, the *T. maritima* and *T. neapolitana* xylose isomerase are active only at neutral pH and are only marginally active (10 to 15%) between 60 and 70°C (350). Based on structural information, Meng et al. (245) have mutagenized the *Thermoanaerobacterium thermosulfurigenes* xylose isomerase and increased its catalytic efficiency on glucose (Table 11). Introducing the same substitutions in the *T. neapolitana* xylose isomerase also significantly increased this enzyme's catalytic efficiency on glucose (Table 11). The *T. neapolitana* xylose isomerase Val185Thr mutant derivative is now being used as the template to generate variant enzymes with increased activity at acidic pHs.

Other Industrial and Biotechnological Applications

Cellulose degradation and ethanol production. Cellulose is the most abundant and renewable nonfossil carbon source on Earth (67). Considerable effort has been spent to create an economically feasible ethanol production from cellulose, but without much success. Typically embedded in a network of hemicellulose and lignin, cellulose requires an alkaline pretreatment to become accessible to enzyme action. An enzymatic saccharification step makes cellulose and its degradation products suitable for ethanologenic yeast or bacterial fermentations. One of the main limitations to this three-step process is the low activity (and high cost) of the cellulases used. Since cellulose's alkaline pretreatment is performed at high temperatures, hyperthermophilic cellulases should be the best candidate catalysts for cellulose degradation. The production of cellulases by hyperthermophiles is rare, however. Only recently have endoglucanases and cellobiohydrolases been characterized in the *Thermotogales* (Table 12). Among the enzymes characterized, pairings of endoglucanase and cellobiohydrolase, optimally active either at 95 or at 105°C, represent interesting enzyme combinations to be tested in cellulose processing.

Industrial ethanol production is currently based on corn starch that is first liquefied and saccharified (see above). The oligosaccharide syrup is then used as a feedstock for ethanologenic yeast fermentation. The use of cellulases to increase the yields of starch liquefaction and saccharification has been described (211). Since starch liquefaction is performed at high temperatures, using thermophilic endoglucanases during this step is an option.

TABLE 12. Thermophilic and hyperthermophilic enzymes with potential industrial applications

Enzyme	Origin	Potential application(s)	Properties	Reference(s)
Endo-1,4-β-glucanase	*T. maritima*	Cellulose degradation	Optimal activity at 95°C, pH 6.0–7.5; $t_{1/2}$, 2 h (95°C)	42, 218
	T. neapolitana	Cellulose degradation	Optimal activity at 95°C, pH 6.0; sp act, 1,219 U/mg[a] on CMC[b]	32
	T. neapolitana	Cellulose degradation	Optimal activity at 106°C, pH 6.0–6.6; sp act: 1,536 U/mg on CMC; $t_{1/2}$, 130 min(106°C); transglycosylation activity	32
Cellobiohydrolase	*T. maritima*	Cellulose degradation	Optimal activity at 95°C, pH 6.0–7.5; $t_{1/2}$, 30 min (95°C)	42
Cellobiohydrolase	*Thermotoga* sp. strain FjSS3-B.1	Cellulose degradation	Optimal activity at 105°C. pH 7.0; $t_{1/2}$, 70 min (108°C)	286
Endoxylanase	*Thermotoga* sp. strain FjSS3-B.1	Paper pulp bleaching	Optimal activity at pH 6.5; $t_{1/2}$, 22 h (90°C) and 12 h (95°C)	294
	T. thermarum (enzyme II)	Paper pulp bleaching	Optimal activity at 90–100°C, pH 7.0; sp act, 19.5 U/mg; inactive on CMC	324
	Thermoanaerobacterium saccharolyticum	Paper pulp bleaching	Optimal activity at 70°C, pH 5.5–6.0; $t_{1/2}$, 35 min (80°C)	208 207
	Bacillus sp. strain 3D	Paper pulp bleaching	Optimal activity at 75°C, pH 6.0 (3,300 U/mg); stable at 80°C for 24 h (pH 9.0) and 10 h (pH 12.5)	126
β-Xylosidase/ arabinofuranosidase	*Thermotoga* sp. strain FjSS3-B.1	Paper pulp bleaching	Optimal activity at pH 7.0; $t_{1/2}$, 4 h (98°C) (+ 40 mg of bovine serum albumin per ml)	285, 287
β-Mannanase	*Rhodothermus marinus*	Softwood pulp bleaching; coffee bean treatment and coffee extraction	Optimal activity at 85°C, pH 5.0–6.5; $t_{1/2}$, 45.3 h (85°C) and 4.2 h (90°C)	118
β-Xylosidase	*Thermoanaerobacterium saccharolyticum*	Carbohydrate synthesis; xylose production	Optimal activity at 70°C, pH 5.5; $t_{1/2}$, 55 min (75°C); β-1,4, β-1,3, and β-1,1 transglycosylation activities	11, 209
β-Glucosidase	*P. furiosus*	Regio- and stereoselective glucoconjugate synthesis by transglycosylation	Optimal activity at 102–105°C, pH 5.0; K_m of 20 mM and V_{max} of 470 U/mg (95°C) on cellobiose; $t_{1/2}$, 85 h (100°C) and 13 h (110°C)	176
Trehalose synthase	*Thermus caldophilus*	α, α-Trehalose production; used in food, cosmetics, medicine, and organ preservation	Producs 86% α, α-trehalose from 95% maltose at 40°C	189
Hydantoinase	*Bacillus stearothermophilus*	Synthesis of D-amino acids as intermediates in the production of semi-synthetic antibiotics, peptide hormones, pyrethroids, and pesticides	Optimal activity at 65°C, pH 8.0 (+ Mn^{2+}); $t_{1/2}$, 30 min (80°C)	206
Esterase	*P. furiosus*	Transesterification and ester synthesis	Optimal activity at 100°C, pH 7.6; $t_{1/2}$, 34 h (100°C) and 2 h (120°C)	157
Aldolase	*S. solfataricus*	Synthetic chemistry: C—C bond synthesis	Specific for nonphosphorylated substrates; Optimal activity at 90°C; $t_{1/2}$, 7.8 h (90°C) and 2.5 h (100°C)	45
Cytochrome P450	*S. solfataricus*	Selective regio- and stereospecific hydroxylations in chemical synthesis	T_m, 91°C; substrate unknown	242
Secondary alcohol dehydrogenase	*Thermoanaerobacter ethanolicus*	Chemical synthesis: production of enantiomerically pure chiral alcohols	Optimal activity at >90°C; $t_{1/2}$, 1.7 h (90°C)	46, 47, 339
Pectin methylesterase	*T. thermosulfurigenes*	Fruit juice clarification, wine making	Optimal activity at 70°C, pH 6.5; $t_{1/2}$, 30 min (70°C)	296

Continued on following page

TABLE 12—*Continued*

Enzyme	Origin	Potential application(s)	Properties	Reference(s)
Polygalacturonate hydrolase	*T. thermosulfurigenes*	Fruit juice clarification, wine making	Optimal activity at 75°C, pH 5.5; $t_{1/2}$, 30 min (70°C)	296
Pectate lyase	*Thermoanaerobacter italicus*	Fruit juice clarification, wine making, fruit and vegetable maceration	Optimal activity at 80°C; stable at 70°C for 2 h	194
β-Galactosidase	*T. maritima*	Production of lactose-free dietary milk products	Optimal activity at 80°C, pH 5.3	111
β-Fructosidase	*T. maritima*	Confectionery industry; production of invert sugar; hydrolysis of inulin to produce HFCS	Optimal activity at 90–95°C, pH 5.5; no metal requirement; hydrolyzes sucrose (no product inhibition) and inulin	217
β-1,4-Endoglucanase	*P. furiosus*	Animal feed: digestion of barley β-glucan	Hydrolyzes β-1,4 linkages in (1→3),(1→4)-β-D-glucans and cellulose; optimal activity at 100°C, pH 6.0; $t_{1/2}$, 40 h (90°C) and 1.6 h (105°C)	20
Phytase	*Bacillus* sp. strain DS11	Phytate degradation in animal feed	Optimal activity at 70°C, pH 5.0–5.5; $t_{1/2}$, 10 min (90°C) (+ 5 mM $CaCl_2$)	178
Keratinase	*Fervidobacterium pennavorans*	Degradation of poultry feathers and production of rare amino acids (i.e., serine and proline)	Optimal activity at 80°C, pH 10.0	105
Chitinase	*Streptomyces thermoviolaceus*	Chitin utilization as a renewable resource; production of biologically active oligosaccharides	Optimal activity at 80°C, pH 9.0; transglycosylation activity	340
α-Galactosidase	*T. maritima*	Oil and gas industry: well stimulation by galactomannan hydrolysis; sugar beet processing: removal of raffinose from sucrose syrups; oligosaccharide synthesis through glycosyl transfer reactions	Optimal activity at 90–95°C, pH 5.0–5.5; $t_{1/2}$, 48 h (80°C) and 70 min (90°C); hydrolyzes raffinose and melibiose	219
Alkaline phosphatase	*T. neapolitana*	Diagnostics: enzyme-labeling applications where high stability is required	Optimal activity at 85°C, pH 9.9; $t_{1/2}$, 4 h (90°C) (+ Co^{2+}); Sp act, 1,352 U/mg (85°C) with pNPP[b] as substrate	87

[a] 1 U corresponds to an OD_{430} change of 0.1/min.
[b] CMC, carboxymethyl cellulose.
[c] pNPP, *p*-nitrophenyl phosphate.

Paper pulp bleaching. In the paper production process, pulping is the step during which wood fibers are broken apart and most of the lignin is removed. Pulping often corresponds to a chemical hot-alkali treatment of the wood fibers. The remaining lignin is removed by a multistep bleaching process. Performed with chlorine and/or chlorine dioxide at high temperatures, pulp bleaching generates high volumes of polluting wastes (333). The amount of chemical used—and, therefore, the resulting pollution—can be reduced if the paper pulp is pretreated with hemicellulases. Since pulping and bleaching are both performed at high temperatures, the paper industry needs thermophilic hemicellulases, preferably those active above pH 6.5 or pH 7.0 (358). Hyperthermophilic hemicellulases have only been characterized in the *Thermotogales* (Table 12). These enzymes are active at pHs around 7.0. It is not known if they can withstand higher pHs. It is interesting that the *Bacillus* 3D endoxylanase is at least 100 times more active than the *Thermotoga thermarum* enzyme (Table 12). Although less thermophilic than the *Thermotoga* endoxylanases, the *Bacillus* enzyme is highly stable under alkaline conditions. Other hemicellulases (e.g., α-glucuronidase, β-mannanase, α-L-arabinofuranosidase, and galactosidases) have been shown to contribute to the enzymatic treatment of the pulp. Not many of these enzymes have been characterized from thermophiles and hyperthermophiles (Table 12).

Chemical synthesis. Production of the dipeptide aspartame (L-aspartyl-L-phenylalanine methyl ester) by using thermolysin (68, 172) is the only chemical synthesis process that uses a thermophilic enzyme on an industrial scale. Other thermophilic and hyperthermophilic enzymes have been suggested as potential catalysts for a variety of synthetic processes. A number of thermophilic enzymes (including hydantoinase, cytochrome P450, secondary alcohol dehydrogenase, and various glycosyl hydrolases) show regioselective and/or stereoselective reaction mechanisms that are highly desirable for synthetic chemistry (see examples in Table 12). Active at elevated tem-

peratures and highly resistant to solvent denaturation, hyperthermophilic proteases are also strong candidates for synthesis applications where the highly temperature-dependent solvent viscosity and substrate solubility affect the reaction rate.

Other applications. The use of enzymes (including horseradish peroxidase, alkaline phosphatase, and glucose phosphate dehydrogenase) in immunoassays in the pharmaceutical and food industries is constantly increasing. Highly stable enzymes are desirable for these diagnostic applications only if they are active at moderate temperatures (i.e., under conditions compatible with the biological activity and stability of the other reagents involved in the assay). The thermostable alkaline phosphatase recently characterized from *Thermotoga neapolitana* is highly active at high temperatures (Table 12) but shows almost no activity at room temperature. This enzyme could become valuable if its activity at room temperature is engineered to levels comparable to currently available mesophilic alkaline phosphatases and if its stability can be retained.

Pectin is a branched heteropolysaccharide abundant in plant tissues. Its main chain is a partially methyl-esterified (1, 4)-α-D-polygalacturonate chain. Along the main chain are rhamnopyranose residues, which are the binding sites for side chains composed of neutral sugars. There are two types of pectinolytic enzymes: methylesterases and depolymerases (hydrolases and lyases). These enzymes are widely used in the food industry. In fruit juice extraction and wine making, pectinolytic enzymes increase juice yield, reduce viscosity, and improve color extraction from fruit skin. A few thermophilic pectinolytic enzymes isolated from thermophilic anaerobes (Table 12) show catalytic and stability properties compatible with industrial needs.

Chitin (a linear β-1,4 homopolymer of *N*-acetylglucosamine) is also an abundant carbohydrate in the biosphere. Chitinases could be used for the utilization of chitin as a renewable resource and for the production of oligosaccharides as biologically active substances. Some chitooligosaccharides can be used in phagocyte activation or as growth inhibitors of certain tumors. A few thermophilic chitinases have been characterized. Their potential for an economically competitive chitin degradation process remains to be tested.

Animal feedstock production processes include heat treatments that inactivate potential viral and microbial contaminants. Using thermophilic enzymes (i.e., arabinofuranosidase and phytase) in feedstock production would enhance digestibility and nutrition of the feed while allowing the combination of heat treatment and feed transformation in a single step. Table 12 shows other examples of processes where it may be desirable to use a thermophilic enzyme (including keratinase and others).

CONCLUSIONS AND PERSPECTIVES

Hyperthermophilic enzymes have become model systems to study enzyme evolution, enzyme stability and activity mechanisms, protein structure-function relationships, and biocatalysis under extreme conditions. These applications result from the discovery that molecular biology and biochemical studies such as protein purification and characterization are facilitated by the cloning and expressing of genes from hyperthermophiles in mesophilic hosts. The great diversity of archaeal and bacterial hyperthermophiles represents a large pool of enzymes to chose from for developing new biotechnological applications.

The future of this field is fascinating and boundless. Three questions are particularly intriguing:

First, what is the upper temperature limit for enzyme activity and stability? An answer to this question may come from the discovery of new, natural hyperthermophilic enzymes that are active above 125°C. Another approach is to use hyperthermophilic enzymes whose substrates are stable at very high temperatures and to use genetic engineering tools to select for mutants with higher stability. This approach is being tested by directed evolution with the *P. furiosus* α-amylase gene (85) in F. Arnold's laboratory to determine the upper limits to α-amylase activity.

Second, numerous reports suggest that the stability and activity of thermophilic enzymes can be controlled by separate molecular determinants. Can hyperthermophilic enzymes be used as molecular templates to design highly stable enzymes that have high activity at low temperatures? Such an achievement could greatly enhance the range of applications for hyperthermophilic enzymes in areas including medicine, food, and research reagents. Our laboratory is currently using directed-evolution techniques to transform hyperthermophilic xylose isomerase and alkaline phosphatase into thermostable catalysts that are highly active at moderate temperatures.

Third, how do rigidity and flexibility relate to thermostability and activity, respectively? In other words, is rigidity at room temperature a requirement for enzyme thermostability, and is flexibility a requirement for activity?

As opposed to X-ray crystallography, which gives access only to a static, average enzyme structure, tools such as molecular dynamics, hydrogen exchange, and NMR allow the study of protein flexibility and thermostability, as well as allowing the identification of regions susceptible to unfolding. Coupled with SDM, these tools should help us explore many aspects of enzyme thermostability and activity. In particular, these tools will help answer the three questions mentioned above.

The ever-increasing number of fully sequenced genomes will be an invaluable help in deciphering which sequence variations among homologous proteins are related to stability and which ones are simply a result of evolution. Many algorithms used in computational methods are created using parameters calculated from known protein structures. Despite the many advances in computer algorithms, protein structure prediction remains among the most challenging tasks in computer modeling. While homologous folds (i.e., with the same ancestor) are better predicted than analogous folds (i.e., convergent evolution), totally unknown protein structures are orders of magnitude harder to predict. With protein thermostability often depending on only a small number of noncovalent interactions, even the best predictions of homologous folds might fall short of providing clues for stability. For this reason, using structural genomics to study protein thermostability will probably first answer questions such as Are the different protein folds populated to the same level among the hyperthermophilic and mesophilic enzymes? In other words, are there folds that are favored at high temperatures? In the foreseeable future, the comparison of individual protein thermostabilities will still heavily rely on crystallographic and NMR structural studies.

ACKNOWLEDGMENTS

This research was supported by grants 94–34189–0067 and 9901423 from the U.S. Department of Agriculture and by grant NSF-BES-9529047–63143-Zeikus from the National Science Foundation.

We gratefully acknowledge Paweena Limjaroen for her assistance with the literature search and Dinlaka Sriprapundh for preparing Fig. 6. We also thank our many students and postdoctoral fellows who have worked on and contributed to our knowledge of thermophilic enzymes during the past years, including Dinlaka Sriprapundh, Maris Laivenieks, Doug Burdette, Guoqiang Dong, Chanyong Lee, Yong-Eok Lee, Saroj Mathupala, Ramesh Mathur, Meng-Hsiao Meng, Cindy Petersen, Badal Saha, Alexei Savchenko, Gwo-Jenn Shen, and Vladimir Tchernajenko. We express our deep gratitude to Christopher B. Jambor for his repeated encouragements and his expert editing. Any remaining mistakes are ours.

REFERENCES

1. **Achenbach-Richter, L., R. Gupta, K.-O. Stetter, and C. R. Woese.** 1987. Were the original eubacteria thermophiles? Syst. Appl. Microbiol. **9:**34–39.
2. **Adams, M. W. W.** 1993. Enzymes and proteins from organisms that grow near and above 100°C. Annu. Rev. Microbiol. **47:**627–658.
3. **Adams, M. W. W., and R. M. Kelly.** 1995. Enzymes from microorganisms from extreme environments. C&E News **73:**32–42.
4. **Adams, M. W. W., F. B. Perler, and R. M. Kelly.** 1995. Extremozymes: expanding the limits of biocatalysis. Bio/Technology **13:**662–668.
5. **Aguilar, C. F., I. Sanderson, M. Moracci, M. Ciaramella, R. Nucci, M. Rossi, and L. H. Pearl.** 1997. Crystal structure of the β-glycosidase from the hyperthermophilic archeon *Sulfolobus solfataricus*: resilience as a key factor in thermostability. J. Mol. Biol. **271:**789–802.
6. **Ahern, T. J., and A. M. Klibanov.** 1985. The mechanisms of irreversible enzyme inactivation at 100°C. Science **228:**1280–1284.
7. **Anderson, D. E., W. J. Becktel, and F. W. Dahlquist.** 1990. pH-induced denaturation of proteins: a single salt bridge contributes 3–5 kcal/mol to the free energy of folding of T4 lysozyme. Biochemistry **29:**2403–2408.
8. **Andrä, S., G. Frey, R. Jaenicke, and K. O. Stetter.** 1998. The thermosome from *Methanopyrus kandleri* possesses an NH_4^+-dependent ATPase activity. Eur. J. Biochem. **255:**93–99.
9. **Andreotti, G., M. V. Cubellis, G. Nitti, G. Sannia, X. Mai, M. W. Adams, and G. Marino.** 1995. An extremely thermostable aromatic aminotransferase from the hyperthermophilic archaeon *Pyrococcus furiosus*. Biochim. Biophys. Acta **1247:**90–96.
10. **Argos, P., M. G. Rossmann, U. M. Grau, H. Zuber, G. Frank, and J. D. Tratschin.** 1979. Thermal stability and protein structure. Biochemistry **18:** 5698–5703.
11. **Armand, S., C. Vieille, C. Gey, A. Heyraud, J. G. Zeikus, and B. Henrissat.** 1996. Stereochemical course and reaction products of the action of β-xylosidase from *Thermoanaerobacterium saccharolyticum* strain B6A-RI. Eur. J. Biochem. **236:**706–713.
12. **Arnold, F. H.** 1993. Engineering proteins for nonnatural environments. FASEB J. **7:**744–749.
13. **Arnold, U., A. Schierhorn, and R. Ulbrich-Hofmann.** 1999. Modification of the unfolding region in bovine pancreatic ribonuclease and its influence on the thermal stability and proteolytic fragmentation. Eur. J. Biochem. **259:** 470–475.
14. **Arnone, M. I., L. Birolo, S. Pascarella, M. V. Cubellis, F. Bossa, G. Sannia, and G. Marino.** 1997. Stability of aspartate aminotransferase from *Sulfolobus solfataricus*. Protein Eng. **10:**237–248.
15. **Auerbach, G., R. Huber, M. Grättinger, K. Zaiss, H. Schurig, R. Jaenicke, and U. Jacob.** 1997. Closed structure of phosphoglycerate kinase from *Thermotoga maritima* reveals the catalytic mechanism and determinants of thermal stability. Structure **5:**1475–1483.
16. **Auerbach, G., R. Ostendorp, L. Prade, I. Korndörfer, T. Dams, R. Huber, and R. Jaenicke.** 1998. Lactate dehydrogenase from the hyperthermophilic bacterium *Thermotoga maritima*: the crystal structure at 2.1 Å resolution reveals strategies for intrinsic protein stabilization. Structure **6:**769–781.
17. **Backmann, J., G. Schäfer, L. Wyns, and H. Bönisch.** 1998. Thermodynamics and kinetics of unfolding of the thermostable trimeric adenylate kinase from the archaeon *Sulfolobus acidocaldarius*. J. Mol. Biol. **284:**817–833.
18. **Barns, S. M., C. F. Delwiche, J. D. Palmer, and N. R. Pace.** 1996. Perspectives on archaeal diversity, thermophily and monophyly from environmental rRNA sequences. Proc. Natl. Acad. Sci. USA **93:**9188–9193.
19. **Barns, S. M., R. E. Fundyga, M. W. Jeffries, and N. R. Pace.** 1994. Remarkable archaeal diversity detected in a Yellowstone National Park hot spring environment. Proc. Natl. Acad. Sci. USA **91:**1609–1613.
20. **Bauer, M. W., L. E. Driskill, W. Callen, M. A. Snead, E. J. Mathur, and R. M. Kelly.** 1999. An endoglucanase, EglA, from the hyperthermophilic archaeon *Pyrococcus furiosus* hydrolyzes β-1,4 bonds in mixed-linkage (1→3), (1→4)-β-D-glucans and cellulose. J. Bacteriol. **181:**284–290.
21. **Bauer, M. W., L. E. Driskill, and R. M. Kelly.** 1998. Glycosyl hydrolases from hyperthermophilic microorganisms. Curr. Opin. Biotechnol. **9:**141–145.
22. **Bauer, M. W., and R. M. Kelly.** 1998. The family 1 β-glucosidases from *Pyrococcus furiosus* and *Agrobacterium faecalis* share a common catalytic mechanism. Biochemistry **37:**17170–17178.
23. **Beaucamp, N., A. Hofmann, B. Kellerer, and R. Jaenicke.** 1997. Dissection of the gene of the bifunctional PGK-TIM fusion protein from the hyperthermophilic bacterium *Thermotoga maritima*: design and characterization of the separate triosephosphate isomerase. Protein Sci. **6:**2159–2165.
24. **Belkin, S., C. O. Wirsen, and H. W. Jannasch.** 1986. A new sulfur-reducing, extremely thermophilic eubacterium from a submarine thermal vent. Appl. Environ. Microbiol. **51:**1180–1185.
25. **Bentley, I. S., and E. C. Williams.** 1996. Starch conversion, p. 339–357. *In* T. Godfrey and S. I. West (ed.), Industrial enzymology, 2nd ed. Stockton Press, New York, N.Y.
26. **Bergquist, P. L., and H. W. Morgan.** 1992. The molecular genetics and biotechnological application of enzymes from extremely thermophilic eubacteria, p. 44–75. *In* R. A. Herbert and R. J. Sharp (ed.), Molecular biology and biotechnology of extremophiles. Chapman & Hall, New York, N.Y.
27. **Bertoldo, C., F. Duffner, P. L. Jorgensen, and G. Antranikian.** 1999. Pullulanase type I from *Fervidobacterium pennavorans* Ven5: cloning, sequencing, and expression of the gene and biochemical characterization of the recombinant enzyme. Appl. Environ. Microbiol. **65:**2084–2091.
28. **Blöchl, E., R. Rachel, S. Burggraf, D. Hafenbradl, H. W. Jannasch, and K. O. Stetter.** 1997. *Pyrolobus fumarii*, gen. and sp. nov., represents a novel group of archaea, extending the upper temperature limit for life to 113°C. Extremophiles **1:**14–21.
29. **Bock, A. K., J. Glasemacher, R. Schmidt, and P. Schönheit.** 1999. Purification and characterization of two extremely thermostable enzymes, phosphate acetyltransferase and acetate kinase, from the hyperthermophilic eubacterium *Thermotoga maritima*. J. Bacteriol. **181:**1861–1867.
30. **Boel, E., L. Brady, A. M. Brzozowski, Z. Derewenda, G. G. Dodson, V. J. Jensen, S. B. Petersen, H. Swift, L. Thim, and H. F. Woldike.** 1990. Calcium binding in α-amylases: an X-ray diffraction study at 2.1-Å resolution of two enzymes from *Aspergillus*. Biochemistry **29:**6244–6249.
31. **Böhm, G., and R. Jaenicke.** 1994. Relevance of sequence statistics for the properties of extremophilic proteins. Int. J. Pept. Protein Res. **43:**97–106.
32. **Bok, J. D., D. A. Yernool, and D. E. Eveleigh.** 1998. Purification, characterization, and molecular analysis of thermostable cellulases CelA and CelB from *Thermotoga neapolitana*. Appl. Environ. Microbiol. **64:**4774–4781.
33. **Bonch-Osmolovskaya, E. A., M. L. Miroshnichenko, N. A. Kostrikina, N. A. Chernych, and G. A. Zavarzin.** 1990. *Thermoproteus uzoniensis* sp. nov., a new extremely thermophilic archaebacterium from Kamchatka continental hot springs. Arch. Microbiol. **154:**556–559.
34. **Bonch-Osmolovskaya, E. A., A. I. Slesarev, M. L. Miroshnichenko, T. P. Svetlichnaya, and V. A. Alekseev.** 1988. Characteristic of *Desulfurococcus amylolyticus* n. sp.—a new extremely thermophilic archaebacterium isolated from thermal springs of Kamchatka and Kunashir island. Microbiology **57:**78–85.
35. **Bönisch, H., J. Backmann, T. Kath, D. Naumann, and G. Schäfer.** 1996. Adenylate kinase from *Sulfolobus acidocaldarius*: expression in *Escherichia coli* and characterization by Fourier transform infrared spectroscopy. Arch. Biochem. Biophys. **333:**75–84.
36. **Breitung, J., G. Börner, S. Scholz, D. Linder, K. O. Stetter, and R. K. Thauer.** 1992. Salt dependence, kinetic properties and catalytic mechanism of *N*-formylmethanofuran: tetrahydromethanopterin formyltransferase from the extreme thermophile *Methanopyrus kandleri*. Eur. J. Biochem. **210:**971–981.
37. **Breitung, J., R. A. Schmitz, K. O. Stetter, and R. K. Thauer.** 1991. N^5,N^{10}-methenyltetrahydromethanopterin cyclohydrolase from the extreme thermophile *Methanopyrus kandleri*: increase of catalytic efficiency (k_{cat}/K_M) and thermostability in the presence of salts. Arch. Microbiol. **156:**517–524.
38. **Britton, K. L., P. J. Baker, K. M. M. Borges, P. C. Engel, A. Pasquo, D. W. Rice, F. T. Robb, R. Scandurra, T. J. Stillman, and K. S. P. Yip.** 1995. Insights into thermal stability from a comparison of the glutamate dehydrogenases from *Pyrococcus furiosus* and *Thermococcus litoralis*. Eur. J. Biochem. **229:**688–695.
39. **Brock, T. D.** 1967. Life at high temperatures. Science **158:**1012–1019.
40. **Brock, T. D., K. M. Brock, R. T. Belly, and R. L. Weiss.** 1972. *Sulfolobus*: a new genus of sulfur oxidizing bacteria living at low pH and high temperature. Arch. Mikrobiol. **84:**54–68.
41. **Brock, T. D., and H. Freeze.** 1969. *Thermus aquaticus* gen. n. and sp. n., a nonsporulating extreme thermophile. J. Bacteriol. **98:**289–297.
42. **Bronnenmeier, K., A. Kern, W. Liebl, and W. L. Staudenbauer.** 1995. Purification of *Thermotoga maritima* enzymes for the degradation of cellulosic materials. Appl. Environ. Microbiol. **61:**1399–1407.
43. **Brown, S. H., and R. M. Kelly.** 1993. Characterization of amylolytic enzymes, having both α-1,4 and α-1,6 hydrolytic activity, from the thermophilic archaea *Pyrococcus furiosus* and *Thermococcus litoralis*. Appl. Environ. Microbiol. **59:**2614–2621.

44. **Brown, S. H., C. Sjøholm, and R. M. Kelly.** 1993. Purification and characterization of a highly thermostable glucose isomerase produced by the extremely thermophilic eubacterium *Thermotoga maritima*. Biotechnol. Bioeng. **41:**878–886.
45. **Buchanan, C. L., H. Connaris, M. J. Danson, C. D. Reeve, and D. W. Hough.** 1999. An extremely thermostable aldolase from *Sulfolobus solfataricus* with specificity for non-phosphorylated substrates. Biochem. J. **343:** 563–570.
46. **Burdette, D. S., F. Secundo, R. S. Phillips, J. Dong, R. A. Scott, and J. G. Zeikus.** 1997. Biophysical and mutagenic analysis of *Thermoanaerobacter ethanolicus* secondary-alcohol dehydrogenase activity and specificity. Biochem. J. **326:**717–724.
47. **Burdette, D. S., C. Vieille, and J. G. Zeikus.** 1996. Cloning and expression of the gene encoding the *Thermoanaerobacter ethanolicus* 39E secondary-alcohol dehydrogenase and biochemical characterization of the enzyme. Biochem. J. **316:**115–22.
48. **Burggraf, S., H. Fricke, A. Neuner, J. Kristjansson, P. Rouvier, L. Mandelco, C. R. Woese, and K. O. Stetter.** 1990. *Methanococcus igneus* sp. nov., a novel hyperthermophilic methanogen from a shallow submarine hydrothermal system. Syst. Appl. Microbiol. **13:**263–269.
49. **Burggraf, S., H. W. Jannasch, B. Nicolaus, and K. O. Stetter.** 1990. *Archaeoglobus profundus* sp. nov., represents a new species within the sulfate-reducing archaebacteria. Syst. Appl. Microbiol. **13:**24–28.
50. **Burley, S. K., and G. A. Petsko.** 1985. Aromatic-aromatic interaction: a mechanism of protein structure stabilization. Science **229:**23–28.
51. **Cacciapuoti, G., S. Fusco, N. Caiazzo, V. Zappia, and M. Porcelli.** 1999. Heterologous expression of 5′-methylthioadenosine phosphorylase from the archaeon *Sulfolobus solfataricus*: characterization of the recombinant protein and involvement of disulfide bonds in thermophilicity and thermostability. Protein Expression Purif. **16:**125–135.
52. **Cacciapuoti, G., M. Porcelli, C. Bertoldo, M. De Rosa, and V. Zappia.** 1994. Purification and characterization of extremely thermophilic and thermostable 5′-methylthioadenosine phosphorylase from the archaeon *Sulfolobus solfataricus*. Purine nucleoside phosphorylase activity and evidence for intersubunit disulfide bonds. J. Biol. Chem. **269:**24762–24769.
53. **Caflisch, A., and M. Karplus.** 1995. Acid and thermal denaturation of barnase investigated by molecular dynamics simulations. J. Mol. Biol. **252:** 672–708.
54. **Caflisch, A., and M. Karplus.** 1994. Molecular dynamics simulation of protein denaturation: solvation of the hydrophobic cores and secondary structure of barnase. Proc. Natl. Acad. Sci. USA **91:**1746–1750.
55. **Camacho, M. L., R. A. Brown, M. J. Bonete, M. J. Danson, and D. W. Hough.** 1995. Isocitrate dehydrogenases from *Haloferax volcanii* and *Sulfolobus solfataricus*: enzyme purification, characterisation and N-terminal sequence. FEMS Microbiol. Lett. **134:**85–90.
56. **Canganella, F., C. M. Andrade, and G. Antranikian.** 1994. Characterization of amylolytic and pullulytic enzymes from thermophilic archaea and from a new *Fervidobacterium* species. Appl. Microbiol. Biotechnol. **42:**239–245.
57. **Canganella, F., W. J. Jones, A. Gambacorta, and G. Antranikian.** 1998. *Thermococcus guaymasensis* sp. nov. and *Thermococcus aggregans* sp. nov., two novel thermophilic archaea isolated from the Guaymas Basin hydrothermal vent site. Int. J. Syst. Bacteriol. **48:**1181–1185.
58. **Cannio, R., G. Fiorentino, P. Carpinelli, M. Rossi, and S. Bartolucci.** 1996. Cloning and overexpression in *Escherichia coli* of the genes encoding NAD-dependent alcohol dehydrogenase from two *Sulfolobus* species. J. Bacteriol. **178:**301–305.
59. **Chan, M. K., S. Mukund, A. Kletzin, M. W. W. Adams, and D. C. Rees.** 1995. Structure of a hyperthermophilic tungstopterin enzyme, aldehyde ferredoxin oxidoreductase. Science **267:**1463–1469.
60. **Chen, C.-C., R. Adolphson, J. F. D. Dean, K.-E. L. Eriksson, M. W. W. Adams, and J. Westpheling.** 1997. Release of lignin from kraft pulp by a hyperthermophilic xylanase from *Thermotoga maritima*. Enzyme Microb. Technol. **20:**39–45.
61. **Chen, K., and F. H. Arnold.** 1991. Enzyme engineering for nonaqueous solvents: random mutagenesis to enhance activity of subtilisin E in polar organic media. Bio/Technology **9:**1073–1077.
62. **Chen, L., and M. F. Roberts.** 1999. Characterization of a tetrameric inositol monophosphatase from the hyperthermophilic bacterium *Thermotoga maritima*. Appl. Environ. Microbiol. **65:**4559–4567.
63. **Chi, Y. I., L. A. Martinez-Cruz, J. Jancarik, R. V. Swanson, D. E. Robertson, and S. H. Kim.** 1999. Crystal structure of the β-glycosidase from the hyperthermophile *Thermosphaera aggregans*: insights into its activity and thermostability. FEBS Lett. **445:**375–383.
64. **Choi, I.-G., W.-G. Bang, S.-H. Kim, and Y. G. Yu.** 1999. Extremely thermostable serine-type protease from *Aquifex pyrophilus*. Molecular cloning, expression, and characterization. J. Biol. Chem. **274:**881–888.
65. **Chung, Y. C., T. Kobayashi, H. Kanai, T. Akiba, and T. Kudo.** 1995. Purification and properties of extracellular amylase from the hyperthermophilic archaeon *Thermococcus profundus* DT5432. Appl. Environ. Microbiol. **61:**1502–1506.
66. **Colombo, S., S. D' Auria, P. Fusi, L. Zecca, C. A. Raia, and P. Tortora.** 1992. Purification and characterization of a thermostable carboxypeptidase from the extreme thermophilic archaebacterium *Sulfolobus solfataricus*. Eur. J. Biochem. **206:**349–357.
67. **Coughlan, M. P.** 1990. Cellulose degradation by fungi, p. 1–36. *In* W. M. Fogarty and C. T. Kelly (ed.), Microbial enzymes and biotechnology, 2nd ed. Elsevier Applied Science, London, United Kingdom.
68. **Cowan, D., R. Daniel, and H. Morgan.** 1985. Thermophilic proteases: properties and potential applications. Trends Biotechnol. **3:**68–72.
69. **Crabb, W. D., and C. Mitchinson.** 1997. Enzymes involved in the processing of starch to sugars. Trends Biotechnol. **15:**349–352.
70. **Crameri, A., S. A. Raillard, E. Bermudez, and W. P. Stemmer.** 1998. DNA shuffling of a family of genes from diverse species accelerates directed evolution. Nature **391:**288–291.
71. **Creveld, L. D., A. Amadei, R. C. van Schaik, H. A. Pepermans, J. de Vlieg, and H. J. Berendsen.** 1998. Identification of functional and unfolding motions of cutinase as obtained from molecular dynamics computer simulations. Proteins **33:**253–264.
72. **Crueger, A., and W. Crueger.** 1990. Glucose transforming enzymes, p. 177–226. *In* W. M. Fogarty and C. T. Kelly (ed.), Microbial enzymes and biotechnology, 2nd ed. Elsevier Science, London, United Kingdom.
73. **Daggett, V.** 2000. Long timescale simulations. Curr. Opin. Struct. Biol. **10:**160–164.
74. **Daggett, V., and M. Levitt.** 1993. Protein unfolding pathways explored through molecular dynamics simulations. J. Mol. Biol. **232:**600–619.
75. **Dams, T., G. Auerbach, G. Bader, U. Jacob, T. Ploom, R. Huber, and R. Jaenicke.** 2000. The crystal structure of dihydrofolate reductase from *Thermotoga maritima*: molecular features of thermostability. J. Mol. Biol. **297:** 659–672.
76. **Dams, T., and R. Jaenicke.** 1999. Stability and folding of dihydrofolate reductase from the hyperthermophilic bacterium *Thermotoga maritima*. Biochemistry **38:**9169–9178.
77. **D'Auria, S., A. Morana, F. Febbraio, V. Carlo, M. De Rosa, and R. Nucci.** 1996. Functional and structural properties of the homogeneous β-glycosidase from the extreme thermoacidophilic archaeon *Sulfolobus solfataricus* expressed in *Saccharomyces cerevisiae*. Protein Expression Purif. **7:**299–308.
78. **D'Auria, S., R. Nucci, M. Rossi, E. Bertoli, F. Tanfani, I. Gryczynski, H. Malak, and J. R. Lakowicz.** 1999. β-Glycosidase from the hyperthermophilic archaeon *Sulfolobus solfataricus*: structure and activity in the presence of alcohols. J. Biochem. **126:**545–552.
79. **Davies, G. J., S. J. Gamblin, J. A. Littlechild, and H. C. Watson.** 1993. The structure of a thermally stable 3-phosphoglycerate kinase and a comparison with its mesophilic equivalent. Proteins Struct. Funct. Genet. **15:**283–289.
80. **de Bakker, P. I., P. H. Hünenberger, and J. A. McCammon.** 1999. Molecular dynamics simulations of the hyperthermophilic protein Sac7d from *Sulfolobus acidocaldarius*: contribution of salt bridges to thermostability. J. Mol. Biol. **285:**1811–1830.
81. **Deckert, G., P. V. Warren, T. Gaasterland, W. G. Young, A. L. Lenox, D. E. Graham, R. Overbeek, M. A. Snead, M. Keller, M. Aujay, R. Huber, R. A. Feldman, J. M. Short, G. J. Olsen, and R. V. Swanson.** 1998. The complete genome of the hyperthermophilic bacterium *Aquifex aeolicus*. Nature **392:** 353–358.
82. **De Montigny, C., and J. Sygusch.** 1996. Functional characterization of an extreme thermophilic class II fructose-1,6-bisphosphate aldolase. Eur. J. Biochem. **241:**243–248.
83. **Dill, K. A.** 1990. Dominant forces in protein folding. Biochemistry **29:**7133–7155.
84. **Dirmeier, R., M. Keller, D. Hafenbradl, F. J. Braun, R. Rachel, S. Burggraf, and K. O. Stetter.** 1998. *Thermococcus acidaminovorans* sp. nov., a new hyperthermophilic alkalophilic archaeon growing on amino acids. Extremophiles **2:**109–114.
85. **Dong, G., C. Vieille, A. Savchenko, and J. G. Zeikus.** 1997. Cloning, sequencing, and expression of the gene encoding extracellular α-amylase from *Pyrococcus furiosus* and biochemical characterization of the recombinant enzyme. Appl. Environ. Microbiol. **63:**3569–3576.
86. **Dong, G., C. Vieille, and J. G. Zeikus.** 1997. Cloning, sequencing, and expression of the gene encoding amylopullulanase from *Pyrococcus furiosus* and biochemical characterization of the recombinant enzyme. Appl. Environ. Microbiol. **63:**3577–3584.
87. **Dong, G., and J. G. Zeikus.** 1997. Purification and characterization of alkaline phosphatase from *Thermotoga neapolitana*. Enzyme Microb. Technol. **21:**335–340.
88. **Dougherty, D. A.** 1996. Cation-π interactions in chemistry and biology: a new view of benzene, Phe, Tyr, and Trp. Science **271:**163–168.
89. **Duffaud, G. D., O. B. D'Hennezel, A. S. Peek, A. Reysenbach, and R. M. Kelly.** 1998. Isolation and characterization of *Thermococcus barossii*, sp. nov., a hyperthermophilic archaeon isolated from a hydrothermal vent flange formation. Syst. Appl. Microbiol. **21:**40–49.
90. **Durbecq, V., T. L. Thia-Toong, D. Charlier, V. Villeret, M. Roovers, R. Wattiez, C. Legrain, and N. Glansdorff.** 1999. Aspartate carbamoyltransferase from the thermoacidophilic archaeon *Sulfolobus acidocaldarius*. Cloning, sequence analysis, enzyme purification and characterization. Eur. J. Biochem. **264:**233–241.
91. **Edmondson, S. P., L. Qui, and J. W. Shriver.** 1995. Solution structure of the

DNA-binding protein sac7d from the hyperthermophile *Sulfolobus acidocaldarius*. Biochemistry **34:**13289–13304.
92. **Eidsness, M. K., K. A. Richie, A. E. Burden, D. M. Kurtz, Jr., and R. A. Scott.** 1997. Dissecting contributions to the thermostability of *Pyrococcus furiosus* rubredoxin: β-sheet chimeras. Biochemistry **36:**10406–10413.
93. **Eijsink, V. G., G. Vriend, F. Hardy, O. R. Veltman, B. Van der Vinne, B. Van der Burg, B. W. Dijkstra, J. R. Van der Zee, and G. Venema.** 1993. Structural determinants of the thermostability of thermolysin-like *Bacillus* neutral proteases, p. 91–99. *In* W. J. Van den Tweel, A. Harder, and R. M. Buitelaar (ed.), Stability and stabilization of enzymes. Elsevier Science Publishers BV, Amsterdam, The Netherlands.
94. **Elcock, A. H.** 1998. The stability of salt bridges at high temperatures: implications for hyperthermophilic proteins. J. Mol. Biol. **284:**489–502.
95. **Erauso, G., A.-L. Reysenbach, A. Godfroy, J.-R. Meunier, B. Crump, F. Partensky, J. A. Baross, V. Marteinsson, G. Barbier, N. R. Pace, and D. Prieur.** 1993. *Pyrococcus abyssi sp. nov.*, a new hyperthermophilic archaeon isolated from a deep-sea hydrothermal vent. Arch. Microbiol. **160:**338–349.
96. **Ermler, U., M. C. Merckel, R. K. Thauer, and S. Shima.** 1997. Formylmethanofuran:tetrahydromethanopterin formyltransferase from *Methanopyrus kandleri*—new insights into salt-dependence and thermostability. Structure **5:**635–646.
97. **Erra-Pujada, M., P. Debeire, F. Duchiron, and M. J. O'Donohue.** 1999. The type II pullulanase of *Thermococcus hydrothermalis*: molecular characterization of the gene and expression of the catalytic domain. J. Bacteriol. **181:**3284–3287.
98. **Fabry, S., and R. Hensel.** 1987. Purification and characterization of D-glyceraldehyde-3-phosphate dehydrogenase from the thermophilic archaebacterium *Methanothermus fervidus*. Eur. J. Biochem. **165:**147–155.
99. **Facchiano, A. M., G. Colonna, and R. Ragone.** 1998. Helix stabilizing factors and stabilization of thermophilic proteins: an X-ray based study. Protein Eng. **11:**753–760.
100. **Faguy, D. M., S. F. Koval, and K. F. Jarrell.** 1992. Correlation between glycosylation of flagellin proteins and sensitivity of flagellar filaments to Triton X-100 in methanogens. FEMS Microbiol. Lett. **69:**129–134.
101. **Faraone-Mennella, M. R., A. Gambacorta, B. Nicolaus, and B. Farina.** 1998. Purification and biochemical characterization of a poly(ADP-ribose) polymerase-like enzyme from the thermophilic archaeon *Sulfolobus solfataricus*. Biochem. J. **335:**441–447.
102. **Fiala, G., and K. O. Stetter.** 1986. *Pyrococcus furiosus* sp. nov. represents a novel genus of marine heterotrophic archaebacteria growing optimally at 100°C. Arch. Microbiol. **145:**56–61.
103. **Fiala, G., K. O. Stetter, H. W. Jannasch, T. A. Langworthy, and J. Madon.** 1986. *Staphylothermus marinus* sp. nov. represents a novel genus of extremely thermophilic submarine heterotrophic archaebacteria growing up to 98°C. System. Appl. Microbiol. **8:**106–113.
104. **Fischer, F., W. Zillig, K. O. Stetter, and G. Schreiber.** 1983. Chemolithoautotrophic metabolism of anaerobic extremely thermophilic archaebacteria. Nature **301:**511–513.
105. **Friedrich, A. B., and G. Antranikian.** 1996. Keratin degradation by *Fervidobacterium pennavorans*, a novel thermophilic anaerobic species of the order *Thermotogales*. Appl. Environ. Microbiol. **62:**2875–2882.
106. **Fuchs, T., H. Huber, S. Burggraf, and K. O. Stetter.** 1996. 16S rDNA-based phylogeny of the archaeal order *Sulfolobales* and reclassification of *Desulfurolobus ambivalens* as *Acidianus ambivalens* comb. nov. Syst. Appl. Microbiol. **19:**59–60.
107. **Fujii, T., Y. Hata, M. Oozeki, H. Moriyama, T. Wakagi, N. Tanaka, and T. Oshima.** 1997. The crystal structure of zinc-containing ferredoxin from the thermoacidophilic archaeon *Sulfolobus* sp. strain 7. Biochemistry **36:**1505–1513.
108. **Fujiwara, S., S. Lee, M. Haruki, S. Kanaya, M. Takagi, and T. Imanaka.** 1996. Unusual enzyme characteristics of aspartyl-tRNA synthetase from hyperthermophilic archaeon *Pyrococcus* sp. KOD1. FEBS Lett. **394:**66–70.
109. **Fukusumi, S., A. Kamizono, S. Horinouchi, and T. Beppu.** 1988. Cloning and nucleotide sequence of a heat-stable amylase gene from an anaerobic thermophile, *Dictyoglomus thermophilum*. Eur. J. Biochem. **174:**15–21.
110. **Fusek, M., X. Lin, and J. Tang.** 1990. Enzymic properties of thermopsin. J. Biol. Chem. **265:**1496–1501.
111. **Gabelsberger, J., W. Liebl, and K.-H. Schleifer.** 1993. Cloning and characterization of β-galactoside and β-glycoside hydrolysing enzymes of *Thermotoga maritima*. FEMS Microbiol. Lett. **109:**131–138.
112. **Ganghofner, D., J. Kellermann, W. L. Staudenbauer, and K. Bronnenmeier.** 1998. Purification and properties of an amylopullulanase, a glucoamylase, and an α-glucosidase in the amylolytic enzyme system of *Thermoanaerobacterium thermosaccharolyticum*. Biosci. Biotechnol. Biochem. **62:**302–308.
113. **Gantelet, H., and F. Duchiron.** 1999. A new pullulanase from a hyperthermophilic archaeon for starch hydrolysis. Biotechnol. Lett. **21:**71–75.
114. **Gershenson, A., J. A. Schauerte, L. Giver, and F. H. Arnold.** 2000. Tryptophan fluorescence study of enzyme flexibility and unfolding in laboratory-evolved thermostable esterases. Biochemistry **39:**4658–4665.
115. **Ghosh, M., A. M. Grunden, D. M. Dunn, R. Weiss, and M. W. Adams.** 1998. Characterization of native and recombinant forms of an unusual cobalt-dependent proline dipeptidase (prolidase) from the hyperthermophilic archaeon *Pyrococcus furiosus*. J. Bacteriol. **180:**4781–4789.
116. **Giver, L., A. Gershenson, P. Freskgard, and F. H. Arnold.** 1998. Directed evolution of a thermostable esterase. Proc. Natl. Acad. Sci. USA **95:**12809–12813.
117. **Godfroy, A., F. Lesongeur, G. Raguenes, J. Querellou, E. Antoine, J. R. Meunier, J. Guezennec, and G. Barbier.** 1997. *Thermococcus hydrothermalis* sp. nov., a new hyperthermophilic archaeon isolated from a deep-sea hydrothermal vent. Int. J. Syst. Bacteriol. **47:**622–626.
118. **Gomes, J., and W. Steiner.** 1998. Production of a high activity of an extremely thermostable β-mannanase by the thermophilic eubacterium *Rhodothermus marinus*, grown on locust bean gum. Biotechnol. Lett. **20:**729–733.
119. **González, J. M., Y. Masuchi, F. T. Robb, J. W. Ammerman, D. L. Maeder, M. Yanagibayashi, J. Tamaoka, and C. Kato.** 1998. *Pyrococcus horikoshii* sp. nov., a hyperthermophilic archaeon isolated from a hydrothermal vent at the Okinawa Trough. Extremophiles **2:**123–130.
120. **Grabarse, W., M. Vaupel, J. A. Vorholt, S. Shima, R. K. Thauer, A. Wittershagen, G. Bourenkov, H. D. Bartunik, and U. Ermler.** 1999. The crystal structure of methenyltetrahydromethanopterin cyclohydrolase from the hyperthermophilic archaeon *Methanopyrus kandleri*. Struct. Fold. Des. **7:**1257–1268.
121. **Grättinger, M., A. Dankesreiter, H. Schurig, and R. Jaenicke.** 1998. Recombinant phosphoglycerate kinase from the hyperthermophilic bacterium *Thermotoga maritima*: catalytic, spectral and thermodynamic properties. J. Mol. Biol. **280:**525–533.
122. **Grogan, D., P. Palm, and W. Zillig.** 1990. Isolate B12, which harbours a virus-like element, represents a new species of the archaebacterial genus *Sulfolobus, Sulfolobus shibatae*, sp. nov. Arch. Microbiol. **154:**594–599.
123. **Guagliardi, A., A. Napoli, M. Rossi, and M. Ciaramella.** 1997. Annealing of complementary DNA strands above the melting point of the duplex promoted by an archaeal protein. J. Mol. Biol. **267:**841–848.
124. **Haney, P. J., M. Stees, and J. Konisky.** 1999. Analysis of thermal stabilizing interactions in mesophilic and thermophilic adenylate kinases from the genus *Methanococcus*. J. Biol. Chem. **274:**28453–28458.
125. **Hardy, F., G. Vriend, O. R. Veltman, B. Van Der Vinne, G. Venema, and V. G. Eijsink.** 1993. Stabilization of *Bacillus stearothermophilus* neutral protease by introduction of prolines. FEBS Lett. **317:**89–92.
126. **Harris, G. W., R. W. Pickersgill, I. Connerton, P. Debeire, J. P. Touzel, C. Breton, and S. Perez.** 1997. Structural basis of the properties of an industrially relevant thermophilic xylanase. Proteins **29:**77–86.
127. **Hashimoto, H., T. Inoue, M. Nishioka, S. Fujiwara, M. Takagi, T. Imanaka, and Y. Kai.** 1999. Hyperthermostable protein structure maintained by intra and inter-helix ion-pairs in archaeal O^6-methylguanine-DNA methyltransferase. J. Mol. Biol. **292:**707–716.
128. **Hedrick, D. B., R. D. Pledger, D. C. White, and J. A. Baross.** 1992. In situ microbial ecology of hydrothermal vent sediments. FEMS Microbiol. Ecol. **101:**1–10.
129. **Hei, D. J., and D. S. Clark.** 1994. Pressure stabilization of proteins from extreme thermophiles. Appl. Environ. Microbiol. **60:**932–939.
130. **Hennig, M., B. Darimont, R. Sterner, K. Kirschner, and J. N. Jansonius.** 1995. 2.0 Å structure of indole-3-glycerol phosphate synthase from the hyperthermophile *Sulfolobus solfataricus*: possible determinants of protein stability. Structure **3:**1295–1306.
131. **Hennig, M., R. Sterner, K. Kirschner, and J. N. Jansonius.** 1997. Crystal structure at 2.0 Å resolution of phosphoribosyl anthranilate isomerase from the hyperthermophile *Thermotoga maritima*: possible determinants of protein stability. Biochemistry **36:**6009–6016.
132. **Hensel, R., I. Jakob, H. Scheer, and F. Lottspeich.** 1992. Proteins from hyperthermophilic archaea: stability towards covalent modification of the peptide chain. Biochem. Soc. Symp. **58:**127–133.
133. **Hensel, R., S. Laumann, J. Lang, H. Heumann, and F. Lotispeich.** 1987. Characterization of two D-glyceraldehyde-3-phosphate dehydrogenases from the extremely thermophilic archaebacterium *Thermoproteus tenax*. Eur. J. Biochem. **170:**325–333.
134. **Hernández, G., F. E. Jenney, Jr., M. W. Adams, and D. M. LeMaster.** 2000. Millisecond time scale conformational flexibility in a hyperthermophile protein at ambient temperature. Proc. Natl. Acad. Sci. USA **97:**3166–3170.
135. **Herrington, C. S., and J. J. O'Leary (ed.).** 1997. PCR in situ hybridization. IRL Press, Oxford, United Kingdom.
136. **Hess, D., K. Kruger, A. Knappik, P. Palm, and R. Hensel.** 1995. Dimeric 3-phosphoglycerate kinases from hyperthermophilic archaea. Cloning, sequencing and expression of the 3-phosphoglycerate kinase gene of *Pyrococcus woesei* in *Escherichia coli* and characterization of the protein. Structural and functional comparison with the 3-phosphoglycerate kinase of *Methanothermus fervidus*. Eur. J. Biochem. **233:**227–237.
137. **Hess, J. M., and R. M. Kelly.** 1999. Influence of polymolecular events on inactivation behavior of xylose isomerase from *Thermotoga neapolitana* 5068. Biotechnol. Bioeng. **62:**509–517.
138. **Hettmann, T., C. L. Schmidt, S. Anemuller, U. Zahringer, H. Moll, A. Petersen, and G. Schäfer.** 1998. Cytochrome b558/566 from the archaeon *Sulfolobus acidocaldarius*. A novel highly glycosylated, membrane-bound

b-type hemoprotein. J. Biol. Chem. **273:**12032–12040.
139. **Hicks, P. M., M. W. W. Adams, and R. M. Kelly.** 1999. Enzymes, extremely thermostable, p. 987–1004. *In* M. C. Flickinger and S. W. Drew (ed.), Encyclopedia of bioprocess technology: fermentation, biocatalysis, and bioseparation. John Wiley & Sons, Inc., New York, N.Y.
140. **Hicks, P. M., and R. M. Kelly.** 1999. Thermophilic microorganisms, p. 2536–2552. *In* M. C. Flickinger and S. W. Drew (ed.), Encyclopedia of bioprocess technology: fermentation, biocatalysis, and bioseparation. John Wiley & Sons, Inc., New York, N.Y.
141. **Hiller, R., Z. H. Zhou, M. W. Adams, and S. W. Englander.** 1997. Stability and dynamics in a hyperthermophilic protein with melting temperature close to 200°C. Proc. Natl. Acad. Sci. USA **94:**11329–11332.
142. **Hollien, J., and S. Marqusee.** 1999. A thermodynamic comparison of mesophilic and thermophilic ribonucleases H. Biochemistry **38:**3836–3836.
143. **Hopfner, K. P., A. Eichinger, R. A. Engh, F. Laue, W. Ankenbauer, R. Huber, and B. Angerer.** 1999. Crystal structure of a thermostable type B DNA polymerase from *Thermococcus gorgonarius*. Proc. Natl. Acad. Sci. USA **96:**3600–3605.
144. **Horikoshi, K., and W. D. Grant (ed.).** 1998. Extremophiles. Microbial life in extreme environments. Wiley-Liss, New York, N.Y.
145. **Huber, R., S. Burggraf, T. Mayer, S. M. Barns, P. Rossnagel, and K. O. Stetter.** 1995. Isolation of a hyperthermophilic archaeum predicted by in situ RNA analysis. Nature **376:**57–58.
146. **Huber, R., D. Dyba, H. Huber, S. Burggraf, and R. Rachel.** 1998. Sulfur-inhibited *Thermosphaera aggregans* sp. nov., a new genus of hyperthermophilic archaea isolated after its prediction from environmentally derived 16S rRNA sequence. Int. J. Syst. Bacteriol. **48:**31–38.
147. **Huber, R., W. Eder, S. Heldwein, G. Wanner, H. Huber, R. Rachel, and K. O. Stetter.** 1998. *Thermocrinis ruber* gen. nov., sp. nov., a pink-filament-forming hyperthermophilic bacterium isolated from Yellowstone National Park. Appl. Environ. Microbiol. **64:**3576–3583.
148. **Huber, R., J. K. Kristjansson, and K. O. Stetter.** 1987. *Pyrobaculum* gen. nov., a new genus of neutrophilic, rod-shaped archaebacteria from continental solfataras growing optimally at 100°C. Arch. Microbiol. **149:**95–101.
149. **Huber, R., M. Kurr, H. W. Jannasch, and K. O. Stetter.** 1989. A novel group of abyssal methanogenic archaebacteria (*Methanopyrus*) growing at 110°C. Nature **342:**833–834.
150. **Huber, R., T. A. Langworthy, H. König, M. Thomm, C. R. Woese, U. B. Sleytr, and K. O. Stetter.** 1986. *Thermotoga maritima* sp. nov. represents a new genus of unique extremely thermophilic eubacteria growing up to 90°C. Arch. Microbiol. **144:**324–333.
151. **Huber, R., J. Stöhr, S. Hohenhaus, R. Rachel, S. Burggraf, H. W. Jannasch, and K. O. Stetter.** 1995. *Thermococcus chitonophagus* sp. nov., a novel, chitin-degrading, hyperthermophilic archaeum from a deep-sea hydrothermal vent environment. Arch. Microbiol. **164:**255–264.
152. **Huber, R., T. Wilharm, D. Huber, A. Trincone, S. Burggraf, H. König, R. Rachel, I. Rockinger, H. Fricke, and K. O. Stetter.** 1992. *Aquifex pyrophilus* gen. nov. sp. nov., represents a novel group of marine hyperthermophilic hydrogen-oxidizing bacteria. Syst. Appl. Microbiol. **15:**340–351.
153. **Huser, B. A., B. K. Patel, R. M. Daniel, and H. W. Morgan.** 1986. Isolation and characterisation of a novel extremely thermophilic, anaerobic, chemo-organotrophic eubacterium. FEMS Microbiol. Lett. **37:**121–127.
154. **Hyun, H. H., and J. G. Zeikus.** 1985. General biochemical characterization of thermostable extracellular β-amylase from *Clostridium thermosulfurogenes*. Appl. Environ. Microbiol. **49:**1162–1167.
155. **Ibragimova, G. T., and R. C. Wade.** 1999. Stability of the beta-sheet of the WW domain: a molecular dynamics simulation study. Biophys. J. **77:**2191–2198.
156. **Ichikawa, J. K., and S. Clarke.** 1998. A highly active protein repair enzyme from an extreme thermophile: the L-isoaspartyl methyltransferase from *Thermotoga maritima*. Arch. Biochem. Biophys. **358:**222–231.
157. **Ikeda, M., and D. S. Clark.** 1998. Molecular cloning of extremely thermostable esterase gene from hyperthermophilic archaeon *Pyrococcus furiosus* in *Escherichia coli*. Biotechnol. Bioeng. **57:**624–629.
158. **Ishikawa, K., H. Nakamura, K. Morikawa, and S. Kanaya.** 1993. Stabilization of *Escherichia coli* ribonuclease HI by cavity-filling mutations within a hydrophobic core. Biochemistry **32:**6171–6178.
159. **Ishikawa, K., M. Okumura, K. Katayanagi, S. Kimura, S. Kanaya, H. Nakamura, and K. Morikawa.** 1993. Crystal structure of ribonuclease H from *Thermus thermophilus* HB8 refined at 2.8 Å resolution. J. Mol. Biol. **230:**529–542.
160. **Isupov, M. N., T. M. Fleming, A. R. Dalby, G. S. Crowhurst, P. C. Bourne, and J. A. Littlechild.** 1999. Crystal structure of the glyceraldehyde-3-phosphate dehydrogenase from the hyperthermophilic archaeon *Sulfolobus solfataricus*. J. Mol. Biol. **291:**651–660.
161. **Jacobs, D. J., L. A. Kuhn, and M. F. Thorpe.** 1999. Flexible and rigid regions in proteins, p. 357–384. *In* M. F. Thorpe and P. Duxbury (ed.), Rigidity theory and applications. Kluwer Academic/Plenum Publishers, New York, N.Y.
162. **Jaenicke, R.** 1991. Protein stability and molecular adaptation to extreme conditions. Eur. J. Biochem. **202:**715–728.
163. **Jaenicke, R.** 1998. What ultrastable globular proteins teach us about protein stabilization. Biochemistry **63:**312–321.
164. **Jaenicke, R., and G. Böhm.** 1998. The stability of proteins in extreme environments. Curr. Opin. Struct. Biol. **8:**738–748.
165. **Jeanthon, C., S. L'Haridon, A. L. Reysenbach, E. Corre, M. Vernet, P. Messner, U. B. Sleytr, and D. Prieur.** 1999. *Methanococcus vulcanius* sp. nov., a novel hyperthermophilic methanogen isolated from East Pacific Rise, and identification of *Methanococcus* sp. DSM 4213T as *Methanococcus fervens* sp. nov. Int. J. Syst. Bacteriol. **49:**583–589.
166. **Jeanthon, C., S. L'Haridon, A. L. Reysenbach, M. Vernet, P. Messner, U. B. Sleytr, and D. Prieur.** 1998. *Methanococcus infernus* sp. nov., a novel hyperthermophilic lithotrophic methanogen isolated from a deep-sea hydrothermal vent. Int. J. Syst. Bacteriol. **48:**913–919.
167. **Jones, W. J., J. A. Leigh, F. Mayer, C. R. Woese, and R. S. Wolfe.** 1983. *Methanococcus jannaschii* sp. nov., an extremely thermophilic methanogen from a submarine hydrothermal vent. Arch. Microbiol. **136:**254–261.
168. **Kanaya, S., and M. Itaya.** 1992. Expression, purification, and characterization of a recombinant ribonuclease H from *Thermus thermophilus* HB8. J. Biol. Chem. **267:**10184–10192.
169. **Karshikoff, A., and R. Ladenstein.** 1998. Proteins from thermophilic and mesophilic organisms essentially do not differ in packing. Protein Eng. **11:**867–872.
170. **Kashiwabara, S., S. Ogawa, N. Miyoshi, M. Oda, and Y. Suzuki.** 1999. Three domains comprised in thermostable molecular weight 54,000 pullulanase of type I from *Bacillus flavocaldarius* KP1228. Biosci. Biotechnol. Biochem. **63:**1736–1748.
171. **Kasumi, T., K. Hayashai, and N. Tsumura.** 1982. Roles of magnesium and cobalt in the reaction of glucose isomerase from *Streptomyces griseofuscus* S-41. Agric. Biol. Chem. **9:**21–30.
172. **Katchalski-Katzir, E.** 1993. Immobilized enzymes — learning from past successes and failures. Trends Biotechnol. **11:**471–478.
173. **Kawamura, S., Y. Kakuta, I. Tanaka, K. Hikichi, S. Kuhara, N. Yamasaki, and M. Kimura.** 1996. Glycine-15 in the bend between two α-helices can explain the thermostability of DNA binding protein HU from *Bacillus stearothermophilus*. Biochemistry **35:**1195–1200.
174. **Kawamura, S., I. Tanaka, N. Yamasaki, and M. Kimura.** 1997. Contribution of a salt bridge to the thermostability of DNA binding protein HU from *Bacillus stearothermophilus* determined by site-directed mutagenesis. J. Biochem. **121:**448–455.
175. **Kawarabayasi, Y., Y. Hino, H. Horikawa, S. Yamasaki, Y. Haikawa, K. Jin-No, M. Takahashi, M. Sekine, S.-I. Baba, A. Ankai, H. Kosugi, A. Hosoyama, S. Fukui, Y. Nagai, K. Nishijima, H. Nakazawa, M. Takamiya, S. Masuda, T. Funahashi, T. Tanaka, Y. Kudoh, J. Yamazaki, N. Kushida, A. Oguchi, K.-I. Aoki, K. Kubota, Y. Nakamura, N. Nomura, Y. Sako, and H. Kikuchi.** 1999. Complete genome sequence of an aerobic hyper-thermophilic Crenarchaeon, *Aeropyrum pernix* K1. DNA Res. **6:**83–101, 145–152.
176. **Kengen, S. W., E. V. Luesink, A. J. Stams, and A. J. Zehnder.** 1993. Purification and characterization of an extremely thermostable β-glucosidase from the hyperthermophilic archaeon *Pyrococcus furiosus*. Eur. J. Biochem. **213:**305–312.
177. **Kim, C.-H., O. Nashiru, and J. H. Ko.** 1996. Purification and biochemical characterization of pullulanase type I from *Thermus caldophilus*. FEMS Microbiol. Lett. **138:**147–152.
178. **Kim, Y.-O., H.-K. Kim, K.-S. Bae, J.-H. Yu, and T.-K. Oh.** 1998. Purification and properties of a thermostable phytase from *Bacillus* sp. DS11. Enzyme Microb. Technol. **22:**2–7.
179. **Kimura, S., S. Kanaya, and H. Nakamura.** 1992. Thermostabilization of *Escherichia coli* ribonuclease HI by replacing left-handed helical Lys^{95} with Gly or Asn. J. Biol. Chem. **267:**22014–22017.
180. **Kirino, H., M. Aoki, M. Aoshima, Y. Hayashi, M. Ohba, A. Yamagishi, T. Wakagi, and T. Oshima.** 1994. Hydrophobic interaction at the subunit interface contributes to the thermostability of 3-isopropylmalate dehydrogenase from an extreme thermophile, *Thermus thermophilus*. Eur. J. Biochem. **220:**275–281.
181. **Klein, A. R., J. Breitung, D. Linder, K. O. Stetter, and R. K. Thauer.** 1993. N^5, N^{10}-methenyltetrahydromethanopterin cyclohydrolase from the extremely thermophilic sulfate reducing *Archaeoglobus fulgidus*: comparison of its properties with those of the cyclohydrolase from the extremely thermophilic *Methanopyrus kandleri*. Arch. Microbiol. **159:**213–219.
182. **Klingeberg, M., B. Galunsky, C. Sjøholm, V. Kasche, and G. Antranikian.** 1995. Purification and properties of a highly thermostable, sodium dodecyl sulfate-resistant and stereospecific proteinase from the extremely thermophilic archaeon *Thermococcus stetteri*. Appl. Environ. Microbiol. **61:**3098–3104.
183. **Knapp, S., W. M. de Vos, D. Rice, and R. Ladenstein.** 1997. Crystal structure of glutamate dehydrogenase from the hyperthermophilic eubacterium *Thermotoga maritima* at 3.0 Å resolution. J. Mol. Biol. **267:**916–932.
184. **Knapp, S., S. Kardinahl, N. Hellgren, G. Tibbelin, G. Schäfer, and R. Ladenstein.** 1999. Refined crystal structure of a superoxide dismutase from the hyperthermophilic archaeon *Sulfolobus acidocaldarius* at 2.2 Å resolution. J. Mol. Biol. **285:**689–702.
185. **Knöchel, T. R., M. Henning, A. Merz, B. Darimont, K. Kirschner, and J. N.**

Jansonius. 1996. The crystal structure of indole-3-glycerol phosphate synthase from the hyperthermophilic archaeon *Sulfolobus solfataricus* in three different crystal forms: effects of ionic strength. J. Mol. Biol. **262:**502–515.
186. **Kobayashi, T., Y. S. Kwak, T. Akiba, T. Kudo, and K. Horikoshi.** 1994. *Thermococcus profundus* sp. nov., a new hyperthermophilic archaeon isolated from a deep-sea hydrothermal vent. Syst. Appl. Microbiol. **17:**232–236.
187. **Koch, R., F. Canganella, H. Hippe, K. D. Jahnke, and G. Antranikian.** 1997. Purification and properties of a thermostable pullulanase from a newly isolated thermophilic anaerobic bacterium, *Fervidobacterium pennavorans* ven5. Appl. Environ. Microbiol. **63:**1088–1094.
188. **Koch, R., A. Spreinat, K. Lemke, and G. Antranikian.** 1991. Purification and properties of a hyperthermoactive α-amylase from the archaeobacterium *Pyrococcus woesei*. Arch. Microbiol. **155:**572–578.
189. **Koh, S., H.-J. Shin, J. S. Kim, D.-S. Lee, and S. Y. Lee.** 1998. Trehalose synthesis from maltose by a thermostable trehalose synthase from *Thermus caldophilus*. Biotechnol. Lett. **20:**757–761.
190. **Kohen, A., R. Cannio, S. Bartolucci, and J. P. Klinman.** 1999. Enzyme dynamics and hydrogen tunnelling in a thermophilic alcohol dehydrogenase. Nature **399:**496–499.
191. **Kojoh, K., H. Matsuzawa, and T. Wakagi.** 1999. Zinc and an N-terminal extra stretch of the ferredoxin from a thermoacidophilic archaeon stabilize the molecule at high temperature. Eur. J. Biochem. **264:**85–91.
192. **Korndörfer, I., B. Steipe, R. Huber, A. Tomschy, and R. Jaenicke.** 1995. The crystal structure of holo-glyceraldehyde-3-phosphate dehydrogenase from the hyperthermophilic bacterium *Thermotoga maritima* at 2.5 Å resolution. J. Mol. Biol. **246:**511–521.
193. **Kort, R., W. Liebl, B. Labedan, P. Forterre, R. I. L. Eggen, and W. M. Vos.** 1997. Glutamate dehydrogenase from the hyperthermophilic bacterium *Thermotoga maritima*: molecular characterization and phylogenetic implications. Extremophiles **1:**52–60.
194. **Kozianowski, G., F. Canganella, F. A. Rainey, H. Hippe, and G. Antranikian.** 1997. Purification and characterization of thermostable pectate-lyases from a newly isolated thermophilic bacterium, *Thermoanaerobacter italicus* sp. nov. Extremophiles **1:**171–182.
195. **Kujo, C., and T. Oshima.** 1998. Enzymological characteristics of the hyperthermostable NAD-dependent glutamate dehydrogenase from the archaeon *Pyrobaculum islandicum* and effects of denaturants and organic solvents. Appl. Environ. Microbiol. **64:**2152–2157.
196. **Kumar, S., and R. Nussinov.** 1999. Salt bridge stability in monomeric proteins. J. Mol. Biol. **293:**1241–1255.
197. **Kunow, J., D. Linder, K. O. Stetter, and R. K. Thauer.** 1994. $F_{420}H_2$: quinone oxidoreductase from *Archaeoglobus fulgidus*. Characterization of a membrane-bound multisubunit complex containing FAD and iron-sulfur clusters. Eur. J. Biochem. **223:**503–511.
198. **Larrick, J. W. (ed.).** 1997. The PCR technique: quantitative PCR. Eaton Publishing, Natick, Mass.
199. **Lawyer, F. C., S. Stoffel, R. K. Saiki, K. Myambo, and D. H. Gelfand.** 1989. Isolation, characterization, and expression in *Escherichia coli* of the DNA polymerase gene from *Thermus aquaticus*. J. Biol. Chem. **264:**6427–6437.
200. **Lazaridis, T., and M. Karplus.** 1997. "New view" of protein folding reconciled with the old through multiple unfolding simulations. Science **278:**1928–1931.
201. **Lazaridis, T., I. Lee, and M. Karplus.** 1997. Dynamics and unfolding pathways of a hyperthermophilic and a mesophilic rubredoxin. Protein Sci. **6:**2589–2605.
202. **Lebbink, J. H., R. I. Eggen, A. C. Geerling, V. Consalvi, R. Chiaraluce, R. Scandurra, and W. M. de Vos.** 1995. Exchange of domains of glutamate dehydrogenase from the hyperthermophilic archaeon *Pyrococcus furiosus* and the mesophilic bacterium *Clostridium difficile*: effects on catalysis, thermoactivity and stability. Protein Eng. **8:**1287–1294.
203. **Lebbink, J. H. G., S. Knapp, J. van der Oost, D. Rice, R. Ladenstein, and W. M. de Vos.** 1999. Engineering activity and stability of *Thermotoga maritima* glutamate dehydrogenase. II: construction of a 16-residue ion-pair network at the subunit interface. J. Mol. Biol. **289:**357–369.
204. **Lee, C. Y., and J. G. Zeikus.** 1991. Purification and characterization of thermostable glucose isomerase from *Clostridium thermosulfurogenes* and *Thermoanaerobacter* strain B6A. Biochem. J. **273:**565–571.
205. **Lee, J. T., H. Kanai, T. Kobayashi, T. Akiba, and T. Kudo.** 1996. Cloning, nucleotide sequence, and hyperexpression of α-amylase gene from an archaeon, *Thermococcus profundus*. J. Ferment. Bioeng. **82:**432–438.
206. **Lee, S. G., D. C. Lee, S. P. Hong, M. H. Sung, and H. S. Kim.** 1995. Thermostable D-hydantoinase from thermophilic *Bacillus stearothermophilus* DS-1: characteristics of purified enzyme. Appl. Microbiol. Biotechnol. **43:**270–276.
207. **Lee, Y. E., S. E. Lowe, B. Henrissat, and J. G. Zeikus.** 1993. Characterization of the active site and thermostability regions of endoxylanase from *Thermoanaerobacterium saccharolyticum* B6A-RI. J. Bacteriol. **175:**5890–5898.
208. **Lee, Y. E., S. E. Lowe, and J. G. Zeikus.** 1993. Gene cloning, sequencing, and biochemical characterization of endoxylanase from *Thermoanaerobacterium saccharolyticum* B6A-RI. Appl. Environ. Microbiol. **59:**3134–3137.
209. **Lee, Y. E., and J. G. Zeikus.** 1993. Genetic organization, sequence and biochemical characterization of recombinant β-xylosidase from *Thermoanaerobacterium saccharolyticum* strain B6A-RI. J. Gen. Microbiol. **139:**1235–1243.
210. **Lehmacher, A., and H. Bisswanger.** 1990. Comparative kinetics of D-xylose and D-glucose isomerase activities of the D-xylose isomerase from *Thermus aquaticus* HB8. Biol. Chem. Hoppe-Seyler **371:**527–536.
211. **Lewis, S. M.** 1996. Fermentation alcohol, p. 11–48. *In* T. Godfrey and S. I. West (ed.), Industrial enzymology, 2nd ed. Stockton Press, New York, N.Y.
212. **Li, A., and V. Daggett.** 1994. Characterization of the transition state of protein unfolding by use of molecular dynamics: chymotrypsin inhibitor 2. Proc. Natl. Acad. Sci. USA **91:**10430–10434.
213. **Li, A., and V. Daggett.** 1996. Identification and characterization of the unfolding transition state of chymotrypsin inhibitor 2 by molecular dynamics simulations. J. Mol. Biol. **257:**412–429.
214. **Li, A., and V. Daggett.** 1997. Molecular dynamics simulation of the unfolding of barnase: characterization of the major intermediate. J. Mol. Biol. **275:**677–694.
215. **Li, C., J. Heatwole, S. Soelaiman, and M. Shoham.** 1999. Crystal structure of a thermophilic alcohol dehydrogenase substrate complex suggests determinants of substrate specificity and thermostability. Proteins Struct. Funct. Genet. **37:**619–627.
216. **Li, W., R. A. Grayling, K. Sandman, S. Edmondson, J. W. Shriver, and J. N. Reeve.** 1998. Thermodynamic stability of archaeal histones. Biochemistry **37:**10563–10572.
217. **Liebl, W., D. Brem, and A. Gotschlich.** 1998. Analysis of the gene for β-fructosidase (invertase, inulinase) of the hyperthermophilic bacterium *Thermotoga maritima*, and characterisation of the enzyme expressed in *Escherichia coli*. Appl. Microbiol. Biotechnol. **50:**55–64.
218. **Liebl, W., P. Ruile, K. Bronnenmeier, K. Riedel, F. Lottspeich, and I. Greif.** 1996. Analysis of a *Thermotoga maritima* DNA fragment encoding two similar thermostable cellulases, CelA and CelB, and characterization of the recombinant enzymes. Microbiology **142:**2533–2542.
219. **Liebl, W., B. Wagner, and J. Schellhase.** 1998. Properties of an α-galactosidase, and structure of its gene *galA*, within an α- and β-galactoside utilization gene cluster of the hyperthermophilic bacterium *Thermotoga maritima*. Syst. Appl. Microbiol. **21:**1–11.
220. **Lim, J. H., Y. G. Yu, Y. S. Han, S. Cho, B. Y. Ahn, S. H. Kim, and Y. Cho.** 1997. The crystal structure of an Fe-superoxide dismutase from the hyperthermophile *Aquifex pyrophilus* at 1.9 Å resolution: structural basis for thermostability. J. Mol. Biol. **270:**259–274.
221. **Liu, S. Y., J. Wiegel, and F. C. Gherardini.** 1996. Purification and cloning of a thermostable xylose (glucose) isomerase with an acidic pH optimum from *Thermoanaerobacterium* strain JW/SL-YS 489. J. Bacteriol. **178:**5938–5945.
222. **Londesborough, J.** 1980. The causes of sharply bent or discontinuous Arrhenius plots for enzyme-catalyzed reactions. Eur. J. Biochem. **105:**211–215.
223. **Lowe, S. E., M. K. Jain, and J. G. Zeikus.** 1993. Biology, ecology, and biotechnological applications of anaerobic bacteria adapted to environmental stresses in temperature, pH, salinity, or substrates. Microbiol. Rev. **57:**451–509.
224. **Ma, K., D. Linder, K. O. Stetter, and R. K. Thauer.** 1991. Purification and properties of N^5, N^{10}-methylenetetrahydromethanopterin reductase (coenzyme F_{420}-dependent) from the extreme thermophile *Methanopyrus kandleri*. Arch. Microbiol. **155:**593–600.
225. **Ma, K., C. Zirngibl, D. Linder, K. O. Stetter, and R. K. Thauer.** 1991. N^5,N^{10}-methylenetetrahydromethanopterin dehydrogenase (H_2-forming) from the extreme thermophile *Methanopyrus kandleri*. Arch. Microbiol. **156:**43–48.
226. **Macedo-Ribeiro, S., B. Darimont, R. Sterner, and R. Huber.** 1996. Small structural changes account for the high thermostability of 1[4Fe-4S] ferredoxin from the hyperthermophilic bacterium *Thermotoga maritima*. Structure **4:**1290–1301.
227. **Maes, D., J. P. Zeelen, N. Thanki, N. Beaucamp, M. Alvarez, M. H. Thi, J. Backmann, J. A. Martial, L. Wyns, R. Jaenicke, and R. K. Wierenga.** 1999. The crystal structure of triosephosphate isomerase (TIM) from *Thermotoga maritima*: a comparative thermostability structural analysis of ten different TIM structures. Proteins **37:**441–453.
228. **Malakauskas, S. M., and S. L. Mayo.** 1998. Design, structure and stability of a hyperthermophilic protein variant. Nat. Struct. Biol. **5:**470–475.
229. **Manco, G., E. Giosuè, S. D'Auria, P. Herman, G. Carrea, and M. Rossi.** 2000. Cloning, overexpression, and properties of a new thermophilic and thermostable esterase with sequence similarity to hormone-sensitive lipase subfamily from the archaeon *Archaeoglobus fulgidus*. Arch. Biochem. Biophys. **373:**182–192.
230. **Mansfeld, J., G. Vriend, B. W. Dijkstra, O. R. Veltman, B. Van den Burg, G. Venema, R. Ulbrich-Hofmann, and V. G. H. Eijsink.** 1997. Extreme stabilization of a thermolysin-like protease by an engineered disulfide bond. J. Biol. Chem. **272:**11152–11156.
231. **Maras, B., V. Consalvi, R. Chiaraluce, L. Politi, M. De Rosa, F. Bossa, R. Scandurra, and D. Barra.** 1992. The protein sequence of glutamate dehy-

drogenase from *Sulfolobus solfataricus*, a thermoacidophilic archaebacterium. Is the presence of N-ε-methyllysine related to thermostability? Eur. J. Biochem. **203:**81–87.
232. **Marg, G. A., and D. S. Clark.** 1990. Activation of the glucose isomerase by divalent cations: evidence for two distinct metal-binding sites. Enzyme Microb. Technol. **12:**367–373.
233. **Marteinsson, V. T., J. L. Birrien, A. L. Reysenbach, M. Vernet, D. Marie, A. Gambacorta, P. Messner, U. B. Sleytr, and D. Prieur.** 1999. *Thermococcus barophilus* sp. nov., a new barophilic and hyperthermophilic archaeon isolated under high hydrostatic pressure from a deep-sea hydrothermal vent. Int. J. Syst. Bacteriol. **49:**351–359.
234. **Mathupala, S., B. C. Saha, and J. G. Zeikus.** 1990. Substrate competition and specificity at the active site of amylopullulanase from *Clostridium thermohydrosulfuricum*. Biochem. Biophys. Res. Commun. **166:**126–132.
235. **Mathupala, S. P., S. E. Lowe, S. M. Podkovyrov, and J. G. Zeikus.** 1993. Sequencing of the amylopullulanase (*apu*) gene of *Thermoanaerobacter ethanolicus* 39E, and identification of the active site by site-directed mutagenesis. J. Biol. Chem. **268:**16332–16344.
236. **Mathupala, S. P., and J. G. Zeikus.** 1993. Improved purification and biochemical characterization of extracellular amylopullulanase from *Thermoanaerobacter ethanolicus* 39E. Appl. Microbiol. Biotechnol. **39:**487–493.
237. **Matsumura, M., G. Signor, and B. W. Matthews.** 1989. Substantial increase of protein stability by multiple disulphide bonds. Nature **342:**291–293.
238. **Matthews, B. W., H. Nicholson, and W. J. Becktel.** 1987. Enhanced protein thermostability from site-directed mutations that decrease the entropy of unfolding. Proc. Natl. Acad. Sci. USA **84:**6663–6667.
239. **Matussek, K., P. Moritz, N. brunner, C. Eckerskorn, and R. Hensel.** 1998. Cloning, sequencing, and expression of the gene encoding cyclic 2,3-diphosphoglycerate synthetase, the key enzyme of cyclic 2,3-diphosphoglycerate metabolism in *Methanothermus fervidus*. J. Bacteriol. **180:**5997–6004.
240. **McAfee, J. G., S. P. Edmondson, P. K. Datta, J. W. Shriver, and R. Gupta.** 1995. Gene cloning, expression, and characterization of the Sac7 proteins from the hyperthermophile *Sulfolobus acidocaldarius*. Biochemistry **34:**10063–10077.
241. **McCrary, B. S., S. P. Edmondson, and J. W. Shriver.** 1996. Hyperthermophile protein folding thermodynamics: differential scanning calorimetry and chemical denaturation of Sac7d. J. Mol. Biol. **264:**784–805.
242. **McLean, M. A., S. A. Maves, K. E. Weiss, S. Krepich, and S. G. Sligar.** 1998. Characterization of a cytochrome P450 from the acidothermophilic archaea *Sulfolobus solfataricus*. Biochem. Biophys. Res. Commun. **252:**166–172.
243. **Meissner, H., and W. Liebl.** 1998. *Thermotoga maritima* maltosyltransferase, a novel type of maltodextrin glycosyltransferase acting on starch and malto-oligosaccharides. Eur. J. Biochem. **258:**1050–1058.
244. **Meng, M., M. Bagdasarian, and J. G. Zeikus.** 1993. Thermal stabilization of xylose isomerase from *Thermoanaerobacterium thermosulfurigenes*. Bio/Technology **11:**1157–1161.
245. **Meng, M., C. Lee, M. Bagdasarian, and J. G. Zeikus.** 1991. Switching substrate preference of thermophilic xylose isomerase from D-xylose to D-glucose by redesigning the substrate binding pocket. Proc. Natl. Acad. Sci. USA **88:**4015–4019.
246. **Merz, A., T. Knöchel, J. N. Jansonius, and K. Kirschner.** 1999. The hyperthermostable indoleglycerol phosphate synthase from *Thermotoga maritima* is destabilized by mutational disruption of two solvent-exposed salt bridges. J. Mol. Biol. **288:**753–763.
247. **Michels, P. C., and D. S. Clark.** 1997. Pressure-enhanced activity and stability of a hyperthermophilic protease from a deep-sea methanogen. Appl. Environ. Microbiol. **63:**3985–3991.
248. **Miller, J. F., C. M. Nelson, J. M. Ludlow, N. N. Shah, and D. S. Clark.** 1989. High pressure-temperature bioreactor: assays of thermostable hydrogenase with fiber optics. Biotechnol. Bioeng. **34:**1015–1021.
249. **Miroshnichenko, M. L., E. A. Bonch-Osmolovskaya, A. Neuner, N. A. Kostrikina, N. A. Chernych, and V. A. Alekseev.** 1989. *Thermococcus stetteri* sp. nov., a new extremely thermophilic marine sulfur-metabolizing archaebacterium. Sys. Appl. Microbiol. **12:**257–262.
250. **Moriyama, H., K. Onodera, M. Sakurai, N. Tanaka, H. Kirino-Kagawa, T. Oshima, and Y. Katsube.** 1995. The crystal structures of mutated 3-isopropylmalate dehydrogenase from *Thermus thermophilus* HB8 and their relationship to the thermostability of the enzyme. J. Biochem. **117:**408–413.
251. **Mozhaev, V. V.** 1993. Mechanism-based strategies for protein thermostabilization. Trends Biotechnol. **11:**88–95.
252. **Mrabet, N. T., A. Van den Broeck, I. Van den Brande, P. Stanssens, Y. Laroche, A. M. Lambeir, G. Matthijssens, J. Jenkins, M. Chiadmi, H. van Tilbeurgh, F. Rey, J. Janin, W. J. Quax, I. Lasters, M. De Maeyer, and S. J. Wodak.** 1992. Arginine residues as stabilizing elements in proteins. Biochemistry **31:**2239–2253.
253. **Muheim, A., R. J. Todd, D. R. Casimiro, H. B. Gray, and F. H. Arnold.** 1993. Ruthenium-mediated protein cross-linking and stabilization. J. Am. Chem. Soc. **115:**5312–5313.
254. **Muir, J. M., R. J. Russell, D. W. Hough, and M. J. Danson.** 1995. Citrate synthase from the hyperthermophilic archaeon, *Pyrococcus furiosus*. Protein Eng. **8:**583–592.
255. **Nakai, T., K. Okada, S. Akutsu, I. Miyahara, S. Kawaguchi, R. Kato, S. Kuramitsu, and K. Hirotsu.** 1999. Structure of *Thermus thermophilus* HB8 aspartate aminotransferase and its complex with maleate. Biochemistry **38:**2413–2424.
256. **Neet, K. E., and D. E. Timm.** 1994. Conformational stability of dimeric proteins: quantitative studies by equilibrium denaturation. Protein Sci. **3:**2167–2174.
257. **Nelson, C. M., M. R. Schuppenhauer, and D. S. Clark.** 1992. High pressure, high-temperature bioreactor for comparing effects of hyperbaric and hydrostatic pressure on bacterial growth. Appl. Environ. Microbiol. **58:**1789–1793.
258. **Nelson, K. E., R. A. Clayton, S. R. Gill, M. L. Gwinn, R. J. Dodson, D. H. Haft, E. K. Hickey, J. D. Peterson, W. C. Nelson, K. A. Ketchum, L. McDonald, T. R. Utterback, J. A. Malek, K. D. Linher, M. M. Garrett, A. M. Stewart, M. D. Cotton, M. S. Pratt, C. A. Phillips, D. Richardson, J. Heidelberg, G. G. Sutton, R. D. Fleischmann, J. A. Eisen, O. White, S. L. Salzberg, H. O. Smith, J. C. Venter, and C. M. Fraser.** 1999. Evidence for lateral gene transfer between archaea and bacteria from genome sequence of *Thermotoga maritima*. Nature **399:**323–329.
259. **Nesper, M., S. Nock, E. Sedlak, M. Antalik, D. Podhradsky, and M. Sprinzl.** 1998. Dimers of *Thermus thermophilus* elongation factors Ts are required for its function as a nucleotide exchange factor of elongation factor Tu. Eur. J. Biochem. **255:**81–86.
260. **Neuner, A., H. W. Jannasch, S. Belkin, and K. O. Stetter.** 1990. *Thermococcus litoralis* sp. nov.: a new species of extremely thermophilic marine archaebacteria. Arch. Microbiol. **153:**205–207.
261. **Nicholls, A., K. A. Sharp, and B. Honig.** 1991. Protein folding and association: insights from the interfacial and thermodynamic properties of hydrocarbons. Proteins **11:**281–296.
262. **Nicholson, H., W. J. Becktel, and B. W. Matthews.** 1988. Enhanced protein thermostability from designed mutations that interact with α-helix dipoles. Nature **336:**651–656.
263. **Niehaus, F., C. Bertoldo, M. Kahler, and G. Antranikian.** 1999. Extremophiles as a source of novel enzymes for industrial application. Appl. Microbiol. Biotechnol. **51:**711–729.
264. **Nojima, H., K. Hon-Nami, T. Oshima, and H. Noda.** 1978. Reversible thermal unfolding of thermostable cytochrome *c*-552. J. Mol. Biol. **122:**33–42.
265. **Nojima, H., A. Ikai, T. Oshima, and H. Noda.** 1977. Reversible unfolding of thermostable phosphoglycerate kinase. Thermostability associated with mean zero enthalpy change. J. Mol. Biol. **116:**429–442.
266. **Ogasahara, K., E. A. Lapshina, M. Sakai, Y. Izu, S. Tsunasawa, I. Kato, and K. Yutani.** 1998. Electrostatic stabilization in methionine aminopeptidase from hyperthermophile *Pyrococcus furiosus*. Biochemistry **37:**5939–5946.
267. **Olsen, O., and K. K. Thomsen.** 1991. Improvement of bacterial β-glucanase thermostability by glycosylation. J. Gen. Microbiol. **137:**579–585.
268. **Ostendorp, R., G. Auerbach, and R. Jaenicke.** 1996. Extremely thermostable L(+)-lactate dehydrogenase from *Thermotoga maritima*: cloning, characterization, and crystallization of the recombinant enzyme in its tetrameric and octameric state. Protein Sci. **5:**862–873.
269. **Pace, C. N.** 1992. Contribution of the hydrophobic effect to globular protein stability. J. Mol. Biol. **226:**29–35.
270. **Pappenberger, G., H. Schurig, and R. Jaenicke.** 1997. Disruption of an ionic network leads to accelerated thermal denaturation of D-glyceraldehyde-3-phosphate dehydrogenase from the hyperthermophilic bacterium *Thermotoga maritima*. J. Mol. Biol. **274:**676–683.
271. **Perler, F. B., D. G. Comb, W. E. Jack, L. S. Moran, B. Qiang, R. B. Kucera, J. Benner, B. E. Slatko, D. O. Nwankwo, S. K. Hempstead, C. K. Carlow, and H. Jannasch.** 1992. Intervening sequences in an archaea DNA polymerase gene. Proc. Natl. Acad. Sci. USA **89:**5577–5581.
272. **Perutz, M. F.** 1978. Electrostatic effects in proteins. Science **201:**1187–1191.
273. **Perutz, M. F., and H. Raidt.** 1975. Stereochemical basis of heat stability in bacterial ferredoxins and in haemoglobin A2. Nature **255:**256–259.
274. **Pfeil, W., U. Gesierich, G. R. Kleemann, and R. Sterner.** 1997. Ferredoxin from the hyperthermophile *Thermotoga maritima* is stable beyond the boiling point of water. J. Mol. Biol. **272:**591–596.
275. **Piper, P. W., C. Emson, C. E. Jones, C. D. A., T. M. Fleming, and J. A. Littlechild.** 1996. Complementation of a *pgk* deletion mutation in *Saccharomyces cerevisiae* with expression of the phosphoglycerate-kinase gene from the hyperthermophilic archaeon *Sulfolobus solfataricus*. Curr. Genet. **29:**594–596.
276. **Pley, U., J. Schipka, A. Gambacorta, H. W. Jannasch, H. Fricke, R. Rachel, and K. O. Stetter.** 1991. *Pyrodictium abyssi* sp. nov. represents a novel heterotrophic marine archaeal hyperthermophile growing at 110°C. Syst. Appl. Microbiol. **14:**245–253.
277. **Privalov, P. L., and N. N. Khechinashvili.** 1974. A thermodynamic approach to the problem of stabilization of globular protein structure: a calorimetric study. J. Mol. Biol. **86:**665–684.
278. **Purcarea, C., G. Erauso, D. Prieur, and G. Hervé.** 1994. The catalytic and regulatory properties of aspartate transcarbamoylase from *Pyrococcus abyssi*, a new deep-sea hyperthermophilic archaebacterium. Microbiology **140:**1967–1975.

279. **Quax, W. J., N. T. Mrabet, R. G. Luiten, P. W. Schuurhuizen, P. Stanssens, and I. Lasters.** 1991. Enhancing the thermostability of glucose isomerase by protein engineering. Bio/Technology **9:**738–442.
280. **Rahman, R. N. Z. A., S. Fujiwara, H. Nakamura, M. Takagi, and T. Imanaka.** 1998. Ion pairs involved in maintaining a thermostable structure of glutamate dehydrogenase from a hyperthermophilic archaeon. Biochem. Biophys. Res. Commun. **248:**920–926.
281. **Reysenbach, A.-L., and J. W. Deming.** 1991. Effects of hydrostatic pressure on growth of hyperthermophilic archaebacteria from the Juan de Fuca Ridge. Appl. Environ. Microbiol. **57:**1271–1274.
282. **Roovers, M., C. Hethke, C. Legrain, M. Thomm, and N. Glansdorff.** 1997. Isolation of the gene encoding *Pyrococcus furiosus* ornithine carbamoyltransferase and study of its expression profile *in vivo* and *in vitro*. Eur. J. Biochem. **247:**1038–1045.
283. **Rüdiger, A., P. L. Jorgensen, and G. Antranikian.** 1995. Isolation and characterization of a heat-stable pullulanase from the hyperthermophilic archaeon *Pyrococcus woesei* after cloning and expression of its gene in *Escherichia coli*. Appl. Environ. Microbiol. **61:**567–575.
284. **Russell, R. J., J. M. Ferguson, D. W. Hough, M. J. Danson, and G. L. Taylor.** 1997. The crystal structure of citrate synthase from the hyperthermophilic archaeon *Pyrococcus furiosus* at 1.9 Å resolution. Biochemistry **36:**9983–9994.
285. **Ruttersmith, L. D., and R. M. Daniel.** 1993. Thermostable β-glucosidase and β-xylosidase from *Thermotoga* sp. strain FjSS3-B.1. Biochim. Biophys. Acta **1156:**167–172.
286. **Ruttersmith, L. D., and R. M. Daniel.** 1991. Thermostable cellobiohydrolase from the thermophilic eubacterium *Thermotoga* sp. strain FjSS3-B.1. Biochem. J. **277:**887–890.
287. **Ruttersmith, L. D., R. M. Daniel, and H. D. Simpson.** 1992. Cellulolytic and hemicellulolytic enzymes functional above 100°C. Ann. N. Y. Acad. Sci. **672:**137–141.
288. **Saha, B., and J. G. Zeikus.** 1991. Characterization of thermostable α-glucosidase from *Clostridium thermohydrosulfuricum* 39E. Appl. Microbiol. Biotechnol. **35:**568–571.
289. **Saha, B., and J. G. Zeikus.** 1989. Novel highly thermostable pullulanase from thermophiles. Trends Biotechnol. **7:**234–239.
290. **Sako, Y., P. C. Croocker, and Y. Ishida.** 1997. An extremely heat-stable extracellular proteinase (aeropyrolysin) from the hyperthermophilic archaeon *Aeropyrum pernix* K1. FEBS Lett. **415:**329–334.
291. **Sako, Y., N. Nomura, A. Uchida, Y. Ishida, H. Morii, Y. Koga, T. Hoaki, and T. Maruyama.** 1996. *Aeropyrum pernix* gen. nov., sp. nov., a novel aerobic hyperthermophilic archaeon growing at temperatures up to 100°C. Int. J. Syst. Bacteriol. **46:**1070–1077.
292. **Sako, Y., K. Takai, A. Uchida, and Y. Ishida.** 1996. Purification and characterization of phosphoenolpyruvate carboxylase from the hyperthermophilic archaeon *Methanothermus sociabilis*. FEBS Lett. **392:**148–152.
293. **Sanz-Aparicio, J., J. A. Hermoso, M. Martinez-Ripoll, B. Gonzalez, C. Lopez-Camacho, and J. Polaina.** 1998. Structural basis of increased resistance to thermal denaturation induced by single amino acid substitution in the sequence of β-glucosidase A from *Bacillus polymyxa*. Proteins Struct. Funct. Gene. **33:**567–576.
294. **Saul, D. S., L. C. Williams, R. A. Reeves, M. D. Gibbs, and P. L. Bergquist.** 1995. Sequence and expression of a xylanase gene from the hyperthermophile *Thermotoga* sp. strain FjSS3-B.1 and characterization of the recombinant enzyme and its activity on kraft pulp. Appl. Environ. Microbiol. **61:**4110–4113.
295. **Schäfer, S., C. Barkowski, and G. Fuchs.** 1986. Carbon assimilation by the autotrophic thermophilic archaebacterium *Thermoproteus neutrophilus*. Arch. Microbiol. **146:**301–308.
296. **Schink, B., and J. G. Zeikus.** 1983. Characterization of pectinolytic enzymes of *Clostridium thermosulfurogenes*. FEMS Microbiol. Lett. **17:**295–298.
297. **Schmidt-Dannert, C., and F. H. Arnold.** 1999. Directed evolution of industrial enzymes. Trends Biotechnol. **17:**135–136.
298. **Schuliger, J. W., S. H. Brown, J. A. Baross, and R. M. Kelly.** 1993. Purification and characterization of a novel amylolytic enzyme from ES4, a marine hyperthermophilic archaeum. Mol. Marine Biol. Biotechnol. **2:**76–87.
299. **Schultes, V., R. Deutzmann, and R. Jaenicke.** 1990. Complete amino-acid sequence of glyceraldehyde-3-phosphate dehydrogenase from the hyperthermophilic eubacterium *Thermotoga maritima*. Eur. J. Biochem. **192:**25–31.
300. **Schumann, J., A. Wrba, R. Jaenicke, and K. O. Stetter.** 1991. Topographical and enzymatic characterization of amylases from the extremely thermophilic eubacterium *Thermotoga maritima*. FEBS Lett. **282:**122–126.
301. **Segerer, A., A. Neuner, J. K. Kristjansson, and K. O. Stetter.** 1986. *Acidianus infernus* gen. nov., sp. nov., and *Acidianus brierleyi* comb. nov.: facultative aerobic, extremely acidophilic thermophilic sulfur-metabolizing archaebacteria. Int. J. Syst. Bacteriol. **36:**559–564.
302. **Segerer, A. H., A. Trincone, M. Gahrtz, and K. O. Stetter.** 1991. *Stygiolobus azoricus* gen. nov., sp. nov. represents a novel genus of anaerobic, extremely thermoacidophilic archaebacteria of the order *Sulfolobales*. Int. J. Syst. Bacteriol. **41:**495–501.
303. **Serrano, L., M. Bycroft, and A. R. Fersht.** 1991. Aromatic-aromatic interactions and protein stability. Investigation by double-mutant cycles. J. Mol. Biol. **218:**465–475.
304. **Shen, G. J., B. C. Saha, Y. E. Lee, L. Bhatnagar, and J. G. Zeikus.** 1988. Purification and characterization of a novel thermostable β-amylase from *Clostridium thermosulfurogenes*. Biochem. J. **254:**835–840.
305. **Shima, S., D. A. Hérault, A. Berkessel, and R. K. Thauer.** 1998. Activation and thermostabilization effects of cyclic 2,3-diphosphoglycerate on enzymes from the hyperthermophilic *Methanococcus kandleri*. Arch. Microbiol. **170:**469–472.
306. **Shima, S., C. Tziatzios, D. Schubert, H. Fukada, K. Takahashi, U. Ermler, and R. K. Thauer.** 1998. Lyotropic-salt-induced changes in monomer/dimer/tetramer association equilibrium of formyltransferase from the hyperthermophilic *Methanopyrus kandleri* in relation to the activity and thermostability of the enzyme. Eur. J. Biochem. **258:**85–92.
307. **Shirley, B. A., P. Stanssens, U. Hahn, and C. N. Pace.** 1992. Contribution of hydrogen bonding to the conformational stability of ribonuclease T1. Biochemistry **31:**725–732.
308. **Siebert, P. (ed.).** 1998. The PCR technique: RT-PCR. Eaton Publishing, Natick, Mass.
309. **Simpson, H. D., U. R. Haufler, and R. M. Daniel.** 1991. An extremely thermostable xylanase from the thermophilic eubacterium *Thermotoga*. Biochem. J. **277:**413–417.
310. **Singleton, M., M. Isupov, and J. Littlechild.** 1999. X-ray structure of pyrrolidone carboxyl peptidase from the hyperthermophilic archaeon *Thermococcus litoralis*. Struct. Fold Des. **7:**237–244.
311. **Smith, C. A., H. S. Toogood, H. M. Baker, R. M. Daniel, and E. N. Baker.** 1999. Calcium-mediated thermostability in the subtilisin superfamily: the crystal structure of *Bacillus* Ak.1 protease at 1.8 Å resolution. J. Mol. Biol. **294:**1027–1040.
312. **Specka, U., F. Mayer, and G. Antranikian.** 1991. Purification and properties of a thermoactive glucoamylase from *Clostridium thermosaccharolyticum*. Appl. Environ. Microbiol. **57:**2317–2323.
313. **Sriprapundh, D., C. Vieille, and J. G. Zeikus.** 2000. Molecular determinants of xylose isomerase thermal stability and activity: analysis by site-directed mutagenesis. Protein Eng. **13:**259–265.
314. **Stemmer, W. P.** 1994. Rapid evolution of a protein in vitro by DNA shuffling. Nature **370:**389–391.
315. **Sterner, R., G. R. Kleemann, H. Szadkowski, A. Lustig, M. Hennig, and K. Kirschner.** 1996. Phosphoribosyl anthranilate isomerase from *Thermotoga maritima* is an extremely stable and active homodimer. Protein Sci. **5:**2000–2008.
316. **Stetter, K. O.** 1988. *Archaeoglobus fulgidus* gen. nov., sp.: a new taxon of extremely thermophilic archaebacteria. Syst. Appl. Microbiol. **10:**172–173.
317. **Stetter, K. O.** 1999. Extremophiles and their adaptation to hot environments. FEBS Lett. **452:**22–25.
318. **Stetter, K. O.** 1996. Hyperthermophiles in the history of life. Ciba Found. Symp. **202:**1–10.
319. **Stetter, K. O.** 1998. Hyperthermophiles: isolation, classification, and properties, p. 1–24. *In* K. Horikoshi and W. D. Grant (ed.), Extremophiles: microbial life in extreme environments. Wiley-Liss, New York, N.Y.
320. **Stetter, K. O.** 1996. Hyperthermophilic procaryotes. FEMS Microbiol. Rev. **18:**149–158.
321. **Stetter, K. O.** 1982. Ultrathin mycelia-forming organisms from submarine volcanic areas having an optimum growth temperature of 105°C. Nature **300:**258–260.
322. **Stetter, K. O., H. König, and B. Stackebrandt.** 1983. *Pyrodictium* gen. nov., a new genus of submarine disc-shaped sulphur reducing archaebacteria growing optimally at 105°C. Syst. Appl. Microbiol. **4:**535–551.
323. **Stetter, K. O., M. Thomm, J. Winter, G. Wildgruber, H. Huber, W. Zillig, D. Janecovic, H. König, P. Palm, and S. Wunderl.** 1981. *Methanothermus fervidus*, sp. nov., a novel extremely thermophilic methanogen isolated from an iceland hot spring. Zentbl. Bakteriol. Mikrobiol. Hyg. I Abt Orig. C**2:**166–178.
324. **Sunna, A., J. Puls, and G. Antranikian.** 1996. Purification and characterization of two thermostable endo-1, 4-β-D-xylanases from *Thermotoga thermarum*. Biotechnol. Appl. Biochem. **24:**177–185.
325. **Suzuki, Y., K. Hatagaki, and H. Oda.** 1991. A hyperthermostable pullulanase produced by an extreme thermophile, *Bacillus flavocaldarius* KP 1228, and evidence for the proline theory of increasing protein thermostability. Appl. Microbiol. Biotechnol. **34:**707–714.
326. **Tachibana, Y., A. Kuramura, N. Shirasaka, Y. Suzuki, T. Yamamoto, S. Fujiwara, M. Takagi, and T. Imanaka.** 1999. Purification and characterization of an extremely thermostable cyclomaltodextrin glucanotransferase from a newly isolated hyperthermophilic archaeon, a *Thermococcus* sp. Appl. Environ. Microbiol. **65:**1991–1997.
327. **Tahirov, T. H., H. Oki, T. Tsukihara, K. Ogasahara, K. Yutani, K. Ogata, Y. Izu, S. Tsunasawa, and I. Kato.** 1998. Crystal structure of methionine aminopeptidase from hyperthermophile, *Pyrococcus furiosus*. J. Mol. Biol. **284:**101–124.
328. **Takai, K., Y. Sako, A. Uchida, and Y. Ishida.** 1997. Extremely thermostable phosphoenolpyruvate carboxylase from an extreme thermophile, *Rhodo-*

thermus obamensis. J. Biochem. **122:**32–40.
329. **Takai, K., A. Sugai, T. Itoh, and K. Horikoshi.** 2000. *Palaeococcus ferrophilus* gen. nov., sp. nov., a barophilic, hyperthermophilic archaeon from a deep-sea hydrothermal vent chimney. Int. J. Syst. Evol. Microbiol. **50:**489–500.
330. **Tanner, J. J., R. M. Hecht, and K. L. Krause.** 1996. Determinants of enzyme thermostability observed in the molecular structure of *Thermus aquaticus* D-glyceraldehyde-3-phosphate dehydrogenase at 2.5 Å resolution. Biochemistry **35:**2597–2609.
331. **Teplyakov, A. V., I. P. Kuranova, E. H. Harutyunyan, B. K. Vainshtein, C. Frommel, W. E. Hohne, and K. S. Wilson.** 1990. Crystal structure of thermitase at 1.4 Å resolution. J. Mol. Biol. **214:**261–279.
332. **Thoma, R., M. Hennig, R. Sterner, and K. Kirschner.** 2000. Structure and function of mutationally generated monomers of dimeric phosphoribosylanthranilate isomerase from *Thermotoga maritima*. Structure **8:**265–276.
333. **Tolan, J. S.** 1996. Pulp and paper, p. 327–338. *In* T. Godfrey and S. West (ed.), Industrial enzymology, 2nd ed. Stockton Press, New York, N.Y.
334. **Tomazic, S. J., and A. M. Klibanov.** 1988. Mechanisms of irreversible thermal inactivation of *Bacillus* α-amylases. J. Biol. Chem. **263:**3086–3091.
335. **Tomazic, S. J., and A. M. Klibanov.** 1988. Why is one *Bacillus* α-amylase more resistant against irreversible thermoinactivation than another? J. Biol. Chem. **263:**3092–3096.
336. **Tomizawa, H., H. Yamada, Y. Hashimoto, and T. Imoto.** 1995. Stabilization of lysozyme against irreversible inactivation by alterations of the Asp-Gly sequences. Protein Eng. **8:**1023–1028.
337. **Tomschy, A., G. Böhm, and R. Jaenicke.** 1994. The effect of ion pairs on the thermal stability of D-glyceraldehyde 3-phosphate dehydrogenase from the hyperthermophilic bacterium *Thermotoga maritima*. Protein Eng. **7:**1471–1478.
338. **Tomschy, A., R. Glockshuber, and R. Jaenicke.** 1993. Functional expression of D-glyceraldehyde-3-phosphate dehydrogenase from the hyperthermophilic eubacterium *Thermotoga maritima* in *Escherichia coli*. Authenticity and kinetic properties of the recombinant enzyme. Eur. J. Biochem. **214:**43–50.
339. **Tripp, A. E., D. S. Burdette, J. G. Zeikus, and R. S. Phillips.** 1998. Mutation of serine-39 to threonine in thermostable secondary alcohol dehydrogenase from *Thermoanaerobacter ethanolicus* changes enantiospecificity. J. Am. Chem. Soc. **120:**5137–5140.
340. **Tsujibo, H., K. Minoura, K. Miyamoto, H. Endo, M. Moriwaki, and Y. Inamori.** 1993. Purification and properties of a thermostable chitinase from *Streptomyces thermoviolaceus* OPC-520. Appl. Environ. Microbiol. **59:**620–622.
341. **Tsunasawa, S., Y. Izu, M. Miyagi, and I. Kato.** 1997. Methionine aminopeptidase from the hyperthermophilic archaeon *Pyrococcus furiosus*: molecular cloning and overexpression in *Escherichia coli* of the gene, and characteristics of the enzyme. J. Biochem. **122:**843–850.
342. **Tsunasawa, S., S. Nakura, T. Tanigawa, and I. Kato.** 1998. Pyrrolidone carboxyl peptidase from the hyperthermophilic Archaeon *Pyrococcus furiosus*: cloning and overexpression in *Escherichia coli* of the gene, and its application to protein sequence analysis. J. Biochem. **124:**778–783.
343. **Uemori, T., Y. Ishino, H. Toh, K. Asada, and I. Kato.** 1993. Organization and nucleotide sequence of the DNA polymerase gene from the archaeon *Pyrococcus furiosus*. Nucleic Acids Res. **21:**259–265.
344. **Uriarte, M., A. Marina, S. Ramon-Maiques, I. Fita, and V. Rubio.** 1999. The carbamoyl-phosphate synthetase of *Pyrococcus furiosus* is enzymologically and structurally a carbamate kinase. J. Biol. Chem. **274:**16295–16303.
345. **Ursby, T., B. S. Adinolfi, S. Al-Karadaghi, E. De Vendittis, and V. Bocchini.** 1999. Iron superoxide dismutase from the archaeon *Sulfolobus solfataricus*: analysis of structure and thermostability. J. Mol. Biol. **286:**189–205.
346. **Van den Burg, B., G. Vriend, O. R. Veltman, G. Venema, and V. G. Eijsink.** 1998. Engineering an enzyme to resist boiling. Proc. Natl. Acad. Sci. USA **95:**2056–2060.
347. **Veltman, O. R., G. Vriend, P. J. Middlehoven, B. Van Den Burg, G. Venema, and V. G. H. Eijsink.** 1996. Analysis of structural determinants of the stability of thermolysin-like proteases by molecular modelling and site-directed mutagenesis. Protein Eng. **9:**1181–1189.
348. **Vetriani, C., D. L. Maeder, N. Tolliday, K. S. Yip, T. J. Stillman, K. L. Britton, D. W. Rice, H. H. Klump, and F. T. Robb.** 1998. Protein thermostability above 100°C: a key role for ionic interactions. Proc. Natl. Acad. Sci. USA **95:**12300–12305.
349. **Vieille, C., D. S. Burdette, and J. G. Zeikus.** 1996. Thermozymes. Biotechnol. Annu. Rev. **2:**1–83.
350. **Vieille, C., J. M. Hess, R. M. Kelly, and J. G. Zeikus.** 1995. *xylA* cloning and sequencing and biochemical characterization of xylose isomerase from *Thermotoga neapolitana*. Appl. Environ. Microbiol. **61:**1867–1875.
351. **Vihinen, M.** 1987. Relationship of protein flexibility to thermostability. Protein Eng. **1:**477–480.
352. **Villa, A., L. Zecca, P. Fusi, S. Colombo, G. Tedeschi, and P. Tortora.** 1993. Structural features responsible for kinetic thermal stability of a carboxypeptidase from the archaebacterium *Sulfolobus solfataricus*. Biochem. J. **295:**827–831.
353. **Volkin, D. B., and A. M. Klibanov.** 1987. Thermal destruction processes in proteins involving cystine residues. J. Biol. Chem. **262:**2945–2950.
354. **Volkin, D. B., and C. R. Middaugh.** 1992. The effect of temperature on protein structure, p. 215–247. *In* T. J. Ahern and M. C. Manning (ed.), Stability of protein pharmaceuticals. A Chemical and physical pathways of protein degradation. Plenum Press, New York, N.Y.
355. **Völkl, P., R. Huber, E. Drobner, R. Rachel, S. Burggraf, A. Trincone, and K. O. Stetter.** 1993. *Pyrobaculum aerophilum* sp. nov., a novel nitrate-reducing hyperthermophilic archaeum. Appl. Environ. Microbiol. **59:**2918–2926.
356. **Vonrhein, C., H. Bönisch, G. Schäfer, and G. E. Schulz.** 1998. The structure of a trimeric archaeal adenylate kinase. J. Mol. Biol. **282:**167–179.
357. **Voorhorst, W. G., R. I. Eggen, E. J. Luesink, and W. M. De Vos.** 1995. Characterization of the *celB* gene coding for β-glucosidase from the hyperthermophilic archaeon *Pyrococcus furiosus* and its expression and site-directed mutation in *Escherichia coli*. J. Bacteriol. **177:**7105–7111.
358. **Wakarchuk, W. W., W. L. Sung, R. L. Campbell, A. Cunningham, D. C. Watson, and M. Yaguchi.** 1994. Thermostabilization of the *Bacillus circulans* xylanase by the introduction of disulfide bonds. Protein Eng. **7:**1379–1386.
359. **Wang, C., M. Eufemi, C. Turano, and A. Giartosio.** 1996. Influence of the carbohydrate moiety on the stability of glycoproteins. Biochemistry **35:**7299–7307.
360. **Wang, L., Y. Duan, R. Shortle, B. Imperiali, and P. A. Kollman.** 1999. Study of the stability and unfolding mechanism of BBA1 by molecular dynamics simulations at different temperatures. Protein Sci. **8:**1292–1304.
361. **Watanabe, K., T. Masuda, H. Ohashi, H. Mihara, and Y. Suzuki.** 1994. Multiple proline substitutions cumulatively thermostabilize *Bacillus cereus* ATCC7064 oligo-1,6-glucosidase. Eur. J. Biochem. **226:**277–283.
362. **Wearne, S. J., and T. E. Creighton.** 1989. Effect of protein conformation on rate of deamidation: ribonuclease A. Proteins **5:**8–12.
363. **Whitlow, M., A. J. Howard, B. C. Finzel, T. L. Poulos, E. Winborne, and G. L. Gilliland.** 1991. A metal-mediated hydride shift mechanism for xylose isomerase based on the 1.6 Å *Streptomyces rubiginosus* structures with xylitol and D-xylose. Proteins **9:**153–173.
364. **Wilquet, V., J. A. Gaspar, M. van de Lande, M. Van de Casteele, C. Legrain, E. M. Meiering, and N. Glansdorff.** 1998. Purification and characterization of recombinant *Thermotoga maritima* dihydrofolate reductase. Eur. J. Biochem. **255:**628–637.
365. **Winterhalter, C., P. Heinrich, A. Candussio, G. Wich, and W. Liebl.** 1995. Identification of a novel cellulose-binding domain within the multidomain 120 kDa xylanase XynA of the hyperthermophilic bacterium *Thermotoga maritima*. Mol. Microbiol. **15:**431–444.
366. **Wrba, A., A. Schweiger, V. Schultes, R. Jaenicke, and P. Zavodsky.** 1990. Extremely thermostable D-glyceraldehyde-3-phosphate dehydrogenase from the eubacterium *Thermotoga maritima*. Biochemistry **29:**7584–7592.
367. **Wright, H. T.** 1991. Nonenzymatic deamidation of asparaginyl and glutamyl residues in proteins. Crit. Rev. Biochem. Mol. Biol. **26:**1–52.
368. **Yip, K. S., T. J. Stillman, K. L. Britton, P. J. Artymiuk, P. J. Baker, S. E. Sedelnikova, P. C. Engel, A. Pasquo, R. Chiaraluce, V. Consalvi, R. Scandurra, and D. W. Rice.** 1995. The structure of *Pyrococcus furiosus* glutamate dehydrogenase reveals a key role for ion-pair networks in maintaining enzyme stability at extreme temperatures. Structure **3:**1147–1158.
368b. **Yip, K. S., K. L. Britton, T. J. Stillman, J. Lebbink, W. M. de Vos, F. T. Robb, C. Vetriani, D. Maeder, and D. W. Rice.** 1998. Insights into the molecular basis of thermal stability from the analysis of ion-pair networks in the glutamate dehydrogenase family. Eur. J. Biochem. **255:**336–346.
369. **Zale, S. E., and A. M. Klibanov.** 1986. Why does ribonuclease irreversibly inactivate at high temperatures? Biochemistry **25:**5432–5444.
370. **Závodszky, P., J. Kardos, Á. Svingor, and G. A. Petsko.** 1998. Adjustment of conformational flexibility is a key event in the thermal adaptation of proteins. Proc. Natl. Acad. Sci. USA **95:**7406–7411.
371. **Zeikus, J. G., S. E. Lowe, and B. C. Saha.** 1990. Biocatalysis in anaerobic extremophiles, p. 255–276. *In* D. A. Abramowicz (ed.), Biocatalysis. Van Nostrand Reinhold, New York, N.Y.
372. **Zeikus, J. G., and R. S. Wolfe.** 1972. *Methanobacterium thermoautotrophicus* sp. nov., an anaerobic, autotrophic, extreme thermophile. J. Bacteriol. **109:**707–715.
373. **Zhang, X. J., W. A. Baase, and B. W. Matthews.** 1992. Multiple alanine replacements within alpha-helix 126–134 of T4 lysozyme have independent, additive effects on both structure and stability. Protein Sci. **1:**761–776.
374. **Zhao, H., and F. H. Arnold.** 1999. Directed evolution converts subtilisin E into a functional equivalent of thermitase. Protein Eng. **12:**47–53.
375. **Zhu, W., K. Sandman, G. E. Lee, J. N. Reeve, and M. F. Summers.** 1998. NMR structure and comparison of the archaeal histone HFoB from the mesophile *Methanobacterium formicicum* with HMfB from the hyperthermophile *Methanothermus fervidus*. Biochemistry **37:**10573–10580.
376. **Zillig, W., A. Gierl, G. Schreiber, S. Wunderl, D. Janekovic, K. O. Stetter, and H. P. Klenk.** 1983. The archaebacterium *Thermofilum pendens* represents a novel genus of the thermophilic, anaerobic sulfur respiring *Thermoproteales*. Syst. Appl. Microbiol. **4:**79–87.
377. **Zillig, W., I. Holz, D. Janekovic, H. Klenk, E. Imsel, J. Trent, S. Wunderl, V. H. Forjaz, R. Coutinho, and T. Ferreira.** 1990. *Hyperthermus butylicus*, a

hyperthermophilic sulfur-reducing archaebacterium that ferments peptides. J. Bacteriol. **172:**3959–3965.

378. **Zillig, W., I. Holz, D. Janekovic, W. Schäfer, and W. D. Reiter.** 1983. The archaebacterium *Thermococcus celer* represents, a novel genus within the thermophilic branch of the archaebacteria. Syst. Appl. Microbiol. **4:**88–94.
379. **Zillig, W., I. Holz, H. Klenk, J. Trent, S. Wunderl, D. Janekovic, E. Imsel, and B. Hass.** 1987. *Pyrococcus woesei*, sp. nov., an ultra-thermophilic marine archaebacterium, representing a novel order, *Thermococcales*. Syst. Appl. Microbiol. **9:**62–70.
380. **Zillig, W., A. Kletzin, C. Schleper, I. Holz, D. Janekovic, J. Hain, M. Lanzendörfer, and J. K. Kristjansson.** 1994. Screening for *Sulfolobales*, their plasmids and their viruses in icelandic solfataras. Syst. Appl. Microbiol. **16:**609–628.
381. **Zillig, W., K. O. Stetter, D. Prangishvilli, W. Schäfer, S. Wunderl, D. Janekovic, I. Holz, and P. Palm.** 1982. *Desulfurococcaceae*, the second family of the extremely thermophilic, anaerobic, sulfur-respiring *Thermoproteales*. Zentbl. Bakteriol. Mikrobiol. Hyg. I Abt Orig. C **3:**304–317.
382. **Zillig, W., K. O. Stetter, W. Schafer, D. Janekovic, S. Wunderl, I. Holz, and P. Palm.** 1981. Thermoproteales: a novel type of extremely thermoacidophilic anaerobic archaebacteria isolated from icelandic solfataras. Zentbl. Bakteriol. Mikrobiol. Hyg I Abt. Orig. C **2:**205–227.
383. **Zillig, W., K. O. Stetter, S. Wunderl, W. Schulz, H. Priess, and I. Scholz.** 1980. The *Sulfolobus-Caldariella* group: taxonomy on the basis of the structure of DNA-dependent RNA polymerases. Arch. Microbiol. **125:**259–269.
384. **Zillig, W., S. Yeats, I. Holz, A. Bock, M. Rettenberger, F. Gropp, and G. Simon.** 1986. *Desulfurolobus ambivalens*, gen. nov., sp. nov., an autotrophic archaebacterium facultatively oxidizing or reducing sulfur. Syst. Appl. Microbiol. **8:**197–203.
385. **Zvyagintseva, I. S., and A. L. Tarasov.** 1988. *Caldococcus litoralis* gen. nov. sp. nov.—a new marine, extremely thermophilic, sulfur-reducing archaebacterium. Microbiology **56:**658–664.
386. **Zwickl, P., S. Fabry, C. Bogedain, A. Hass, and R. Hensel.** 1990. Glyceraldehyde-3-phosphate dehydrogenase from the hyperthermophilic archaebacterium *Pyrococcus woesei*: characterization of the enzyme, cloning and sequencing of the gene, and expression in *Escherichia coli*. J. Bacteriol. **172:**4329–4338.